NATURE AND COMPOSITION OF THE CONTINENTAL CRUST: A LOWER CRUSTAL PERSPECTIVE

Roberta L. Rudnick[1]
Research School of Earth Sciences
The Australian National University, Canberra

David M. Fountain
Department of Geology and Geophysics
University of Wyoming, Laramie

Abstract. Geophysical, petrological, and geochemical data provide important clues about the composition of the deep continental crust. On the basis of seismic refraction data, we divide the crust into type sections associated with different tectonic provinces. Each shows a three-layer crust consisting of upper, middle, and lower crust, in which *P* wave velocities increase progressively with depth. There is large variation in average *P* wave velocity of the lower crust between different type sections, but in general, lower crustal velocities are high (>6.9 km s^{-1}) and average middle crustal velocities range between 6.3 and 6.7 km s^{-1}. Heat-producing elements decrease with depth in the crust owing to their depletion in felsic rocks caused by granulite facies metamorphism and an increase in the proportion of mafic rocks with depth. Studies of crustal cross sections show that in Archean regions, 50–85% of the heat flowing from the surface of the Earth is generated within the crust. Granulite terrains that experienced isobaric cooling are representative of middle or lower crust and have higher proportions of mafic rocks than do granulite terrains that experienced isothermal decompression. The latter are probably not representative of the deep crust but are merely upper crustal rocks that have been through an orogenic cycle. Granulite xenoliths provide some of the deepest samples of the continental crust and are composed largely of mafic rock types. Ultrasonic velocity measurements for a wide variety of deep crustal rocks provide a link between crustal velocity and lithology. Meta-igneous felsic, intermediate and mafic granulite, and amphibolite facies rocks are distinguishable on the basis of *P* and *S* wave velocities, but metamorphosed shales (metapelites) have velocities that overlap the complete velocity range displayed by the meta-igneous lithologies. The high heat production of metapelites, coupled with their generally limited volumetric extent in granulite terrains and xenoliths, suggests they constitute only a small proportion of the lower crust. Using average *P* wave velocities derived from the crustal type sections, the estimated areal extent of each type of crust, and the average compositions of different types of granulites, we estimate the average lower and middle crust composition. The lower crust is composed of rocks in the granulite facies and is lithologically heterogeneous. Its average composition is mafic, approaching that of a primitive mantle-derived basalt, but it may range to intermediate bulk compositions in some regions. The middle crust is composed of rocks in the amphibolite facies and is intermediate in bulk composition, containing significant K, Th, and U contents. Average continental crust is intermediate in composition and contains a significant proportion of the bulk silicate Earth's incompatible trace element budget (35–55% of Rb, Ba, K, Pb, Th, and U).

1. INTRODUCTION

Continents cover 41% of the Earth's surface [*Cogley*, 1984] and sit at high elevations compared to the ocean basins owing to the presence of lower-density, evolved rock types. ("Evolved" is defined, along with other specialized terminology, in the glossary following this introduction.) The evolved rocks that dominate the upper portions of the Earth's continental crust are unique in our solar system [*Taylor*, 1989] and are probably ultimately linked to the presence of liquid water on Earth [*Campbell and Taylor*, 1985]. Whereas the upper crust is accessible to geological sampling and measurements, the deeper portions of the crust are relatively inaccessible. To date, the deepest drill hole has penetrated only 12 km of crust [*Kremenetsky and Ovchinnikov*, 1986]. Nevertheless, these deep portions of the crust contain important information related to the bulk composition of the continental crust as well as how it forms.

The lower crust (below ~20–25 km depth) is believed to consist of metamorphic rocks in the granulite facies (referred to simply as granulites throughout this paper), which are accessible either as large tracts of surface outcrop (terrains) or as tiny fragments carried from great depths in volcanic conduits (xenoliths). The

[1]Now at Department of Earth and Planetary Sciences, Harvard University, Cambridge, Massachusetts.

Reviews of Geophysics, 33, 3 / *August 1995*
pages 267–309
8755-1209/95/95RG-01302$15.00
Paper number 95RG01302

middle crust (i.e., between 10–15 and 20–25 km depth) may contain rocks in the amphibolite facies, which are also found in surface outcrop or as xenoliths. Amphibolite facies rocks may also be important in the lowermost crust in areas of high water flux (such as in island arc settings where hydrous oceanic lithosphere is subducted and dewatered [e.g., *Kushiro*, 1990].

The role the lower crust plays in continental tectonics is poorly understood. For example, are the rheological and compositional differences between upper and lower crust sufficient to promote delamination of the lower crust at continent-continent collision zones? How much lower crust might be recycled back into the mantle at convergent margin settings, and how much remains within the crust under conditions of high-grade metamorphism?

Our understanding of the deep continental crust has improved dramatically over the last decade as a result of detailed seismological studies and numerous studies of lower crustal rocks. However, the composition of the deep crust remains the largest uncertainty in determining the crust's overall composition. This is due to (1) the large compositional differences between granulites that occur in surface tracts (granulite terrains, in which felsic rocks dominate) and those that are carried as small fragments to the Earth's surface in rapidly ascending magmas (xenoliths, which are dominated by mafic rocks), (2) the very heterogeneous nature of the lower crust as observed in granulite terrains, and (3) the difficulty in determining rock type(s) from average seismic velocities derived from refraction studies.

In this contribution we review our knowledge of the deep continental crust from both geophysical-based and sample-based studies. Of the various geophysical methods (seismic, thermal, electrical, potential field), seismological data and heat flow studies reveal most about the composition of the crust. We will focus on these two methods here. (The interested reader is referred to *Jones* [1992] and *Shive et al.* [1992] for reviews of electrical and magnetic properties of the lower crust, respectively.) We then integrate both data sets in order to derive a bulk composition for the lower, middle, and bulk continental crust. Our subdivision of the crust into upper, middle, and lower is based on observations from seismic studies as summarized by *Holbrook et al.* [1992].

2. GLOSSARY

Sources of definitions are *Bates and Jackson* [1980], *Fowler* [1990], and *Sheriff* [1991].

Accessory phase: mineral present in low abundances in rocks but which may contain a significant proportion of the incompatible trace element inventory of the rock. Examples include monazite and allanite.

Acoustic impedance: the product of velocity and density.

Amphibolite: a mafic rock consisting dominantly of amphibole.

Amphibolite facies: the set of metamorphic mineral assemblages in which mafic rocks are composed of amphibole and plagioclase. The facies is typical of regional metamorphism at moderate to high pressures and temperatures (i.e., >300 MPa, 450°–700°C).

Anisotropy: see seismic anisotropy.

Anorthosite: a plutonic igneous rock composed almost entirely of plagioclase feldspar (see *Ashwal* [1993] for an excellent review).

Constructive interference: see interference.

Continent-continent collision zone: a special type of convergent margin where a continent on the subducting plate collides with another on the overriding plate.

Convergent margin: the zone where two tectonic plates converge and one is subducted beneath the other.

Craton: an area of crust that has remained stable for very long periods of time.

Critical angle: the angle of incidence of a seismic wave at which a head wave (or refracted wave) is generated.

Critical distance: offset at which reflection time equals refraction time.

Cumulate: an igneous rock formed by accumulation of crystallizing phases.

Delamination: a process by which dense segments of the lower crust (and lithospheric mantle) sink into the convecting asthenosphere as a result of their negative buoyancy.

Ductile: generally regarded as the capacity of a material to sustain substantial change in shape without gross faulting [see *Paterson*, 1978], though there are numerous, and sometimes conflicting, uses of the word.

Ductile shear zones: a fault zone in which the deformation is ductile.

Eclogite: a high-pressure mafic rock composed of garnet and Na-rich clinopyroxene (omphacite); also a metamorphic facies defined by the appearance of these phases in mafic rocks.

Eu anomaly: $Eu/Eu^* = 2Eu_n/(Sm_n\ Gd_n)^{0.5}$, where the subscripted n indicates that the values are normalized to chondritic meteorites. Eu is one the only rare earth element (REE) that can occur in the 2+ valance state under oxygen fugacity conditions found in the Earth. Eu^{2+} is larger than its REE^{3+} neighbors and has a charge and radius similar to that of Sr. It therefore substitutes for Sr in feldspars, and fractionation of feldspar will lead to a Eu anomaly.

Evolved: said of an intermediate or felsic igneous rock (or its metamorphosed equivalent) that is derived from a rock of a more mafic composition through the

processes of magmatic differentiation or partial melting.

Felsic: said of a rock composed mainly of light-colored minerals.

Granulite: a rock that exhibits granulite facies mineral assemblages.

Granulite facies: the set of metamorphic mineral assemblages in which mafic rocks are represented by diopside + hypersthene + plagioclase. The facies is typical of deep-seated regional dynamothermal metamorphism at temperatures above 650°C. Although granulites may form at relatively low pressures, we use the term here to imply pressures greater than 600 MPa.

Granulite terrain: a large tract of land composed of rocks at the granulite facies.

Granulite xenolith: a foreign rock fragment in granulite facies that is carried to the Earth's surface by rapidly ascending, mantle-derived magmas.

Head wave: wave characterized by entering and leaving high-velocity medium at critical angle. A head wave corresponds to a refracted wave that travels along the interface of a velocity discontinuity.

Heat-producing elements (HPE): those elements that generate heat as a result of their rapid radioactive decay (i.e., K, Th, and U).

Interference: superposition of two or more waveforms. Constructive interference occurs when waveforms are in phase and destructive interference occurs when waveforms are 180° out of phase.

Island arc: an arcuate string of volcanic islands formed above zones of descending oceanic crust (subduction zones).

Isobaric cooling: pressure-temperature path followed by metamorphic rocks in which temperature decreases while pressure remains high.

Isothermal decompression: pressure-temperature path followed by metamorphic rocks in which pressure decreases while temperature remains high.

Lithospheric mantle: that portion of the Earth's mantle that immediately underlies, and is convectively coupled to, the crust.

Mafic: adjective describing a rock composed mainly of ferromagnesian, dark colored minerals.

Metapelites: metamorphosed shales (fine-grained detrital sedimentary rocks composed largely of consolidated clay, silt, and mud).

Mg #: $100Mg/(Mg + \Sigma Fe)$, where Mg and Fe are expressed as moles.

Modal mineralogy: the volumetric proportion of minerals in a rock.

Mu (μ): the ratio of ^{238}U to ^{204}Pb.

Orogenic belt: a linear or arcuate belt that has been subjected to folding and deformation during a mountain-building event.

Pelitic: said of a sedimentary rock composed of clay.

Peridotite: a rock containing >40% olivine accompanied by Cr-diopside, enstatite, and an aluminous phase (either spinel or garnet, depending on pressure). The upper mantle is believed to be composed mainly of peridotite.

Poisson's ratio: the ratio of elastic contraction to elastic expansion of a material in uniaxial compression. It can be related to elastic wave velocities by $0.5\{1 - 1/[(V_p/V_s)^2 - 1]\}$, where V_p is P (primary, or compressional) wave velocity and V_s is S (secondary, or shear) wave velocity.

Prograde: mineral reactions occurring under increasing temperature and pressure conditions.

Reduced heat flow: the intercept of the linear surface heat production–heat flow relationship.

Reflection coefficient: measure of relative amount of reflected energy from an interface, determined as $RC = [Z_2 - Z_1]/[Z_2 + Z_1]$, where Z_i is acoustic impedance of layer i ($Z_i = \rho_i V_i$, where ρ is density and V is velocity).

Refraction surveys: experiments that utilize refracted waves and/or wide-angle reflected waves from different layers in the crust or mantle to deduce the variation in seismic velocity with depth.

Restite: material remaining behind after extraction of a partial melt.

Retrograde: mineral reactions occurring under decreasing temperature and pressure conditions.

Seismic anisotropy: variation of velocity as a function of direction, usually reported as a percent. Either $A = 100(V_{max} - V_{min})/V_{max}$ or $A = 100(V_{max} - V_{min})/V_{mean}$.

Shot-to-receiver offset (offset): the distance between the energy source (explosion, earthquake, etc.) and the seismometer.

Stacking: adding of seismic traces to increase the signal-to-noise ratio.

Subcritical energy: energy received at distances less than the critical distance.

Supercritical energy: energy received at distances greater than the critical distance.

Supracrustal: said of a rock that forms at the Earth's surface.

Trondhjemite: a plutonic rock composed of sodic plagioclase, quartz, biotite, and little or no potassium feldspar.

Underplating: intrusion of magmas near the base of the crust.

Xenolith: a rock that occurs as a fragment in another, unrelated igneous rock (literally, foreign rock fragment).

3. SEISMIC PROPERTIES OF LOWER CONTINENTAL CRUST

In this section we review the major findings related to the structure and composition of the lower conti-

nental crust derived from seismic surveys. We compare these with ultrasonic velocities measured in different deep crustal rock types. In a later section we use these comparisons to infer the bulk composition of the deep crust.

3.1. Methods

Much of our knowledge about the physical properties of the continental crust is derived from various seismic refraction and reflection methods (see *Holbrook et al.* [1992] and *Mooney and Meissner* [1991] for recent reviews). In these studies, seismic energy generated by natural (e.g., earthquakes) or artificial (e.g., explosions, vibrator trucks, air guns) sources is recorded by seismometers placed at various spacings (receiver spacing) at long distances from the energy source (shot-to-receiver offset). In refraction surveys, the offset is generally long (200–300 km) in order to record arrivals from the upper mantle and Moho, shot spacing is generally 20–100 km, and receiver spacing is highly variable. Receiver spacing in older surveys commonly exceeded 10 km, but in more recent studies it is generally 1–5 km. Receiver spacings less than 1 km have been achieved in surveys that use marine profiling techniques where airguns towed by ships shoot frequently into hydrophone streamers, fixed ocean bottom seismometers, or land-based stations [e.g., *BABEL Working Group*, 1993; *Holbrook et al.*, 1994b]. Small receiver spacing, although expensive in land-based surveys, is highly desirable because of the improved correlation of phases on record sections.

The variety of waves recorded in typical refraction surveys provide the basis for seismic velocity models of the crust. In addition to the direct wave that travels through the uppermost crust (P_g), various waves are reflected and refracted (head wave) from what are traditionally interpreted as first-order velocity discontinuities (see texts of *Bott* [1982] and *Fowler* [1990] for review). For a simple, layered crust, only reflections are recorded from an interface at small offsets. As offset increases, a critical angle of incidence is attained where energy is partitioned into a wide-angle reflected wave and a head wave (refracted wave) that travels along the interface. For the Moho these waves are referred to as P_mP and P_n, respectively. In principle, measurement of travel time of refracted arrivals as a function of offset allows determination of an apparent velocity for the head wave. Because amplitudes of these arrivals are generally smaller than amplitudes of wide-angle reflections at offsets greater than the critical distance, they are difficult to identify and correlate in record sections. Wide-angle reflections from other interfaces can also mask the refracted arrival of interest. Because of this complication, most current interpretations rely heavily on critical and supercritical wide-angle reflections to constrain the position and velocity of deep crustal layers. In the last decade, most analyses of refraction data employ various two-dimensional (2-D) forward modeling methods that attempt to match both observed travel times and the amplitudes of the wide-angle reflection and refraction arrivals with theoretically determined travel times and amplitudes. Such approaches have been improved by travel time inversion methods coupled with amplitude modeling [e.g., *Zelt and Smith*, 1992; *Hole et al.*, 1993; *Holbrook et al.*, 1994b].

Near-vertical reflection surveys record subcritical energy at very small offsets (2–10 km), small receiver spacing (25–100 m), and close shot spacing (50–500 m) relative to refraction surveys. Although subcritical reflections have lower amplitudes than critical to supercritical reflections, the acquisition geometry produces a data redundancy that permits use of a wide array of signal processing methods (e.g., stacking) for amplitude enhancement and correlation of reflected phases over large distances. Additionally, the higher-frequency content of energy sources in near-vertical surveys (e.g., air guns and vibrators) provides higher resolution of the crust than available with lower frequency sources used in refraction surveys. Vertical resolution of reflection data is generally regarded as one-quarter the signal wavelength. For a crustal velocity of 6.0 km s^{-1} and a frequency of 25 Hz, vertical resolution is 60 m [*Mooney and Meissner*, 1991]. Despite this potential for resolving structures in the deep crust with near-vertical reflection methods, there remain numerous problems in the interpretation of reflectors in the deep crust (for instance, complications arise from the effects of geometrical spreading, scattering, attenuation, interference effects, and inadequate knowledge of deep crustal velocities used for migration and stacking). In addition, near-vertical incidence methods provide no direct measure of seismic velocities of reflectors, and the reflection coefficients of reflecting horizons remain unconstrained.

3.2. Lower Crustal Structure

One of the most remarkable features of reflection surveys is the presence of numerous subhorizontal reflectors in the lower crust of many regions, which in most cases disappear at the Moho (see *Barnes* [1994] for discussion of sub-Moho reflectors). In many cases the onset of reflectivity within the crust appears at the top of the lower crust and continues throughout, and in other cases it is confined to the upper and lower boundaries of the lower crust (see *Mooney and Brocher* [1987] for a review). A detailed discussion of the voluminous literature on the causes of deep crustal reflectivity is provided by *Mooney and Meissner* [1992], who summarize the large number of models for the origin of reflections from the deep continental crust. These include (1) acoustic impedance contrasts caused by solidified igneous intrusions within crustal rocks of differing physical properties; (2) fine-scale lithologic layering of metamorphic rocks where reflections can be caused by lithologic variations, seismic

anisotropy (variation of velocity as a function of direction) constructive interference, or a combination of these; (3) faults that juxtapose different rock types; (4) localized ductile shear zones where reflections originate because of seismic anisotropy within the shear zone, metamorphic recrystallization (prograde or retrograde) within the shear zone that is absent outside the zone, constructive interference from enhancement of lithologic layering related to high strain, or the complex interaction of all these effects; (5) local zones containing fluids under high pore fluid pressure (for a critique of this hypothesis see *Mooney and Meissner* [1992] and *Frost and Bucher* [1994]); (6) pervasive ductile flow in the deep crust that enhances layering, anisotropy, and constructive interference; and (7) molten or partially molten bodies in the lower crust [*Suetnova et al.*, 1993]. Support for the second hypothesis is provided by seismic modeling studies where geologic maps of exposed deep crustal terrains (see below) and laboratory measurements of rock velocity are used to calculate theoretical reflection profiles [*Burke and Fountain*, 1990; *Fountain*, 1986; *Fountain and Salisbury*, 1986; *Hale and Thompson*, 1982; *Holliger and Levander*, 1992; *Hurich and Smithson*, 1987; *Reston*, 1990]. In general, the models simulate the reflectivity patterns observed on reflection profiles. Opinion on the fourth hypothesis is mixed. Some studies indicate that strain gradients may diminish ductile shear zone reflectivity [*Rey et al.*, 1994] and that compositional changes associated with retrograde or prograde metamorphism (synkinematic growth of new mineral phases) may be required for ductile shear zone reflectivity [*Fountain et al.*, 1994a; *Kern and Wenk*, 1990]. Other investigations [*Barruol et al.*, 1992; *Christensen and Szymanski*, 1988; *Jones and Nur*, 1984; *McDonough and Fountain*, 1988] show examples where ductile shear zones may be reflective.

Consideration of the near-vertical reflection data for the deep continental crust raises two important points concerning interpretation of seismic velocity models derived from refraction data. First, the prominent reflections observed in many lower crustal sections imply that the lower crust is compositionally and/or structurally heterogeneous at a variety of scales. For example, modeling by *Holliger and Levander* [1992] illustrates that acoustic impedance contrasts from lithological variations with fractal dimensions of 2.7 can cause deep crustal reflectors of the type observed on deep seismic profiles. Thus average velocities determined from refraction surveys represent only an average velocity of the rock units in the layer. Moreover, the absence of reflectors does not imply the absence of compositional (or structural) variability because many rock types have similar acoustic impedances (see below) and geometric effects (destructive interference, scattering, etc.) may diminish reflectivity in a heterogeneous medium. Second, the presence of small-scale heterogeneities within the lower crust may strongly influence both the amplitude and travel time of the wide-angle reflections that figure so heavily in the interpretation of refraction data [see *Levander and Holliger*, 1992; *Long et al.*, 1994; and references therein]. The potential severity of this problem is illustrated by *Levander and Holliger* [1992], who show that random velocity variations superimposed on a first-order discontinuity produce the same seismic response (at intermediate and large offsets) as a velocity gradient with the same magnitude of superimposed fine-scale velocity variations. *Levander and Holliger* [1992] conclude that fine-scale velocity variations in the lower crust may make it difficult to detect large-scale velocity changes in the absence of clear refraction arrivals. However, we note that although *Levander and Holliger* [1992] produce similar theoretical seismic profiles for very different models, the average velocity of the lower crust in both models was the same. Accordingly, we assume that the average velocity of a lower crustal layer is indicative of the average properties of the constituent rock types while recognizing that such an average may be caused by a heterogeneous package of lithologies.

3.3. Seismic Velocities in the Crust

Some of the most useful parameters determined in seismic refraction surveys are average P (compressional) and S (shear) wave velocities, V_p and V_s, respectively for different crustal layers. Velocities are related to the physical environment of the crust (temperature, pressure, porosity, fluid content, etc.) and the intrinsic properties of the rocks (mineralogical composition, chemical composition, metamorphic grade, crystallographic preferred orientation of constituent minerals, etc.) through which the seismic waves pass. Reviews of the relative importance of these parameters in crustal rocks are given by *Christensen and Wepfer* [1989], *Fountain and Christensen* [1989], and *Jackson* [1991]. An excellent review of seismic constraints on lower crustal composition using seismic refraction data and laboratory measurements of rock properties is given by *Holbrook et al.* [1992]; our analysis follows from theirs.

In order to summarize the general characteristics of the lower continental crust of differing tectonic affinities, we used the highest-quality seismic studies compiled by *Holbrook et al.* [1992, Table 1-1] and supplemented these with more recent studies. Because these studies are confined mainly to North America and Europe, we included data of lesser quality (e.g., wide receiver spacing, one-dimensional interpretations) so as to achieve a more thorough sampling of the continents. We divide the crust into the following categories: (1) Precambrian platforms and shields (comprising areas of exposed Precambrian crust plus sedimentary platforms covering Precambrian crust), (2) Paleozoic orogenic belts (e.g., Variscan of western Europe, Appalachians), (3) Mesozoic-Cenozoic exten-

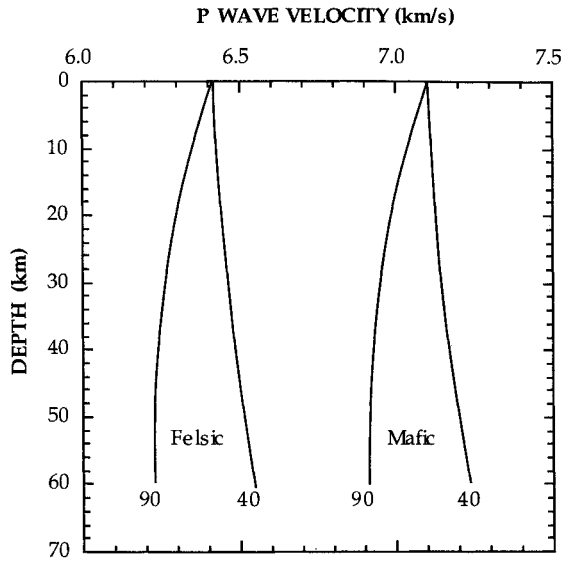

Figure 1. Variation of compressional wave velocity for typical lower crustal felsic and mafic rocks as a function of depth in the crust for geothermal gradients corresponding to surface heat flow values of 40 and 90 mW m^{-2} [*Chapman and Furlong*, 1992]. Mineralogies are constant throughout the illustrated pressure interval.

sional regions (e.g., U.S. Basin and Range), (4) Mesozoic-Cenozoic contractional orogenic belts (e.g., Alps, Himalayas, Canadian Cordillera), (5) continental arcs (e.g., Cascades), (6) active rifts (e.g., Rheingraben), (7) rifted margins (e.g., eastern continental shelf of North America), and (8) forearc regions (e.g., coast of British Columbia). An obvious problem in such a compilation is that many continental regions remain only poorly studied from a seismological viewpoint (i.e., most of Africa, Asia, South America, and Antarctica). It is thus unclear how the picture of crustal structure in different tectonic settings derived from this database might change when more data become available.

Because pressure and temperature can strongly influence the seismic velocities of crustal and mantle rocks it was necessary to correct the crustal refraction data to a common pressure and temperature for purposes of comparison. The potential magnitude of these effects is illustrated in Figure 1 for two different conductive geotherms (corresponding to heat flow of 40 and 90 mW m^{-2}) and two different lithologies, a deep crustal mafic gneiss and a deep crustal felsic rock (see below). We used a typical pressure derivative for V_p determined at confining pressures above 400 MPa ($\sim 2 \times 10^{-4}$ km s^{-1} MPa^{-1}) and typical temperature derivative ($\sim 4 \times 10^{-4}$ km s^{-1} $°C^{-1}$) for crustal rocks (see references in Table 3 and summaries by *Kern* [1982], *Christensen and Wepfer* [1989], *Fountain and Christensen* [1989], *Jackson* [1991], and *Christensen and Mooney* [1995]). For a crustal of constant composition in which the heat flow is low (40 mW m^{-2}, as is observed in cratonic regions) V_p increases slightly with depth. For hotter geotherms, V_p decreases with depth. So that the various refraction models in our compilation could be effectively compared, we corrected all values to a standard pressure of 600 MPa and room temperature. To do so, we estimated the temperature from the family of conductive geotherms presented by *Chapman and Furlong* [1992], determined the pressure of each layer assuming an average crustal density of 2800 kg m^{-3}, and recalculated the velocities for each layer using the derivatives given above. By means of these corrections, the average velocities can also be compared with laboratory measurements of ultrasonic velocities, which are generally performed at room temperature (see below). We assume that the crust is isotropic and that other factors that influence V_p, such as high pore fluid pressures, are not regionally important. Table 1 lists the thicknesses and reported velocities for the profiles used in the compilation as well as the velocities corrected to room temperature and 600 MPa confining pressure. All specific refraction velocity values mentioned henceforth will be corrected velocities.

Although there is considerable and important variation within each crustal type, it appears that some types of crust share comparable velocity structure from place to place. For example, Precambrian shields and platforms are generally characterized by thick crust (43 km) having a high-velocity layer in the lower one third of the crust. (We find no significant differences between Archean and Proterozoic shields in either crustal thickness (43 km for both) or velocity structure [cf. *Durheim and Mooney*, 1994].) In contrast, other types of crust are more highly variable. Paleozoic fold belts in Europe appear to have thinner crust with lower velocity than do non-European Paleozoic fold belts (this may be due to postorogenic extension [*Ménard and Molnar*, 1988]). As might be expected, Cenozoic-Mesozoic contractional orogenic belts have the greatest variability, with crustal thickness varying by nearly a factor of 2 and lower crustal velocity varying by nearly 1 km s^{-1}.

These velocity models were averaged in order to derive crustal type sections (Figure 2, Table 2). All show a three-layer crust with increasing P wave velocity with depth. With the exception of Precambrian shields, the upper crust is characterized by a layer having low velocities (<6.2 km s^{-1}); shield upper crust has a higher average velocity of 6.3 km s^{-1}. The average velocity for the middle crust is variable from section to section. Paleozoic fold belts, Cenozoic-Mesozoic areas, and rifted margins all exhibit middle crusts having velocities between 6.2 and 6.5 km s^{-1}, whereas shields and platforms, continental arcs and rifts have a higher velocity middle crust, between 6.5 and 6.9 km s^{-1}. The lower crust in all profiles exhibits the highest average velocity, between 6.9 and 7.2 km s^{-1}. In general, the type sections in Figure 2 bear

TABLE 1. Summary of Refraction Studies Used in Compilation of Crustal Type Sections

Place	Reference	Fluff, km	Upper			Middle			Lower			Lowest			Moho	Heat Flow	
			Thickness, km	V_p, km s^{-1}		Thickness, km	V_p, km s^{-1}		Thickness, km	V_p, km s^{-1}		Thickness, km	V_p, km s^{-1}		Depth, km	Flow, mW m^{-2}	Reference[a]
				Obs.	Cor.		Obs.	Cor.		Obs.	Cor.		Obs.	Cor.			
Cenozoic-Mesozoic Extensional Terranes																	
Basin and Range	*Stauber* [1983]	3.00	16.00	6.00	6.22				11.00	6.64	6.89				30.00	90	1
Basin and Range	*Valasek et al.* [1987]	3.00	9.50	6.10	6.30	7.00	6.35	6.57	8.50	6.60	6.86	3.00	7.35	7.60	31.00	90	1
Basin and Range transition., Arizona	*Goodwin and McCarthy* [1991]		10.00	5.50	5.50	10.00	6.00	6.21	12.00	6.60	6.86				32.00	90	1
Quesnellia terrane, B.C.	*Zelt et al.* [1993]	2.00	22.00	6.20	6.35				7.00	6.65	6.84	3.00	7.70	7.90	34.00	73	2
Basin and Range	*Zelt and Smith* [1992]		9.00	5.75	5.90	12.00	6.25	6.46	8.00	6.85	7.11				29.00	90	1
Basin and Range	*Holbrook* [1990]		8.00	6.00	6.00	10.00	6.10	6.30	8.00	6.60	6.85	2.00	6.80	7.07	28.00	90	1
Omineca belt	*Kanasewich et al.* [1994]		15.00	5.90	6.06	10.00	6.15	6.36	10.00	6.75	6.98				35.00	83	2
Colorado River corridor	*McCarthy et al.* [1991]		5.00	5.80	5.90	15.00	6.13	6.30	10.00	6.55	6.77				30.00	80	1
Mean		1.00	11.81	5.91	6.03	8.00	6.16	6.37	9.31	6.66	6.90	1.00	7.28	7.52	31.13		
Standard deviation		1.41	5.46	0.22	0.27	5.42	0.12	0.13	1.71	0.10	0.10	1.41	0.45	0.42	2.42		
N		3	8	8	8	6	6	6	8	8	8	3	3	3	8		
Arcs																	
Cascades, Oregon	*Leavert et al.* [1984]		7.60	6.00	6.00	19.40	6.45	6.65	15.00	6.90	7.20	4.00	7.40	7.70	46.00	90	3
Coast plutonic belt, B.C.	*Zelt et al.* [1993]	1.00	12.00	6.30	6.50	8.00	6.80	7.00	15.00	7.03	7.25				36.00	80	2
Trans-Mexico belt	*Valdes et al.* [1986]		4.00	6.00	6.00	12.00	5.90	6.10	30.00	6.90	7.16				46.00	90	1
Honshu, Japan	*Asano et al.* [1985]		19.00	6.00	6.00				20.00	6.80	7.06				39.00	90	4
Northern Honshu, Japan	*Iwasaki et al.* [1994b]		12.00	6.20	6.46	13.00	6.45	6.74	8.00	6.95	7.22				33.00	90	4
Mean		10.92	6.10	6.19	13.10	6.40	6.62	17.60	6.92	7.18				40.00			
Standard deviation		5.62	0.14	0.26	4.72	0.37	0.38	8.14	0.08	0.07				5.87			
N		5	5	5	4	4	4	5	5	5				5			
Forearcs																	
Coast plutonic complex Queen Charlotte	*Yuan et al.* [1992]	4.00	4.00	6.35	6.48	7.00	6.50	6.63	12.00	6.85	6.97	0.50	7.45	7.57	27.50	50	2
Coast plutonic complex Queen Charlotte	*Hole et al.* [1993]		7.00	5.95	6.07	11.00	6.60	6.75	11.00	6.85	6.97				29.00	50	2
Coast plutonic complex Hecate Strait	*Mackie et al.* [1989]		10.00	5.70	5.82	13.00	6.48	6.60	6.00	6.84	6.95				29.00	50	2
Coast plutonic complex Hecate Strait	*Spence and Asudeh* [1993]		7.00	5.60	5.73	8.00	6.40	6.50	14.00	7.05	7.15				29.00	50	2
Coast plutonic complex Hecate Strait	*Spence and Asudeh* [1993]	4.00	4.00	6.10	6.22	12.00	6.48	6.60	6.00	6.90	7.02				26.00	50	2
Vancouver Island, B.C.	*Zelt et al.* [1993]	1.00	12.00	6.30	6.43	9.00	6.65	6.75	8.00	7.00	7.09				30.00	40	2
S. California margin, Salinia	*Howie et al.* [1993]		3.00	5.20	5.33	12.00	6.10	6.25	12.00	6.70	6.88				27.00	70	1
S. California margin	*Howie et al.* [1993]	4.00	10.00	5.63	5.78				6.00	6.90	7.07				20.00	70	1
S. California margin, SLO	*Howie et al.* [1993]		4.00	4.90	5.02	11.00	5.80	5.95	8.00	6.90	7.07				23.00	70	1

TABLE 1. continued

Place	Reference	Fluff, km	Upper			Middle			Lower			Lowest			Moho	Heat Flow	
			Thickness, km	V_p, km s^{-1}		Thickness, km	V_p, km s^{-1}		Thickness, km	V_p, km s^{-1}		Thickness, km	V_p, km s^{-1}		Depth, km	Flow, mW m^{-2}	Reference[a]
				Obs.	Cor.		Obs.	Cor.		Obs.	Cor.		Obs.	Cor.			
Forearcs (continued)																	
Great Valley, Calif., west	*Colburn and Mooney* [1986]	5.00	8.00	5.75	6.00	7.00	6.70	6.87	7.00	7.20	7.38				27.00	70	1
Great Valley, Calif., central	*Holbrook and Mooney* [1987]	4.00	4.00	6.00	6.12	11.00	6.66	6.77	8.00	7.00	7.10				27.00	40	1
Diablo Range, Calif.	*MacGregor-Scott and Walter* [1988]		4.00	3.10	3.22	10.00	5.75	5.86	13.00	6.87	6.97				27.00	40	1
N. California	*Beaudoin et al.* [1994]	1.00	5.00	4.00	4.13	8.00	5.50	5.63	7.00	6.85	6.98				21.00	50	3
NE Japan	*Suyehiro and Nishizawa* [1994]	1.50	2.50	3.80	3.93	13.50	5.99	6.11	4.00	6.90	7.02				21.50	50	17
Mean		1.32	8.54	5.74	5.79	8.25	6.42	6.54	7.79	6.95	7.09				25.89		
Standard deviation		2.30	4.25	0.78	0.76	4.26	0.35	0.35	2.75	0.13	0.13				3.25		
N		8	14	14	14	12	12	12	14	14	14				14		
Active Rifts																	
Black Forest / Rheingraben	*Gajewski and Prodehl* [1987]		13.00	6.00	6.00				12.00	6.65	6.80				25.00	70	5,6
Rheingraben	*Zucca* [1984]		8.00	6.00	6.00				17.00	6.25	6.47				25.00	90	6
Kenya rift south	*Mechie et al.* [1994]	2.00	4.00	5.80	5.95	21.00	6.43	6.64	9.00	6.83	7.07				36.00	90	7
Kenya rift north	*Mechie et al.* [1994]	1.00	3.00	5.80	5.95	6.00	6.30	6.48	10.00	6.61	6.83				20.00	90	7
Salton Sea	*Fuis et al.* [1984]		13.00	6.00	6.00	1.00	6.90	7.11	6.00	7.35	7.58				20.00	90	3
Rio Grande rift	*Sinno et al.* [1986]		12.00	6.00	6.10	8.00	6.10	6.34	10.00	6.67	6.93				30.00	90	3
Dead Sea	*Ginzburg et al.* [1981]	3.00	15.00	6.20	6.40	10.00	6.60	6.84	5.00	7.20	7.43				33.00	80	?
Dead Sea, Jordan	*El-Isa et al.* [1987a, b]		19.00	6.15	6.31				8.00	6.60	6.81	5.00	7.30	7.52	32.00	80	?
Mean		0.75	10.88	5.99	6.09	5.75	6.47	6.68	9.63	6.77	6.99				27.63		
Standard deviation		1.16	5.49	0.14	0.17	7.34	0.30	0.30	3.74	0.35	0.36				5.66		
N		3	8	8	8	5	5	5	8	8	8				8		
Rifted Margins																	
W. Norway 9	*Mutter and Zehnder* [1988]		8.00	6.00	6.00	9.00	6.00	6.13	4.00	7.00	7.15				21.00	60	8
W. Norway 10	*Mutter and Zehnder* [1988]		13.00	6.00	6.00	4.00	6.50	6.65	3.00	7.50	7.60				20.00	60	8
Lofoten, Rost high	*Mjelde* [1992]		6.00	6.00	6.00	12.00	6.40	6.54	9.00	6.80	6.95				27.00	60	8
Lofoten, Voring plateau	*Mjelde* [1992]		10.00	6.00	6.00	2.50	6.40	6.56	2.50	6.80	6.97				15.00	60	8
Goban spur, E. Atlantic	*Horsefield et al.* [1993]	2.00	2.00	5.05	5.18	10.00	6.29	6.45	8.00	6.80	7.00				22.00	70	9
Bay of Biscay	*Ginzburg et al.* [1985]		9.00	6.00	6.00	6.00	6.00	6.15	6.00	6.50	6.66				21.00	60	8
Hatton Bank	*Morgan et al.* [1989]		6.00	6.00	6.00	10.00	6.50	6.65	9.00	7.00	7.23				25.00	70	9
Hatton Bank	*Morgan et al.* [1989]		7.00	6.00	6.00	3.00	6.85	7.00	11.00	7.26	7.43				21.00	70	9
Hatton Bank A	*Fowler et al.* [1989]		7.00	6.00	6.00	3.00	6.35	6.51	17.00	7.00	7.29				27.00	70	9
Hatton Bank C	*Fowler et al.* [1989]	2.50	2.00	6.00	6.00	3.00	6.75	6.92	3.00	7.25	7.41	14.00	7.50	7.67	24.50	70	9
Hatton Bank E	*Fowler et al.* [1989]		4.50	6.00	6.00	3.00	6.20	6.31	14.50	7.40	7.51				22.00	70	9

Carolina trough	*Holbrook et al.* [1994b]		8.00	6.00	6.00	2.00	6.30	6.45	24.00	6.65	6.83	34.00	70	9
Carolina trough	*Holbrook et al.* [1994b]		11.00	6.00	6.00	6.00	6.30	6.47	15.00	7.40	7.58	32.00	70	9
Carolina trough	*Tréhu et al.* [1989]		13.00	6.00	6.00	9.00	6.60	6.77	13.00	7.35	7.54	35.00	70	9
Virginia coast	*Holbrook et al.* [1994a]	8.00	10.00	6.50	6.66	4.00	6.70	6.88	11.00	7.50	7.69	33.00	70	9
Offshore Georgia	*Lizarralde et al.* [1994]	2.00	12.00	6.09	6.24	23.00	6.70	6.89	4.00	7.20	7.40	41.00	70	9
SE of Grand Banks, Newfoundland	*Reid* [1994]	2.00	1.00	5.05	5.18	21.00	6.13	6.29	4.00	6.74	6.93	28.00	70	9
Grand Banks	*Reid* [1993]		4.00	6.00	6.00	20.00	6.10	6.30	6.00	6.73	6.92	30.00	70	9
Jeanne d'Arc basin	*Reid and Keen* [1990]		28.00	6.00	6.00				7.00	6.73	6.91	35.00	70	9
Gulf coastal plain	*Lutter and Nowack* [1990]		11.00	6.00	6.00	5.00	6.20	6.31	12.00	6.85	6.94	28.00	40	3
Baltimore Canyon	*LASE* [1986]		8.00	6.00	6.00	11.00	6.05	6.22	9.00	7.25	7.43	28.00	70	9
E. Greenland 23	*Mutter and Zehnder* [1988]		8.00	6.00	6.00	7.00	7.00	7.15	7.00	7.50	7.68	22.00	70	9
E. Greenland 16	*Mutter and Zehnder* [1988]		13.00	6.00	6.00	3.00	6.50	6.67	4.00	7.00	7.17	20.00	70	9
SW Greenland	*Gohl and Smithson* [1993]	1.00	15.00	6.00	6.00	7.00	6.70	6.87	5.00	7.00	7.19	28.00	70	9
SW Greenland	*Chian and Louden* [1992]		5.00	6.00	6.00	10.00	6.33	6.46	14.00	6.75	6.88	29.00		10
Lincoln Sea, N. Greenland	*Forsyth et al.* [1994]	4.00	8.50	5.88	6.14	5.00	6.50	6.67	5.00	7.50	7.68	22.50	70	9
Red Sea	*Mechie et al.* [1986]		4.00	6.00	6.00	8.00	6.20	6.38	6.00	7.20	7.36	18.00	80	11
Red Sea, Egypt	*Gaulier et al.* [1988]		7.60	6.00	6.00	4.40	6.33	6.52	4.70	7.20	7.44	16.70	80	11
Red Sea, Sudan	*Egloff et al.* [1991]		6.00	6.00	6.00	3.00	5.95	6.11	5.00	6.60	6.78	14.00	80	11
Red Sea, Yemen	*Egloff et al.* [1991]		2.00	6.00	6.00	12.00	6.10	6.26	15.00	6.90	7.11	29.00	80	11
Mean		0.72	8.32	5.95	5.98	7.53	6.38	6.54	8.59	7.05	7.22	25.62		
Standard deviation		1.70	5.21	0.26	0.25	5.69	0.27	0.28	5.12	0.30	0.30	6.46		
N		7	30	30	30	29	29	29	30	30	30	30		
						Paleozoic Orogens								
Swabian Jura	*Gajewski et al.* [1987]		5.00	6.00	6.00	14.00	6.05	6.15	8.00	6.35	6.47	27.00	70	5,6
S. Germany (WF-Z1)	*Zeis et al.* [1990]		3.00	6.00	6.00	15.00	6.05	6.20	12.00	6.65	6.89	30.00	70	5,6
Rhenohercynian	*Aichroth et al.* [1992]		13.00	6.10	6.20				19.00	6.65	6.83	32.00	70	5,6
Saxothuringian	*Aichroth et al.* [1992]		21.00	6.10	6.20				8.00	6.80	6.98	29.00	70	5,6
Moldanubian	*Aichroth et al.* [1992]		23.00	6.00	6.15				10.00	6.70	6.89	33.00	70	5,6
N. German basin	*Aichroth et al.* [1992]		11.00	6.00	6.00	10.00	6.20	6.37	6.00	6.90	7.09	27.00	70	5,6
Ireland	*Jacob et al.* [1985]		10.00	6.20	6.30	13.00	6.50	6.67	8.00	6.90	7.09	31.00	70	6,8,12
Scotland	*Bamford et al.* [1978]		10.00	6.10	6.20	10.00	6.43	6.59	8.00	7.00	7.18	28.00	70	6,8,12
N. England	*Bott et al.* [1985]		4.00	6.00	6.00	24.00	6.48	6.63				28.00	70	6,8,12
Bay of Islands, Nfld.	*Marillier et al.* [1991]	4.00	20.00	6.40	6.51				15.00	7.20	7.35	39.00	60	9
Caledonians, Norway	*Iwasaki et al.* [1994a]	1.00	5.00	6.30	6.42	13.00	6.43	6.59	15.00	6.80	6.98	34.00	70	6,8,12
Appalachians–91-1A	*Marillier et al.* [1994]	4.00	15.00	6.33	6.45				16.00	6.68	6.82	35.00	60	9
Appalachians–91-1B	*Marillier et al.* [1994]	4.00	17.00	6.39	6.53				12.00	6.86	7.01	33.00	60	9
Appalachians–91-2	*Marillier et al.* [1994]	9.00	7.00	6.34	6.40	7.00	6.54	6.65	17.00	6.89	7.03	40.00	60	9
Maine 1	*Luetgert et al.* [1987]	1.00	5.00	6.00	6.10	20.00	6.30	6.42	10.00	6.70	6.81	36.00	53	3
Maine 2—SE	*Luetgert et al.* [1987]	1.00	5.00	6.00	6.12	15.00	6.30	6.42	17.00	7.00	7.11	38.00	53	3
Gander 1	*Hennet et al.* [1991]	1.00	11.00	6.05	6.18	13.00	6.40	6.52	15.00	6.80	6.91	40.00	53	3

TABLE 1. continued

Place	Reference	Fluff, km	Upper			Middle			Lower			Lowest			Moho	Heat Flow	
			Thickness, km	V_p, km s^{-1}		Thickness, km	V_p, km s^{-1}		Thickness, km	V_p, km s^{-1}		Thickness, km	V_p, km s^{-1}		Depth, km	Flow, mW m^{-2}	Reference[a]
				Obs.	Cor.		Obs.	Cor.		Obs.	Cor.		Obs.	Cor.			
Paleozoic Orogens (continued)																	
Gander 2	*Hennet et al.* [1991]	1.00	10.00	6.05	6.18	13.00	6.40	6.53	12.00	6.80	6.91				36.00	53	3
Avalon	*Luetgert and Mann* [1990]		8.00	6.30	6.40	12.00	6.50	6.62	14.00	6.75	6.86				34.00	53	3
Coastal Maine	*Zhu & Ebel* [1994]		10.00	6.03	6.16	10.00	6.40	6.52	12.00	6.70	6.81				32.00	53	3
Central Maine (HKM)	*Zhu & Ebel* [1994]		7.00	6.01	6.13	11.00	6.27	6.39	16.00	6.75	6.87				34.00	53	3
Central Maine (JKM)	*Zhu & Ebel* [1994]	1.00				15.00	6.40	6.53	22.00	6.95	7.06				38.00	53	3
New Hampshire	*Hughes and Luetgert* [1991]	2.00	9.00	6.10	6.20	12.00	6.45	6.57	17.00	6.85	6.96				40.00	53	3
New Hampshire	*Shalev et al.* [1991]		1.50	6.00	6.00	13.50	6.20	6.28	19.50	6.50	6.62				34.50	53	3
New Hampshire (WNH)	*Zhu and Ebel* [1994]		5.00	5.90	6.02	14.00	6.29	6.41	18.50	6.73	6.84				37.50	53	3
Vermont (IVT)	*Zhu and Ebel* [1994]		0.25	6.20	6.32	15.5	6.40	6.52	22.50	6.73	6.84				38.25	53	3
Valley and Ridge	*Prodehl et al.* [1984]		16.00	6.25	6.20	20.00	6.75	6.86	12.00	7.15	7.25				48.00	53	3
Atlantic coast, S. Carolina	*Luetgert et al.* [1994]	1.00	2.00	6.20	6.32	14.00	6.42	6.53	17.00	6.65	6.74				34.00	42	3
Lachlan	*Finlayson et al.* [1980]		10.00	6.00	6.00	23.00	6.40	6.60	11.00	7.20	7.49				44.00	90	13
Mean		1.20	9.42	6.12	6.20	12.11	6.37	6.50	13.43	6.81	6.95				34.84		
Standard deviation		2.08	5.98	0.14	0.16	6.40	0.16	0.16	5.05	0.19	0.21				5.04		
N		12	28	28	28	23	23	23	29	29	29				29		
Paleozoic Orogens: Europe Only																	
Mean			10.50	6.08	6.15	9.90	6.30	6.46	9.40	6.75	6.93				29.90		
Standard deviation			6.93	0.10	0.15	7.85	0.20	0.22	5.15	0.19	0.21				2.51		
N			10	10	10	7	7	7	9	9	9				10		
Paleozoic Orogens: Non-European																	
Mean		1.93	8.82	6.14	6.23	13.41	6.40	6.52	15.55	6.84	6.96				37.43		
Standard deviation		2.43	5.51	0.16	0.17	5.19	0.13	0.13	3.56	0.19	0.22				3.95		
N		11	18	18	18	16	16	16	19	19	19				19		
Cenozoic-Mesozoic Contractional Orogens																	
Canadian Fold and Thrust	*Kanasewich et al.* [1994]		20.00	6.00	6.10	10.00	6.50	6.65	20.00	7.15	7.29				50.00	60	1
Alps BC	*Yan and Mechie* [1989]	2.00	17.00	6.00	6.10	3.00	6.25	6.40	29.00	6.30	6.50				51.00	70	5,6
Alps CD	*Yan and Mechie* [1989]	3.00	17.00	6.00	6.10	4.00			25.00	6.30	6.50				49.00	70	5,6
Alps DE	*Yan and Mechie* [1989]	3.00	17.00	6.10	6.30	3.00			28.00	6.40	6.60				51.00	70	5,6
S. Alps	*Yan and Mechie* [1989]		20.00	6.10	6.20	15.00	6.40	6.60	7.00	7.10	7.30				42.00	70	5,6
S. Alps, Italy	*Deichmann et al.* [1986]		11.00			24.00	6.32	6.51	7.00	7.10	7.29				42.00	70	5,6
Lhasa block, Tibet	*Sapin et al.* [1985]	4.00	9.00			10.00	6.16	6.40	41.00	6.50	6.79	14.00	7.50	7.80	78.00	90	14
Himalaya, S. Lhasa block	*Sapin et al.* [1985]	3.00	15.00			14.00	6.30	6.56	32.00	6.70	6.99	10.00	6.10	6.41	74.00	90	14
Yunnan, E. Himalaya SE	*Kan et al.* [1986]	1.25	13.75			20.00	6.33	6.50	11.30	6.68	6.86				46.30	70	15
Yunnan, E. Himalaya NW	*Kan et al.* [1986]	1.25	19.25			11.00	6.28	6.44	9.50	6.83	7.01				41.00	70	15

Mean		1.75	15.90	6.04	6.16	11.40	6.32	6.51	20.98	6.71	6.91	2.40	6.80	7.11	52.43		
Standard deviation		1.47	3.73	0.05	0.09	7.09	0.10	0.09	11.88	0.33	0.32	5.15	0.99	0.98	13.02		
N		7	5	5	5	8	8	8	10	10	10	2	2	2	10		
							Shields and Platforms										
Kapuskasing (A)	*Boland and Ellis* [1989]		12.00	6.00	6.00	15.00	6.55	6.65	12.00	7.13	7.21	4.00	7.50	7.55	43.00	43	9
E. Superior (A)	*Epili and Mereu* [1991]		2.00	6.00	6.00	15.00	6.20	6.30	16.00	6.75	6.84				33.00	43	9
W. Superior (A)	*Morel-à-l'Huissier et al.* [1987]	1.00	7.00	6.15	6.25	31.00	6.47	6.62	6.00	7.04	7.18				45.00	60	1
SVEKA, North region (A)	*Grad and Luosto* [1987], *Luosto and Korhonen*, [1986], *Luosto et al.* [1989]		10.00	6.00	6.00	7.00	6.30	6.40	8.00	6.63	6.72	30.00	7.18	7.17	55.00	40	6
Karelian (A)	*Luosto et al.* [1989]		10.00	6.10	6.20	17.00	6.58	6.67	20.00	7.10	7.16				47.00	40	6
Kola (A)	*Luosto et al.* [1989]		10.00	6.10	6.30	20.00	6.53	6.65	13.00	7.00	7.10				43.00	51	6
W. India (A)	*Kaila et al.* [1989]		10.00	6.30	6.40	18.00	6.50	6.61	15.00	6.80	6.88				43.00	44	16
Kola 2 (A)	*Azbel et al.* [1989]		10.00	6.20	6.30	32.00	6.60	6.70							42.00	51	6
Kola 3 (A)	*Azbel et al.* [1989]		15.00	6.25	6.40	19.00	6.60	6.75	9.00	7.00	7.10				43.00	51	6
Kaapvaal (A)	*Durrheim and Green* [1992]		7.00	6.00	6.00	10.00	6.20	6.32	15.00	6.60	6.72				32.00	47	7
Kalahari (A)	*Baier et al.* [1983]		17.00	6.45	6.60				30.00	6.90	7.00				47.00	47	7
Grenville–Adirondack (P)	*Hughes and Luetgert* [1992]		17.00	6.60	6.75				26.00	7.10	7.20				43.00	47	1,9
Grenville–Metasedimentary belt (P)	*Zelt and Forsyth* [1994]		7.00	6.31	6.43	19.00	6.60	6.71	18.00	7.21	7.29				44.00	47	1,9
E. Grenville (P)	*Marillier et al.* [1991]		5.00	6.00	6.00	10.00	6.35	6.47	30.00	6.70	6.81				45.00	47	1,9
Grenville, central gneiss (P)	*Mereu et al.* [1986]		8.00	6.30	6.40				32.00	6.65	6.75				40.00	47	9
Colorado plateau (P)	*Wolf and Cipar* [1993]		18.00	6.02	6.16	12.00	6.33	6.50	13.00	6.81	7.00	5.00	7.35	7.54	48.00	68	3
Churchill–Williston	*Kanasewich et al.* [1987]	5.00	15.00	6.20	6.30	15.00	6.50	6.68	10.00	7.10	7.29				45.00	70	9
Churchill–trans-Hudson (P)	*Morel-à-l'Huissier et al.* [1987]		10.00	6.20	6.30	18.00	6.60	6.70	16.00	7.19	7.38				44.00	70	9
Peace River Arch 2 (P)	*Zelt and Ellis* [1989]	4.00	16.00	6.10	6.25	12.00	6.55	6.73	8.00	7.10	7.29				40.00	70	9
Peace River Arch 1 (P)	*Halchuk and Mereu* [1990]	3.00	20.00	6.25	6.40	8.00	6.60	6.79	11.00	7.00	7.19				42.00	70	9
Svecokarelides, S (P)	*Grad and Luosto* [1987]	10.0	5.00	6.30	6.40	10.00	6.63	6.72	30.00	7.18	7.25				55.00	40	6
Svecokarelides, Rapikivi (P)	*Luosto et al.* [1990]		7.00	6.00	6.00	23.00	6.55	6.61	12.00	7.10	7.16				42.00	40	6
Baltic, Lapland (P)	*Luosto et al.* [1989]		12.00	6.05	6.20	18.00	6.52	6.62	12.00	6.85	6.91				42.00	40	6
SvecoNorwegian (P)	*EUGENO-S* [1988]		15.00	6.10	6.25				25.00	6.75	6.83				40.00	40	6
SvecoFennides (P)	*Clowes et al.* [1987]		10.00	6.15	6.30	25.00	6.65	6.74	12.00	7.50	7.55				47.00	40	6
SvecoFennides (P)	*Clowes et al.* [1987]		24.00	6.20	6.31				9.00	6.70	6.79				33.00	40	6
Ukaranian (P)	*Gutерch et al.* [1983]	3.00	19.00	6.45	6.55	13.00	6.75	6.83	9.00	7.30	7.35				44.00	40	6
Saudi Arabia (P)	*Mechie et al.* [1986], *Mooney et al.* [1985]		19.00	6.20	6.30	14.00	6.60	6.70	6.00	7.30	7.38				39.00	45	11
N. Australia 3 (P)	*Finlayson* [1982]		11.00	6.00	6.20	22.00	6.35	6.53	7.00	6.90	7.12	8.00	7.40	7.61	48.00	70	13
N. Australia 2 (P)	*Finlayson* [1982]		27.00	6.15	6.25	0.00			13.00	7.10	7.26	7.00	7.35	7.53	47.00	70	13

TABLE 1. continued

Place	Reference	Fluff, km	Upper			Middle			Lower			Lowest			Moho	Heat Flow	
			Thickness, km	V_p, km s^{-1}		Thickness, km	V_p, km s^{-1}		Thickness, km	V_p, km s^{-1}		Thickness, km	V_p, km s^{-1}		Depth, km	Flow, mW m^{-2}	Reference[a]
				Obs.	Cor.		Obs.	Cor.		Obs.	Cor.		Obs.	Cor.			
Shields and Platforms (continued)																	
Mean		0.90	12.50	6.17	6.27	13.43	6.50	6.63	14.77	6.98	7.09	1.80	7.36	7.48	43.37		
Standard deviation		2.21	5.86	0.15	0.19	8.97	0.14	0.14	8.23	0.32	0.23	5.74	0.12	0.18	5.19		
N		6	30	30	30	24	24	24	29	29	29	5	5	5	30		
Archean Shields																	
Mean		0.09	10.00	6.14	6.22	16.73	6.45	6.57	13.09	6.90	6.99	3.09	7.34	7.36	43.00		
Standard deviation		0.30	4.00	0.15	0.20	9.38	0.16	0.16	7.84	0.19	0.19	9.01	0.23	0.27	6.34		
N		1	11	11	11	10	10	10	11	10	10	11	2	2	11		
Proterozoic Shields																	
Mean		1.39	13.95	6.19	6.30	11.53	6.54	6.67	15.74	7.03	7.15	1.05	7.37	7.56	43.58		
Standard deviation		2.70	6.35	0.16	0.17	8.38	0.12	0.11	8.50	0.24	0.23	2.55	0.03	0.04	4.57		
N		5	19	19	19	14	14	14	19	19	19	3	3	3	19		

[a]Abbreviations are Obs., observed; Cor., corrected to room temperature and 600 MPa; *N*, number of profiles; A, Archean; and P, Proterozoic.

Heat flow references are 1, *Blackwell and Steele* [1991]; 2, *Lewis* [1991]; 3, *Morgan and Gosnold* [1989]; 4, *Nagao and Uyeda* [1989]; 5, *Chapman et al.* [1979]; 6, *Cermák* [1993]; 7, *Nyblade et al.* [1990]; 8, *Cermák* [1979]; 9, *Jessop* [1991]; 10, *Chian and Louden* [1992]; 11, *Gettings et al.* [1986]; 12, *Brock* [1989]; 13, *Cull* [1991]; 14, *Shen* [1991]; 15, *Huang and Wang* [1991]; 16, *Gupta et al.* [1991]; 17, *Okubo and Matsunaga* [1994].

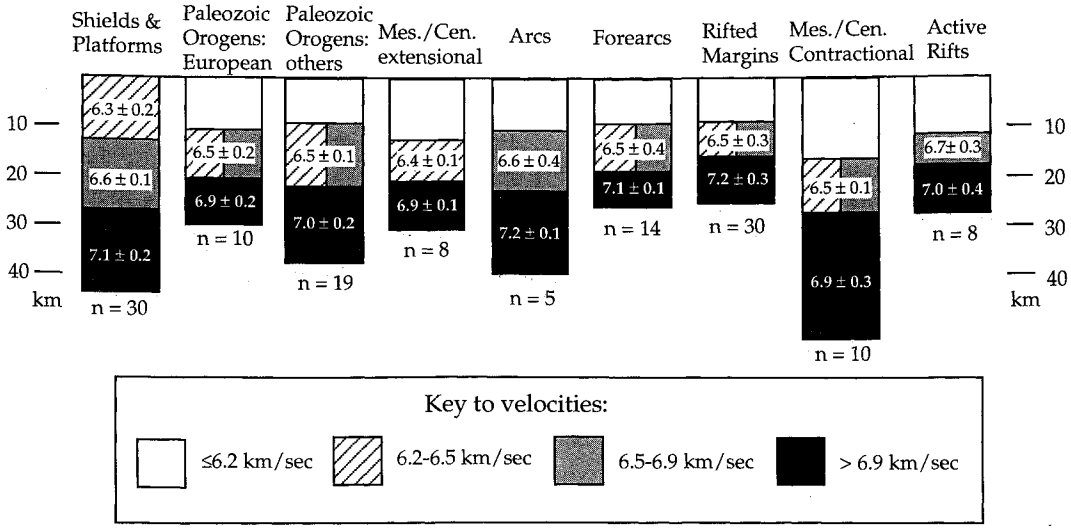

Figure 2. Type sections of continental crust. All velocities are reported at 600 MPa and room temperature; *n* is the number of profiles used to construct each type section.

similarity to those presented by *Mooney and Meissner* [1991] and *Holbrook et al.* [1992].

4. HEAT FLOW STUDIES

Heat flow (thermal conductivity times thermal gradient) through the continental crust is determined by measurement of the thermal gradient and conductivity in shallow boreholes. Values typically range from 30 to 100 mW m^{-2}, and mean values vary systematically depending upon tectonic province [see *Morgan*, 1984, and references therein]. Recognition of a linear relationship between surface heat flow and surface radiogenic heat production due to heat-producing elements (HPE; K, Th, and U) [e.g., *Roy et al.*, 1968] led to the view that heat production decreases with depth in the crust in an exponential, linear, or stepwise manner. However, various complex heat production models can satisfy the surface heat flow and heat production observations [*Fountain et al.*, 1987; *Jaupart*, 1983].

Whatever the exact distribution of heat-producing elements, the abundances observed at the Earth's surface cannot be maintained throughout the crustal column. If they were, all of the heat flow measured at the surface of the continents would be produced within the crust, leaving no heat input from the Earth's mantle, or possibly requiring a negative input from the mantle (i.e., the crustal abundances account for more heat flow than is observed). Thus K, Th, and U abundances must decrease with increasing depth in the crust, but the nature and cause of this decrease are debated.

Both changing composition and increase in metamorphic grade could account for the decrease of HPE with depth in the crust. Mafic granulites generally have lower HPE contents than metasedimentary or more

TABLE 2a. Average Properties of Middle Crust in Different Type Sections

Tectonic Province	*N*	*Thickness, km*	V_p, km s^{-1}	
			Observed	*Corrected*[a]
Cenozoic-Mesozoic extensional regions	8	8.0 ± 5.4	6.2 ± 0.1	6.4 ± 0.1
Continental arcs	5	13.1 ± 4.7	6.4 ± 0.4	6.6 ± 0.4
Forearcs	14	8.2 ± 4.3	6.4 ± 0.3	6.5 ± 0.4
Active rifts	8	5.8 ± 7.3	6.5 ± 0.3	6.7 ± 0.3
Rifted margins	30	7.5 ± 5.6	6.4 ± 0.3	6.5 ± 0.3
Paleozoic orogens	23	12.11 ± 6.4	6.4 ± 0.2	6.5 ± 0.2
Europe only	7	9.9 ± 7.8	6.3 ± 0.2	6.5 ± 0.2
Non-European	16	13.4 ± 5.2	6.4 ± 0.1	6.5 ± 0.1
Cenozoic-Mesozoic contractional orogens	8	11.4 ± 7.1	6.3 ± 0.1	6.5 ± 0.1
Shields and platforms	24	13.4 ± 9.0	6.5 ± 0.1	6.6 ± 0.1
Archean shields	10	16.7 ± 9.4	6.5 ± 0.2	6.6 ± 0.2
Proterozoic shields	14	11.5 ± 8.4	6.5 ± 0.1	6.7 ± 0.1

Values are given as averages ± 1 standard deviation. *N* is number of profiles.
[a]All velocities are corrected to room temperature and 600 MPa.

TABLE 2b. Average Properties of Lower Crust in Different Type Sections

Tectonic Province	N	Thickness, km	V_p, km s^{-1}		Moho Depth, km
			Observed	Corrected[a]	
Cenozoic-Mesozoic extensional regions	8	9.3 ± 1.7	6.7 ± 0.1	6.9 ± 0.1	31.1 ± 2.4
Continental arcs	5	17.6 ± 8.1	6.9 ± 0.1	7.2 ± 0.1	40.0 ± 5.9
Forearcs	14	7.8 ± 2.7	7.0 ± 0.1	7.1 ± 0.1	25.9 ± 3.2
Active rifts	8	9.6 ± 3.7	6.8 ± 0.4	7.0 ± 0.4	27.6 ± 5.7
Rifted margins	30	8.6 ± 5.1	7.0 ± 0.3	7.2 ± 0.3	25.6 ± 6.5
Paleozoic orogens	29	13.4 ± 5.0	6.8 ± 0.2	7.0 ± 0.2	34.8 ± 5.0
Europe only	10	9.4 ± 5.2	6.8 ± 0.2	6.9 ± 0.2	29.9 ± 2.5
Non-European	19	15.5 ± 3.5	6.8 ± 0.2	7.0 ± 0.2	37.4 ± 3.9
Cenozoic-Mesozoic contractional orogens	10	21.0 ± 12	6.7 ± 0.3	6.9 ± 0.3	52.4 ± 13
Shields and platforms	29	14.8 ± 8.2	7.0 ± 0.3	7.1 ± 0.2	43.4 ± 5.2
Archean	10	13.1 ± 7.8	6.9 ± 0.2	7.0 ± 0.2	43.0 ± 6.3
Proterozoic	19	15.7 ± 8.5	7.0 ± 0.2	7.2 ± 0.2	43.6 ± 4.6

Values are given as averages ±1 standard deviation. *N* is number of profiles.
[a]All velocities are corrected to room temperature and 600 MPa.

evolved meta-igneous granulites. In particular, mafic cumulates, which form the bulk of most lower crustal xenoliths, have very low HPE (median heat production of mafic granulite xenoliths is 0.06 μW m^{-3}). Thus if the lower crust is predominantly mafic (cumulates, restites, or simply metabasalts and metagabbros), it would have intrinsically low heat production. In addition, granulite facies metamorphism causes pervasive depletion of U ± Th due to loss of grain boundary fluids and breakdown of accessory phases at higher pressure *P* and temperature *T* [*Rudnick et al.*, 1985]; whether or not K is depleted by metamorphism is still debated [*Rudnick and Presper*, 1990]. So it is possible for HPE depletion due to metamorphism to occur without partial melt removal, hence without a significant change to the bulk composition of the crust. As an example of this, felsic granulites from the Scourian complex in Scotland record some of the lowest HPE concentrations in what are still evolved compositions [*Rudnick et al.*, 1985; *Sheraton et al.*, 1973].

A second observation from heat flow studies is that Archean cratons, and adjacent Proterozoic belts (within 400 km of Archean cratons), have significantly lower heat flow than post-Archean regions [*Morgan*, 1984, and references therein; *Nyblade and Pollack*, 1993]. This may be due to (1) a compositional difference between Archean and post-Archean crust, with the former having markedly lower K, Th, and U concentrations [*Morgan*, 1984; *Taylor and McLennan*, 1985] and (2) the presence of a thick lithospheric mantle beneath Archean cratons that effectively insulates the crust from asthenospheric mantle heat flow in these regions [*Jones*, 1988; *Nicolayson et al.*, 1981; *Nyblade and Pollack*, 1993].

The latter hypothesis is supported by the observation that cratonic mantle xenoliths lie on cooler geotherms (Siberia [*Boyd*, 1984]; Kaapvaal [*Finnerty and Boyd*, 1987]) than mantle xenoliths from post-Archean regions. *Nyblade and Pollack* [1993] calculate that 400 km of lithospheric mantle is required beneath the cratons to account for the difference in heat flow. Lesser thicknesses would require a compositional contrast between Archean and post-Archean crust. Thus although a compositional contrast between Archean and post-Archean crust is permitted by the heat flow data, it is not required to explain the differences in heat flow.

Because of the low and uniform heat flow in Archean provinces (40 ± 2 mW m^{-2}), we turn to these regions in order to evaluate the abundances and depth distribution of HPE in the continental crust. Heat production of Archean crust has been estimated for five regions where deeper crustal levels are exposed. These findings are summarized in Table 3.

1. The Vredefort dome, an upended section through 20 km of Archean crystalline rocks, is composed of granitic gneisses, with mafic rocks becoming more prominent in the lowermost part of the section [*Hart et al.*, 1981; *Nicolayson et al.*, 1981]. The crustal contribution to heat flow, estimated from the radiogenic heat production across the overlying Witwatersrand basin and Vredefort dome, is ~28 mW m^{-2}. The average observed heat flow in the basin is 51 ± 6 mW m^{-2} [*Jones*, 1988] implying a mantle heat flux of 12–22 mW m^{-2}.

2. In the Lewisian complex of NW Scotland, amphibolite facies and granulite facies gneisses consist of felsic meta-igneous rocks with subordinate mafic and ultramafic compositions and minor metasediments [*Weaver and Tarney*, 1980]. An Archean crustal section based on averages of these rock types has a heat production of 0.85 μW m^{-3} [*Weaver and Tarney*, 1984], corresponding to a crustal contribution to heat flow of 34 mW m^{-2}, assuming a 40 km thick crust and proportions of upper, middle and lower crust defined by *Weaver and Tarney* [1984]. For an average Archean heat flow (40 mW m^{-2}) the mantle contribution to heat flow would be only 6 mW m^{-2}. It should be noted, however, that the high crustal heat production in the

TABLE 3. Summary of Heat Production in Cross Sections of Archean Crust

	Reference[a]	Crustal Thickness, km	Exposure Depth, km	Surface Heat Flow, mW m^{-2}	Heat Flow Contribution, mW m^{-2}		Heat Flow From Crust, %
					Exposed Crust	Mantle (Estimated)	
Vredefort	1	36	20	51 ± 6	28	12–17[b]	67–76
Lewisian	2	40[c]	20[c]	40[c]	34	6	85
Kapuskasing	3	43	25	41	22	12–17[b]	58–70
Pikwitonei	4	40[c]	30	41	19	18–21[b]	50–57
S. Norway	5	28	?	21	11	10	52

[a]References are 1, *Nicolayson et al.* [1981]; 2, *Weaver and Tarney* [1984]; 3, *Ashwal et al.* [1987]; 4, *Fountain et al.* [1987]; 5, *Pinet and Jaupart* [1987].
[b]Range represents two assumptions about the heat production of the unexposed lowermost crust. The upper estimate assumes that unexposed crust has heat production equal to that of mafic granulites; the lower estimate assumes a mixture of mafic and HPE-depleted felsic granulites.
[c]Estimated.

Weaver and Tarney model results not from the felsic granulites (which have a very low heat production of 0.12 μW m^{-3}, due to their strongly depleted characteristics), but from the relatively thick upper crustal layer (fully one third of the crust), which has a high heat production (3.25 μW m^{-3}).

3. In the Kapuskasing structural zone (KSZ) a 25-km-thick crustal cross section is composed of greenstone metasedimentary and volcanic rocks in the upper crust (Michipocoten greenstone belt), tonalitic amphibolite facies gneisses in the middle crust, and tonalitic, mafic, and anorthositic granulite facies rocks in the lower crust. Heat flow from the exposed crustal section is 22 mW m^{-2} [*Ashwal et al.*, 1987], yielding a mantle heat flux of 12–18 mW m^{-2} (depending upon the composition of the remaining unexposed crust) and using an average heat flow of 41 mW m^{-2} [*Pinet et al.*, 1991].

4. The Pikwitonei subprovince, northern Superior province, Manitoba, exposes a crustal section ~30 km thick. The upper to middle crust (God's Lake subprovince) is composed of greenstone belts surrounded by felsic gneisses and granitic batholiths, which grade into deeper crust that is dominated by granulite facies tonalitic gneisses and lesser amounts of mafic gneisses, quartzites, trondhjemites, and anorthosites. Heat production in the upper 10 km of crust is highly variable but averages around 0.9 μW m^{-3} [*Fountain et al.*, 1987]. The middle crust is characterized by lower and less variable heat production, averaging 0.6 μW m^{-3}, and the heat production of the lower crust is low and uniform at 0.4 μW m^{-3}. Heat flow from the exposed crustal section is 19 mW m^{-2}, with the mantle heat flow lying between 18 and 21 mW m^{-2} for a 40-km-thick crust (again, depending upon the composition of the unexposed lowermost crust).

5. A section through the deep crust in southern Norway has a heat production of 1.6 μW m^{-3} for amphibolite facies assemblages and 0.4 μW m^{-3} for granulites, the latter containing significant proportions of mafic rocks [*Pinet and Jaupart*, 1987]. The crustal component of heat flow was estimated to be 75% of the regional heat flow, with a mantle heat flow of only 10 mW m^{-2}.

In summary, these observations from Archean crustal sections show that although HPE decrease with depth in the crust, the middle crust may contain significant abundances of HPE. Moreover, radiogenic heat production within the crust accounts for 50–85% of the surface heat flow in Archean regions.

Recent studies in Archean regions have shown that reduced heat flow (the intercept of the linear relationship between surface heat production and heat flow) is higher than the estimated mantle heat flux in shield regions [*Furlong and Chapman*, 1987; *Pinet and Jaupart*, 1987]. This has been attributed to the effects of lateral heterogeneities within the crust that may lead to underestimation of the amount of HPE in the deep crust. The studies of crustal profiles discussed above all estimate mantle heat flux between 6 and 20 mW m^{-2} (or 15–50% of total heat flux), which is in contrast to earlier models that suggested a uniform mantle heat flow of 28 mW m^{-2} [*Vitorello and Pollack*, 1980] irrespective of crustal age. Most of these profiles show increasing proportions of mafic rocks in the lowermost crust, suggesting that lithologic changes, as well as metamorphic depletions, are responsible for the decrease of HPE with depth. It is also apparent that many granulite facies terrains contain large amounts of felsic granulites and have very low heat production (0.4 mW m^{-2} is typical). Thus the low heat flow of Archean cratons cannot be used to infer large proportions (up to 2/3) of mafic lithologies in the crust [cf. *Taylor and McLennan*, 1985]. The heat flow data are consistent with the presence of significant volumes of intermediate and felsic granulites in the middle and lower crust.

5. GRANULITES

Granulites form under high temperature and pressure conditions within the Earth's continental crust.

For this reason, they are widely believed to be the dominant rock type in the lower continental crust, and studies of granulites allow inferences to be made regarding lower crustal composition and physical properties.

Granulites that equilibrated at lower crustal *P-T* conditions are available from two main sources: (1) surface outcrops (terrains), covering areas of hundreds to thousands of square kilometers, and (2) xenoliths, or small rock fragments carried rapidly to the Earth's surface in magmas. The large compositional contrast between these two possible lower crustal sample suites is the fundamental problem encountered in determining a robust estimate of the composition of the bulk lower crust. *Rudnick* [1992] and *Rudnick and Presper* [1990] reviewed many of the chemical and physical properties of these rocks, and the interested reader is referred to these papers. Below we summarize the main features of each type of granulite, incorporating recent data from the literature, and attempt to put these rocks into the context of the lower crust.

5.1. Terrains

Major questions in relating granulite facies terrains to the present-day lower crust are (1) why are they no longer in the lower crust, and (2) by what means were they uplifted? Both these questions relate to the larger question of whether the rocks found in granulite terrains represent actual sections of lower crust or were merely lower crustal transients, passing through high pressure-temperature conditions on their return trip to the surface, such as may occur during a continent-continent collision. Additional questions pertaining to both terrains and xenoliths are what pressures (hence depths) did they equilibrate at, and is there a systematic depth difference between the two [e.g., *Bohlen and Mezger*, 1989]? These latter questions will be addressed in section 5.2.

In order to answer the first set of questions posed above, investigators attempt to define the pressure-temperature-time (*P-T-t*) path followed by granulites during their evolution. To date, the temporal constraints on *P-T* paths have been determined for only a few terrains [see *Mezger*, 1992]; thus we will confine our discussion to *P-T* paths and their possible interpretations. Different tectonic settings may give rise to different *P-T* paths, and although a particular *P-T* path is not necessarily unique to a given tectonic setting, certain generalizations can be made [*Bohlen*, 1991; *Harley*, 1989]. Granulites that cooled at lower crustal depths (isobaric cooling) are regarded as products of magmatic underplating [*Bohlen*, 1991; *Bohlen and Mezger*, 1989; *Mezger*, 1992; *Wells*, 1980], although more complicated scenarios have been suggested [*Harley*, 1989, Figure 14]. In these models, uplift of granulites to the Earth's surface results from tectonic processes unrelated to their formation, and the presence of supracrustal rocks in the terrains is not accounted for (they presumably were tectonically emplaced into the deep crust during an earlier event, such as tectonic burial at convergent plate margins [*von Huene and Scholl*, 1991]). In contrast, isothermal decompression is generally considered to result from double thickening of continental crust [*Harley*, 1989; *Newton and Perkins*, 1982], with the granulites beginning and ending their travels at the Earth's surface. This model accounts for both the presence of supracrustal assemblages and the occurrence of the granulites presently at the Earth's surface.

Most of the *P-T* paths for granulite terrains reviewed by *Harley* [1989] record isothermal decompression, and therefore these rocks may not be truly representative of the lower crust. Yet a significant proportion, about 35%, record isobaric cooling and therefore may have resided for long time periods in the lower crust. Geochronologic constraints, where available, support long-term residence of these terrains in the deep crust (e.g., Enderby Land, Pikwitonei, Adirondacks [see *Mezger*, 1992], and references therein).

These different terrains show an apparent difference in their overall compositions (Figure 3). Those experiencing isothermal decompression are dominated by felsic compositions, whereas those that have cooled isobarically have a significantly larger component of mafic lithologies, resulting in a bimodal distribution of rock types. The higher proportion of mafic lithologies in granulite terrains that represent deep crustal sections is consistent with an increasingly more mafic crust with depth.

5.2. Xenoliths

It is well established that mafic lithologies predominate in granulite xenolith populations (Figure 3). Several questions arise from this contrast with granulite terrains. (1) Are granulite facies xenoliths representative of the lower crust? They may not be representative if they are simply deep-seated manifestations of the volcanism that transports them to the surface. Related to this, are felsic xenoliths underrepresented in xenolith populations because of their dissolution in the host basalt? (2) How do xenoliths relate to isobarically cooled granulite terrains? Do they represent different crustal levels?

Mafic granulite xenoliths could be related to the host volcanism in two ways: (1) they could be cognate inclusions (i.e., cumulates of the magmas that carry them), or (2) they could represent earlier pulses of the basaltic magmatism that intruded the lower crust and equilibrated there. The metamorphic textures and minerals found in the majority of mafic granulite xenoliths preclude the cognate inclusion hypothesis. The second alternative is less easily evaluated: basaltic provinces typically have lifetimes spanning several millions of years [e.g., *Duncan and McDougall*, 1989], so the earliest intrusions in the deep crust have sufficient time to reequilibrate under the generally hot conditions

prevalent there. Determining xenolith ages is therefore crucial in evaluating the second possibility (see *Rudnick* [1992] and *Hanchar and Rudnick* [1995] for a discussion of dating techniques and problems encountered in dating lower crustal xenoliths).

Comparison between age of earliest volcanic activity versus ages of the xenoliths (where they have been established) shows that most mafic xenoliths are not related to their host basalts (Figure 4). Because mafic xenoliths are generally interpreted to have formed by basaltic underplating of the crust [*Rudnick*, 1992], these results demonstrate that basaltic underplating is a recurrent process and thus may be an important means by which the crust grows [*Bohlen and Mezger*, 1989]. Moreover, geochronological studies have established that episodes of basaltic underplating correlate with major regional geologic events [e.g., *Rudnick and Williams*, 1987; *Chen et al.*, 1994], so we consider it unlikely that significant underplating occurs without manifestation at the Earth's surface (e.g., volcanism or tectonism).

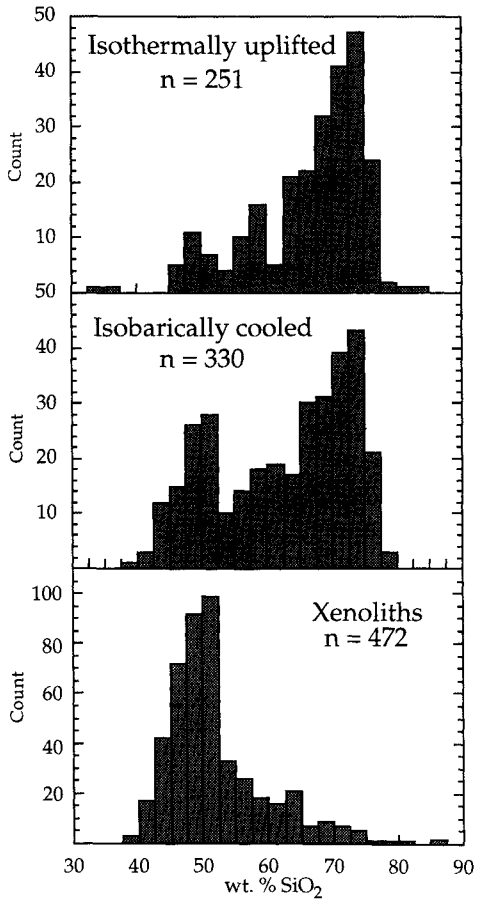

Figure 3. SiO_2 histogram for isothermally uplifted granulite terrains (Limpopo, southern Africa; southern India; Prydz Bay, Antarctica; Rayner complex, Antarctica; Musgrave Ranges, Australia), isobarically cooled granulite terrains (Pikwitonei, Canada; Scourian, Scotland; Napier complex, Antarctica; Furura complex, Tanzania; Ivrea zone, Italy; Adirondack Mountains, U.S.A.), and granulite xenoliths. Geochemistry compiled by *Rudnick and Presper* [1990]; *P-T* paths compiled by *Harley* [1989].

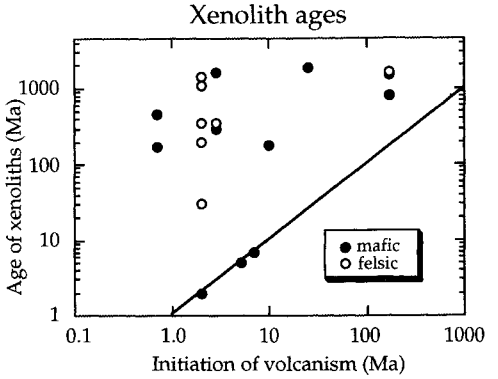

Figure 4. Timing of earliest volcanism associated with host pipe compared to ages of granulite facies xenoliths from these pipes. Age data are as summarized by *Rudnick* [1992], with newer additions from *Wendlandt et al.* [1993] and *Chen et al.* [1994].

Another concern is whether felsic rocks are underrepresented in xenolith suites as a result of their dissolution in the host basalts. Thermal diffusion is very rapid, so even though transport times are short (estimated to be a few hours based on entrainment of dense peridotites [*Spera*, 1980] and fluid dynamical calculations of dike propagation speeds [*Lister and Kerr*, 1991]), most xenoliths will be heated above their solidi, and in some cases liquidi, during transport from the lower crust [*Tsuchiyama*, 1986]. Recent calculations suggest, however, that the degree of dissolution of xenoliths is limited by the diffusion rate of the chemical components, such that minerals >100 μm in diameter within xenoliths will survive transport in basaltic magmas over the short period between entrainment and eruption [*Kerr*, 1995]. We conclude that felsic xenoliths sampled from the lower crust will survive transport by rapidly moving basaltic melts if the lower crust is below its solidus at the time of xenolith entrainment. If the lower crust is instead partially molten, transport of these materials could lead to their disaggregation.

Given that most mafic xenoliths are older than their host volcanics, how do they relate to the isobarically cooled granulite terrains, which contain significantly greater amounts of felsic components? *Bohlen and Mezger* [1989] suggested, on the basis of equilibration pressures, that these two types of granulites are samples of different levels of the crust: isobarically cooled granulite terrains equilibrated at middle to lower-middle crustal levels (0.6 to 0.8 GPa), whereas xenoliths represent the lowermost crust (1.0 to 1.5 GPa). More recent reviews of granulite terrains suggest that many have equilibrated at high pressures, similar to those derived from granulite xenoliths [*Harley*, 1989, 1992]. Moreover, pressures may be calculated only for xenoliths that contain garnet, so it is likely that garnet-free

mafic xenoliths equilibrated at pressures below 1.0–1.5 GPa (e.g., garnet-free mafic granulite xenoliths from northern Mexico are estimated to have equilibrated at <0.72 GPa [*Cameron et al.*, 1992]). Thus it is not possible, on the basis of geobarometry, to distinguish differences in derivation depths between terrains and xenoliths.

The geophysical constraints discussed above, however, lend support to a chemically stratified crust. Seismic velocities increase with depth and typically reach 6.9 km s^{-1} or greater, typical of mafic granulites (see below), at 20–30 km depth in the crust. Likewise, heat production must decrease with depth in the crust, although it is not clear whether the requisite decrease can be accomplished strictly by depletion of HPE due to high-grade metamorphism, or whether mafic lithologies become more abundant with depth. Thus the model of a stratified crust put forward by *Bohlen and Mezger* [1989] is an attractive one, if not entirely supported by their original arguments.

6. TOWARD A BULK DEEP CRUST COMPOSITION

Given the diversity of rock types in granulite facies terrains, the large compositional contrast between terrains and xenoliths, and the nonunique interpretation of seismic data in terms of rock type, it is not surprising that the composition of the lower crust, hence bulk crust, is difficult to quantify. In this section we utilize the existing seismic, heat flow, and geochemical data in order to estimate lower, middle, and total crust compositions. Using the type sections derived above, we assign rock types to match the observed velocities, based on ultrasonic measurements in lower crustal rock types. Utilizing the granulite geochemical database of *Rudnick and Presper* [1990], we obtain an average chemical composition for each layer as well as the whole crust for each type section. We then assign each type section an areal extent based on previous geochronological and tectonic studies and use this, in conjunction with the average crustal thickness of each section, to calculate volumes. From this we calculate the average composition of the lower, middle, and total continental crust.

6.1. Linking Velocity to Lithology: The Laboratory Data Set

In order to interpret the seismic sections in terms of rock type, we need to know the seismic velocities of the different rock types that may exist in the deep crust. *P* and *S* wave velocities for appropriate rock types have been determined by either laboratory ultrasonic measurements [e.g., *Christensen and Fountain*, 1975] or calculations from modal analyses and single-crystal elastic properties [e.g., *Jackson et al.*, 1990]. We compiled the available V_p and V_s data for possible deep crustal and upper mantle rock types and summarize their average properties in Table 4 (a full compilation is available from the authors). Metamorphic rocks of apparent igneous origin in this compilation are grouped by rock composition following the International Union of Geological Sciences (IUGS) scheme for igneous rocks [*Le Bas and Streckeisen*, 1991], where felsic rocks have >63 wt. % SiO_2, intermediate rocks have 52–63 wt. % SiO_2, and mafic rocks have 45–52 wt. % SiO_2. Pelitic rocks are metamorphosed shales, having high Al_2O_3 contents and SiO_2 generally between 55 and 66 wt. %. The pelitic rocks have been further subdivided into two groups: those for which muscovite and biotite are absent or nearly absent ("granulite facies") and those in which biotite and muscovite are abundant phases ("amphibolite facies"). The former are interpreted as residues (restites) of partial melting of pelitic rocks in the lower crust.

The summary in Table 4 includes only laboratory measurements made in at least three orthogonal directions for dry, unaltered samples where confining pressures of 0.6 GPa or greater were attained, assuring complete or near-complete crack closure. In some cases we reclassified samples in a manner different from that of the original investigators based on the reported mineralogy and/or chemical composition in order to be consistent with the categorization described above. Because of the limited number of measurements made on intermediate composition granulite facies rocks, we also include calculated time average *P* wave velocities determined by the Voigt-Reuss-Hill (VRH) method using modal mineralogies reported by *Lambert* [1967] and *Coolen* [1980]. Velocities calculated with the VRH method generally agree with measured values [*Dhaliwal and Graham*, 1991], provided that the rocks are unaltered and contain no glass or decompression features, as some xenolith samples do [*Parsons et al.*, 1995; *Rudnick and Jackson*, 1995]. We believe the latter features are not representative of in situ lower crust, so these xenolith data are not included in our compilation. All mean values in Table 4 are reported at 0.6 GPa and room temperature, the same common reference used for the seismic refraction tabulation.

The resulting mean values in this compilation differ in several ways from results in previous compilations [e.g., *Holbrook et al.*, 1992], perhaps because of the restrictive criteria we used for sample selection. In general, the range of velocities for each category is narrower, and for some categories the average velocities are slightly different. For example, *Holbrook et al.* [1992] report an average V_p of 7.08 ± 0.27 km s^{-1} for mafic granulite facies rocks (this value is derived by subtracting out the temperature correction Holbrook et al. applied to their average velocities in their Table 1–3), whereas we obtain 7.23 ± 0.18 km s^{-1} (both given at 600 MPa and room temperature). Our values compare favorably with those determined for

TABLE 4. Average Properties of Lower and Middle Crustal Rocks at 600 MPa and Room Temperature

	All Samples			*Samples for Which V_s Is Available*					
	Density, g cm^{-3}	*V_p, km s^{-1}*	*SiO_2, wt. %*	*Density, g cm^{-3}*	*V_p, km s^{-1}*	*V_s, km s^{-1}*	*Poisson's Ratio*	*SiO_2, wt. %*	*References*[a]
				Amphibolite Facies					
Felsic gneisses									
Mean	2.690	6.355	70.34	2.733	6.329	3.633	0.254	69.88	2,3,4,6,7,9,
Standard deviation	0.065	0.145	3.22	0.063	0.146	0.104	0.016	2.81	10,11,12,13,
Minimum	2.570	6.060	63.23	2.654	6.060	3.470	0.215	64.10	16,18,27,35,
Maximum	2.857	6.630	77.84	2.857	6.554	3.837	0.281	74.40	36
N	59	59	49	17	17	17	17	13	
Pelitic gneisses									
Mean	2.801	6.477	64.78	2.799	6.506	3.638	0.271	63.77	1,2,7,9,12,
Standard deviation	0.090	0.195	5.38	0.075	0.132	0.136	0.023	4.65	13,14,15,27
Minimum	2.645	6.050	55.40	2.645	6.295	3.363	0.233	55.40	
Maximum	3.058	6.868	76.74	3.002	6.782	3.893	0.312	71.50	
N	35	36	30	15	15	15	15	13	
Mafic gneisses									
Mean	3.028	7.018	48.61	3.043	7.039	3.964	0.267	48.55	1,2,3,4,7,10,
Standard deviation	0.050	0.169	1.75	0.053	0.170	0.154	0.016	1.69	12,13,15,16,
Minimum	2.939	6.720	45.91	2.968	6.738	3.717	0.241	46.23	17,18,23,27,
Maximum	3.120	7.310	52.39	3.120	7.310	4.270	0.304	51.87	31,35
N	24	24	17	12	12	12	12	12	
				Granulite Facies					
Felsic									
Mean	2.706	6.529	68.46	2.718	6.526	3.714	0.260	67.52	3,4,5,6,7,16,
Standard deviation	0.057	0.108	2.93	0.065	0.125	0.088	0.015	2.98	18,19,20,34,
Minimum	2.619	6.289	63.01	2.619	6.289	3.563	0.238	63.01	35
Maximum	2.816	6.870	74.20	2.816	6.870	3.860	0.284	74.20	
N	26	26	20	15	15	15	15	12	
Intermediate: measured									
Mean	2.859	6.727	57.40	2.836	6.661	3.626	0.288	57.56	3,5,6,18,19,
Standard deviation	0.095	0.185	3.73	0.086	0.122	0.151	0.026	3.85	20
Minimum	2.738	6.536	35.32	2.728	6.536	3.434	0.242	53.32	
Maximum	3.020	7.140	62.19	2.992	6.901	3.840	0.322	62.19	
N	9	9	6	7	7	7	7	7	
Intermediate: calculated, VRH time-average									
Mean	2.909	6.657	57.25	2.909	6.657	3.767	0.264	57.25	
Standard deviation	0.090	0.203	3.62	0.090	0.203	0.124	0.014	3.62	
Minimum	2.706	6.035	50.27	2.706	6.035	3.477	0.237	50.27	
Maximum	3.139	7.002	63.57	3.139	7.002	3.998	0.283	63.57	
N	26	26	22	26	26	26	26	22	
Pelitic gneisses									
Mean	3.007	7.091	55.06	3.038	7.069	3.980	0.264	54.37	1,2,5,6,14,
Standard deviation	0.108	0.345	6.29	0.108	0.337	0.125	0.022	6.34	16,21,35
Minimum	2.781	6.417	45.38	2.781	6.417	3.766	0.226	45.38	
Maximum	3.240	7.742	66.56	3.240	7.742	4.297	0.302	66.56	
N	19	19	20	13	13	13	13	13	
Mafic: all									
Mean	3.038	7.226	47.85	3.031	7.209	3.970	0.282	47.74	1,2,3,4,17,
Standard deviation	0.091	0.181	1.97	0.096	0.189	0.127	0.014	1.91	18,19,20,
Minimum	2.899	6.787	43.88	2.899	6.787	3.721	0.243	43.88	26,34
Maximum	3.279	7.500	52.70	3.279	7.500	4.221	0.302	51.99	
N	33	33	27	27	27	27	27	21	
Mafic: garnet-bearing									
Mean	3.099	7.326	48.09	3.113	7.328	4.049	0.280	47.80	1,2,3,4,17,
Standard deviation	0.085	0.136	2.09	0.097	0.152	0.108	0.013	1.95	20,26
Minimum	3.001	7.030	43.88	3.001	7.030	3.838	0.263	43.88	
Maximum	3.279	7.500	52.70	3.279	7.500	4.221	0.302	50.05	
N	12	12	12	7	7	7	7	7	
Mafic: garnet-free									
Mean	3.003	7.169	47.67	3.002	7.167	3.943	0.283	47.71	1,2,4,17,19,
Standard deviation	0.075	0.179	1.84	0.077	0.183	0.121	0.014	1.89	20,34
Minimum	2.899	6.787	45.20	2.899	6.787	3.721	0.243	45.20	
Maximum	3.120	7.450	51.99	3.120	7.450	4.154	0.301	51.99	
N	21	21	15	20	20	20	20	20	

TABLE 4. Continued

	All Samples			*Samples for Which V_s Is Available*					
	Density, g cm^{-3}	*V_p, km s^{-1}*	*SiO_2, wt. %*	*Density, g cm^{-3}*	*V_p, km s^{-1}*	*V_s, km s^{-1}*	*Poisson's Ratio*	*SiO_2, wt. %*	*References*[a]
				Granulite facies (continued)					
Anorthosites: all									
Mean	2.798	7.108	52.28	2.752	6.949	3.728	0.298	53.69	3,7,8,18,20,
Standard deviation	0.098	0.241	1.72	0.036	0.047	0.047	0.009	0.84	22,34
Minimum	2.707	6.810	48.32	2.707	6.888	3.666	0.286	52.52	
Maximum	3.058	7.548	54.42	2.785	7.033	3.801	0.313	54.45	
N	14	14	10	5	5	5	5	3	
Anorthosites: garnet-bearing									
Mean	2.893	7.405	51.94						22
Standard deviation	0.096	0.107	0.81						
Minimum	2.789	7.257	50.86						
Maximum	3.058	7.548	53.22						
N	5	5	5						
Anorthosites: garnet-free									
Mean	2.743	6.944	52.63	2.752	6.949	3.728	0.298	53.69	3,7,8,18,20,
Standard deviation	0.033	0.088	2.24	0.036	0.047	0.047	0.009	0.84	34
Minimum	2.707	6.810	48.33	2.707	6.888	3.666	0.286	52.52	
Maximum	2.785	7.120	54.45	2.785	7.033	3.801	0.313	54.45	
N	9	9	5	5	5	5	5	4	
				Upper Mantle					
Eclogites									
Mean	3.432	8.095	47.35	3.445	8.127	4.583	0.266	47.26	7,16,20,23,
Standard deviation	0.108	0.226	2.09	0.096	0.205	0.151	0.018	2.00	25
Minimum	3.235	7.714	44.52	3.270	7.836	4.277	0.236	44.63	
Maximum	3.585	8.582	51.68	3.585	8.582	4.817	0.288	50.24	
N	24	24	18	12	12	12	12	12	
Ultramafic rocks									
Mean	3.290	8.199	42.60	3.297	8.185	4.681	0.256	42.75	1,2,7,17,24,
Standard deviation	0.028	0.198	2.81	0.026	0.196	0.127	0.021	2.77	27,28,29,30,
Minimum	3.239	7.802	38.40	3.246	7.889	4.430	0.205	39.5	32,33,37
Maximum	3.369	8.590	47.95	3.335	8.590	4.890	0.288	47.95	
N	41	41	12	14	14	14	14	7	

Abbreviations are *N*, number of samples; VRH, Voight-Reuss-Hill.

[a]References are 1, *Fountain* [1976]; 2, *Burke and Fountain* [1990]; 3, *Fountain et al.* [1990]; 4, D. M. Fountain and M. H. Salisbury (manuscript in preparation, 1995); 5, *Kern and Schenk* [1985]; 6, *Kern and Schenk* [1988]; 7, *Birch* [1960]; 8, *Birch* [1961]; 9, *Hughes et al.* [1993]; 10, *McDonough and Fountain* [1988]; 11, *McDonough and Fountain* [1993]; 12, *Christensen* [1965]; 13, *Christensen* [1966b]; 14, *Burlini and Fountain* [1993]; 15, *Padovani et al.* [1982]; 16, *Kern and Richter* [1981]; 17, *Miller and Christensen* [1994]; 18, *Salisbury and Fountain* [1994]; 19, *Christensen and Fountain* [1975]; 20, *Manghnani et al.* [1974]; 21, *Reid et al.* [1989]; 22, *Fountain et al.* 1994a; 23, *Simmons* [1964]; 24, *Christensen* [1974]; 25, *Kumazawa et al.* [1971]; 26, *Fountain et al.* [1994b]; 27, *Kern and Tubia* [1993]; 28, *Christensen and Ramananantoandro* [1971]; 29, *Christensen* [1971]; 30, *Christensen* [1966a]; 31, *Siegesmund et al.* [1989]; 32, *Peselnick and Nicolas* [1978]; 33, *Babuška* [1972]; 34, *Fountain* [1974]; 35, *Kern et al.* [1993]; 36, *Mooney and Christensen* [1994]; 37, *O'Reilly et al.* [1990].

felsic granulite and amphibolite facies rocks by *Christensen and Mooney* [1995]; however, our mafic granulite velocities are slightly higher than theirs, although still within the 1 σ limits (e.g., 7.17 ± 0.18 versus 6.94 ± 0.18 km s^{-1} for garnet-free and 7.33 ± 0.14 versus 7.23 ± 0.18 km s^{-1} for garnet-bearing mafic granulites). The discrepancy for garnet-bearing samples may be due to a difference in the average modal garnet content of the small population in Table 4 (N = 12) compared with Christensen and Mooney's (N = 90). The reason for the discrepancy in garnet-free samples is more difficult to determine. However, because the main phases of mafic granulites have high P wave velocities (e.g., 6.6–7.0 km s^{-1} in plagioclase, 7.7–8.0 km s^{-1} in pyroxenes), we believe the higher average P wave values are correct.

We observe the widely reported trend that seismic velocity increases with rock density for crustal and upper mantle rocks (Figure 5) but the distribution of data, in detail, does not follow well-defined linear trends reported in earlier studies [e.g., *Birch*, 1961]. The data cluster in regions around a mean velocity and density for each lithology and are not dispersed along linear arrays for rocks of the same mean atomic weight as anticipated by *Birch* [1961]. There is some overlap between the groupings, but the concentrations at particular mean values are strong. The calculated values for the intermediate rocks are not shown in this diagram but would fill the gap between the felsic and mafic rocks. The various fields for metapelitic rocks overlap the felsic, intermediate, and mafic rocks.

Our analysis (Figure 5) lends support to the idea

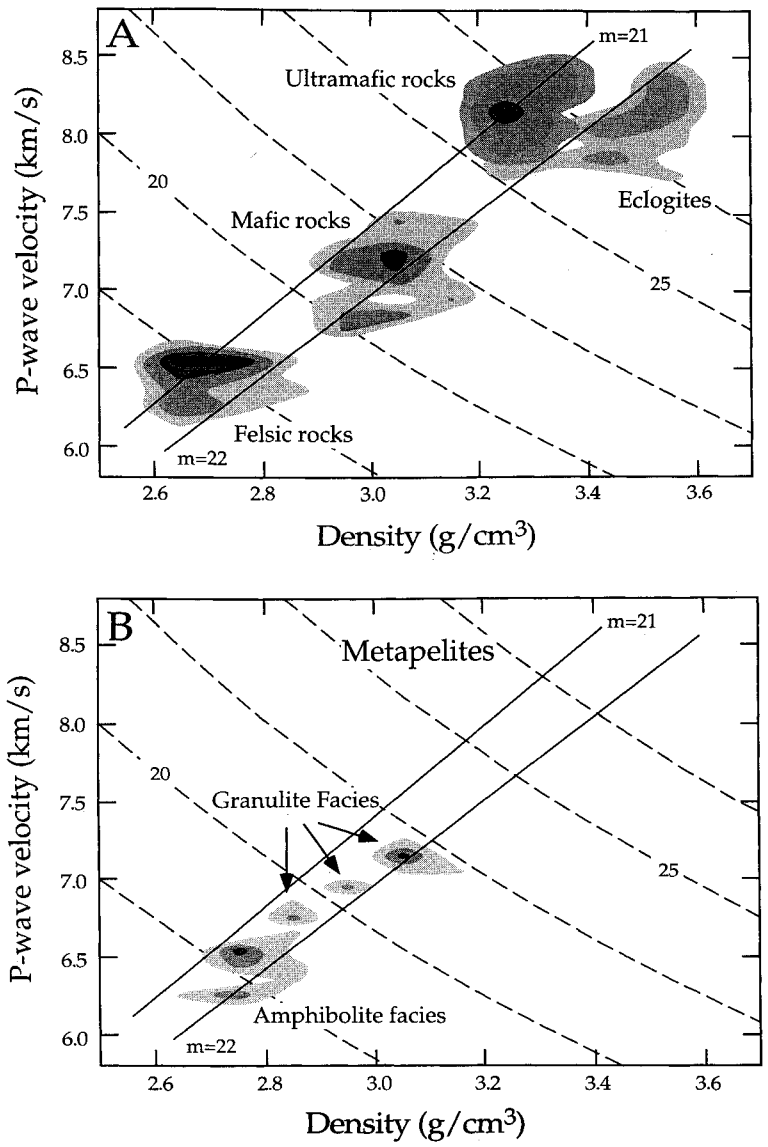

Figure 5. Compressional wave velocities (determined at 600 MPa and room temperature) versus density for (a) felsic and mafic amphibolite to granulite facies rocks, ultramafic rocks, and eclogites and (b) metapelitic rocks. Fields are for each category in Table 4 and are shown as a contoured distribution as 2.5% (lightest), 5%, 10%, 15% (darkest) of the total population of the lithological category for Figure 5a and 5%, 10%, 15% of total population for Figure 5b. Also shown are curves of constant acoustic impedance ($\times 10^6$ kg m^{-2} s^{-1}) and lines of constant mean atomic weight (at 1.0 GPa) from *Birch* [1961].

that there is a bimodal acoustic impedance distribution (the product of velocity and density) in the deep crust [*Goff et al.*, 1994; *Levander et al.*, 1994]. Acoustic impedances for typical felsic and mafic rocks are about 18×10^6 kg m^{-2} s^{-1} and 22.5×10^6 kg m^{-2} s^{-1}, respectively, a difference that corresponds to a reflection coefficient greater than 0.1 for a first-order discontinuity. Thus as was illustrated by *Goff et al.* [1994], strong reflections may be expected from deep crust characterized by layered sequences of mafic and felsic rocks. The situation is not much different if we postulate that pelitic rocks are abundant in the lower crust because of the strong overlap of these fields with those of felsic, intermediate, and mafic rocks. Models of the reflectivity of the Ivrea zone [*Burke and Fountain*, 1990; *Holliger et al.*, 1993] show that lower crust reflectivity is expected where mafic rocks are interlayered with upper amphibolite–lower granulite facies metapelites (metamorphosed shales) but diminishes when mafic rocks are interlayered with higher-grade metapelites.

Compressional wave velocity generally decreases with increasing SiO_2 for high-grade metamorphic rocks (Figure 6) but the relationship is not simple [*Fountain et al.*, 1990]. For laboratory data (Figure 6a), V_p is nearly constant for granulite facies rocks between 65% and 75% SiO_2. Mafic rocks show a wide range of velocities, a range that would be larger yet if mafic eclogite facies rocks were included in this diagram [see *Fountain et al.*, 1994a, Figure 4]. Calculated velocities for granulite facies rocks show the same general trend but exhibit lower values in the felsic range (Figure 6b). The linear trend shown for the calculated velocities is not evident for the measured values. In general, there are only small differences in V_p between amphibolite and granulite facies rocks (Figure 7).

6.2. Comparison With Refraction Data

The velocities given in Table 4 are compared with the mean and range of pressure- and temperature-corrected lower crustal velocities observed for each of

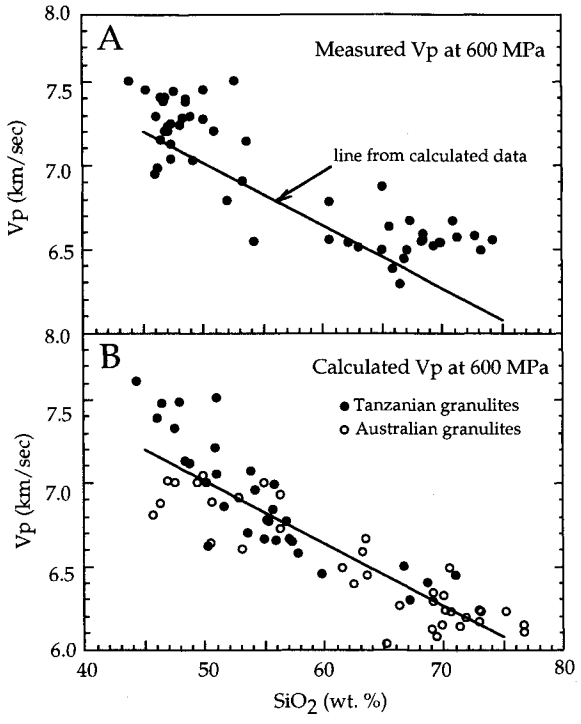

Figure 6. Compressional wave velocities at 600 MPa versus silica for (a) granulite facies rocks measured in the laboratory and (b) granulite facies rocks calculated from modal analyses given by *Lambert* [1967] and *Coolen* [1980]. The least squares line has a slope of -0.038 km s^{-1} (wt. %)$^{-1}$, y-intercept of 8.91 km s, and correlation coefficient of 0.89.

the type sections in Figure 7. The diversity of the lower crust is immediately evident from these diagrams. The mean values for all type sections tend to cluster between 6.9 and 7.2 km s^{-1}, but the ranges can be large, overlapping many rock types. In general, the lower crust of most type sections overlaps mafic rocks, anorthosites, and high-grade metapelites. We reemphasize, however, that near-vertical reflection data and geological observations indicate that the lower crust must be compositionally heterogeneous. Moreover, mean lower crustal refraction values are usually slightly lower than average velocities of mafic rocks (Table 4), suggesting the presence of more evolved granulite facies rocks. A small percentage of these rocks in the deep crust can explain the reflectivity observed in near-vertical incidence profiles. Mean values for several type sections (e.g., contractional orogenic belts, extended terrains) correspond to the lower range of mafic rocks and the upper range of intermediate rocks. The bulk composition of these lower crustal sections may be more intermediate than those with higher mean velocities.

One problem in interpreting P wave velocities in terms of lithology and chemical composition, apparent from these histograms, is that different rock types do not have unique velocities. Intermediate granulite facies rocks overlap with amphibolite facies mafic gneisses and anorthosites, and the latter overlap mafic granulite facies rocks. Perhaps the most important example of this is the overlap between mafic rocks and granulite facies pelites. These metapelites contain relatively low mica and quartz contents, large amounts of high-density phases such as garnet, and Al_2SiO_5 polymorphs and have probably lost a melt fraction [e.g., *Mehnert*, 1975] (see below).

Inclusion of lower crustal S wave data does little to help resolve the aforementioned overlaps (Figure 8, Table 5). There is a clear distinction between mafic and felsic rocks; intermediate rocks generally fill this gap (see Figure 6). However, metapelites exhibit a range of velocities that overlap felsic granulites at the lower end and mafic granulites at the higher end. There is a tendency for the high-V_p metapelites to exhibit slightly higher V_s than mafic granulite facies rocks, but the difference is subtle, and a number are indistinguishable on the basis of P and S wave velocities alone. Metapelites with high P wave velocities commonly exhibit strong preferred orientation of anisotropic phases resulting in high seismic anisotropy [e.g., *Burlini and Fountain*, 1993]. This may ultimately provide a means of distinguishing them from mafic granulite facies rocks, which generally have lower anisotropy. At present, however, there are no measurements of lower crustal anisotropy.

The limited number of S wave data for the lower crust are plotted in Figure 8. Average S wave velocities of lower crust in shields generally plot in the field of mafic rocks, whereas rifts lie intermediate between mafic and felsic rocks. All other crustal types show a large range in P and S wave values, highlighting the heterogeneity of the lower crust from place to place.

In summary, distinguishing between meta-igneous rocks of variable compositions is possible on the basis of their P and S wave velocities. Distinguishing metapelitic rocks from meta-igneous rocks is not possible on the basis of P and S wave velocities alone. Such a distinction is crucial, however, for determining bulk lower crust composition because of the large differences in major and trace element compositions of these rock types (see below). Evaluation of the volume of high-grade metapelites and mafic granulites in the deep crust must therefore rely upon integration of additional data such as seismic anisotropy and heat flow.

6.3. Assigning Lithologies to Type Sections

The first step in our calculation is to assign rock types to the different layers in our type sections. This is perhaps the most difficult aspect of the exercise.

6.3.1. High V_p layers ($\geq$6.9 km s^{-1}). The type sections shown in Figure 2 contain a lowermost layer characterized by high V_p (>6.9 km s^{-1}). Only four of the lower crustal rock types shown in Figure 7 exhibit P wave velocities greater than 6.9 km s^{-1}; these are

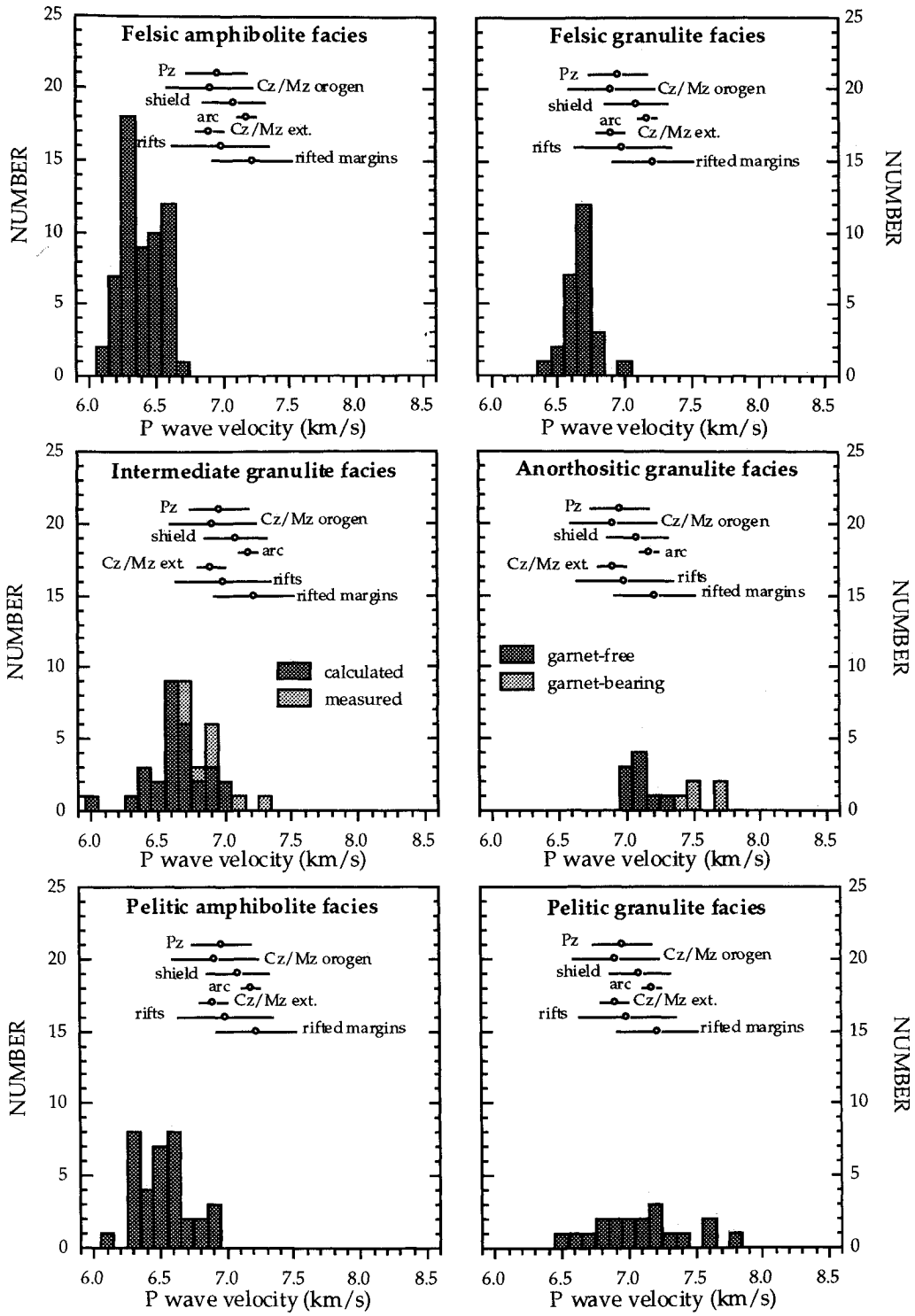

Figure 7. V_p histograms for lower crustal rock types at room temperature and 600 MPa for each lithologic category (Table 4) compared with the mean velocity (circle) and its standard deviation (bar) for each crustal type also at 600 MPa and room temperature (Tables 1 and 2).

mafic granulites, mafic amphibolite facies rocks, anorthosites, and high-grade metapelites. Another possibility is that these layers are composed of a mixture of peridotite (or eclogite) and felsic granulite. However, we consider this unlikely for two reasons: (1) the predominance of mafic granulites and near-absence of felsic granulites in xenolith suites argue against significant amounts of felsic granulites in the lowermost crust, (2) where inferred crust-mantle boundaries are exposed (e.g., Ivrea zone), the lowermost crust is composed of mafic granulite and high-grade metapelite, which may be interlayered with peridotite.

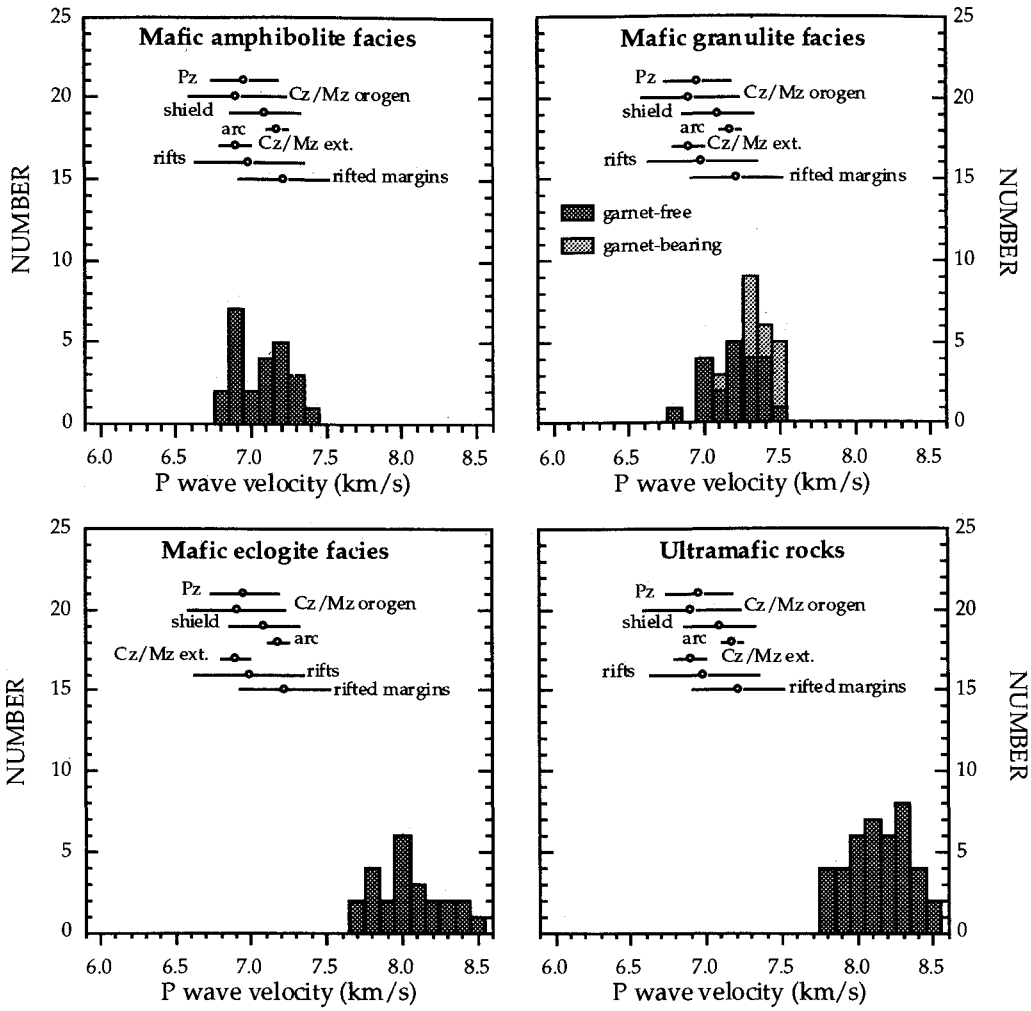

Figure 7. (continued)

We therefore turn our attention to discriminating which of the rock types listed above are most likely to be present in these layers.

Although anorthosites have the requisite velocities for high-V_p crustal layers, we take the rarity of anorthosites in the geologic record, coupled with their shallow emplacement depths [*Ashwal*, 1993], to mean that they form only minor constituents of the lower crust. We therefore did not incorporate anorthosites into our crustal estimates as a unique entity. However, a number of lower crustal xenoliths in the geochemical compilation approach anorthosite compositions (e.g., Chudleigh province, Queensland, Australia [*Rudnick et al.*, 1986]), so anorthositic rocks have been averaged with mafic granulites in the database (see below).

The high V_p of some metapelites suggests that they may be important constituents of the lower crust. The wide range of P wave velocities exhibited by granulite facies metapelites generally correlates with Al_2O_3/SiO_2 (Figure 9), which is a function of the amount of melt depletion they have experienced. Partial melting removes micas, some quartz, and, to a lesser extent, feldspar and leaves the rocks enriched in high-density (and high V_p) phases such as garnet and Al_2SiO_5 polymorphs (kyanite or sillimanite) [*Vielzeuf and Holloway*, 1988]. However, removal of partial melt in a metapelite does not cause uniform depletion of heat-producing elements, as might be expected. This is due to the retention of Th and U in accessory phases, which may remain stable in the residue during partial melting [e.g., *Sawka and Chappell*, 1986] and explains the lack of correlation between Al_2O_3/SiO_2 and heat production in Figure 9.

Heat production in metapelites is about 9 times higher than heat production in mafic granulites (Table 6; Figure 9). This, in conjunction with the relatively low heat flow in Archean shields, allows us to place limits on the amount of metapelite in the high-velocity lower crust of these regions. The Kapuskasing structural zone is the best place to perform this calculation because regional heat flow, heat production to 25 km depth, and seismic structure of the crust are known. A limiting case is made if we assume that the 23 km of unexposed, high-V_p (7.0–7.6 km s^{-1}) crust beneath the KSZ is composed entirely of high-grade metapelite (an assumption that could be consistent with the measured

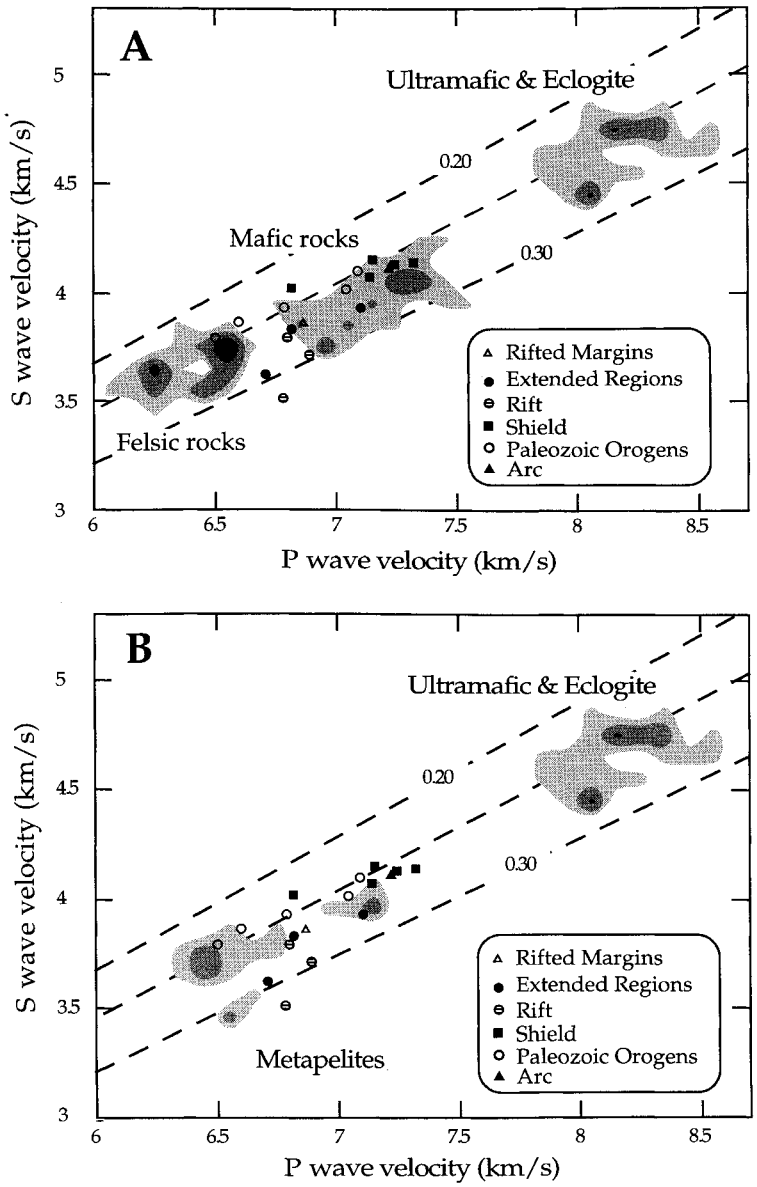

Figure 8. Compressional wave velocity versus shear wave velocity (at 600 MPa and room temperature) for (a) felsic, mafic, ultramafic, and mafic eclogite facies rocks and (b) metapelitic rocks compared with data from refraction experiments (also corrected to 600 MPa and room temperature (Table 5)). Fields (see Figure 5 for explanation) are 5%, 10%, and 15% of the total population. Lines of constant Poisson's ratio ($=0.5\{1 - 1/[(V_p/V_s)^2 - 1]\}$) are superimposed. Also shown are results for individual refraction profiles listed in Table 5.

V_p and V_s of these layers [*Boland and Ellis*, 1989]). Using the median heat production of metapelites (0.57 $\mu W\ m^{-3}$), we calculate a heat flow of 35 $mW\ m^{-2}$ for the present crustal thickness (48 km). The surface heat flow in the Abitibi belt adjacent to the KSZ is 38 $mW\ m^{-2}$ [*Pinet et al.*, 1991]. Thus if all of the deep crust were metapelite, heat production in the crust would account for nearly the entire surface heat flow. This obviously cannot be the case. *Pinet et al.* [1991] estimated the mantle contribution to heat flow to be 12 $mW\ m^{-2}$ in the Superior province. Using this value, a maximum of 20% metapelite may be present in the lower crust underlying the presently exposed KSZ.

Because average seismic velocities of the lower crust of Archean shields are lower than both average mafic granulite and granulitic metapelite (7.0 km s^{-1} versus 7.2 or 7.1 km s^{-1}, respectively), it is likely that felsic and intermediate granulites also exist in the lower crust of Archean cratons (~30% based on average velocities). We therefore conclude that the lower crustal layers in Archean shields is predominantly composed of mafic granulites (or amphibolites) with only 5% metapelite and 30% intermediate or felsic granulites. Post-Archean lower crust can contain up to 10% metapelite in the high-velocity layers. This proportion is consistent with the generally small, but

TABLE 5. Compressional and Shear Wave Velocities for Middle and Lower Continental Crust

Reference	Location	Middle Crust		Lower Crust	
		V_p	V_s	V_p	V_s
	Paleozoic Orogens				
Banda et al. [1981]	Iberian peninsula	6.56	3.57	7.04	4.01
Holbrook et al. [1988]	SW Germany			6.50	3.79
Luetgert et al. [1987]	N. Appalachians	6.41	3.70	6.79	3.93
Luetgert et al. [1987]	N. Appalachians	6.41	3.70	7.09	4.10
Shalev et al. [1991]	Appalachians, N. H.			6.60	3.86
	Shield/Platforms				
Boland and Ellis [1990]	Superior province	6.80	3.90	7.24	4.13
Grad and Luosto [1987]	Baltic shield	7.07	4.02	7.32	4.15
Grad and Luosto [1987]	Baltic shield	6.79	4.03	7.15	4.15
Grad and Luosto [1987]	Baltic shield	7.07	4.02	7.32	4.15
Luosto et al. [1990]	Baltic shield	6.72	3.78	7.14	4.07
Epili and Mereu [1991]	Grenville front			6.82	4.02
	Rifts				
El-Isa et al. [1987a, b]	Jordan			6.89	3.71
El-Isa et al. [1987a, b]	Jordan			6.78	3.51
Holbrook et al. [1988]	Rheingraben			6.80	3.79
	Rifted Margins				
Chian and Louden [1992]	SW Greenland			6.86	3.86
	Extended Regions				
Goodwin and McCarthy [1991]	W. Arizona	6.18	3.62	6.82	3.83
Keller et al. [1975]	Great basin			6.71	3.62
Braile et al. [1982]	Snake River plain	6.60	3.61	7.10	3.93

All velocities are adjusted to room temperature and 600 MPa.

significant, number of metapelites observed in post-Archean lower crustal xenolith suites [*Rudnick*, 1992].

The lower crust of each type section was modeled according to its average *P* wave velocity. Although garnet-bearing mafic granulites have higher average velocities than garnet-free mafic granulites, it is not possible to determine independently their relative proportions in the lower crust. We therefore used the average mafic granulite velocity (7.23 km s^{-1}) to represent mafic lower crustal rocks. We then assume a constant proportion of metapelite (as described in the preceding paragraph) and calculate the amount of intermediate and felsic granulites present in the lower crust of each type section (assuming equal proportions of both). Thus a lower crust having an average velocity of 6.9 km s^{-1} is composed of 40% mafic granulite, 10% metapelite, and 25% each of intermediate and felsic granulite. At the higher end of the velocity scale, a lower crust with a *P* wave velocity of 7.2 km s^{-1} would be composed of 90% mafic granulite and 10% metapelite with no intermediate or felsic granulites.

6.3.2. Intermediate V_p layers (6.5–6.9 km s^{-1}). Layers of intermediate velocities are important in several of the crustal sections shown in Figure 2. These lie directly above the lowermost crust in shields and platforms, arcs, and rifts. Rock types with *P* wave velocities in this range are intermediate granulites and metapelites (Figures 6 and 7). Crustal cross sections [e.g., *Fountain and Salisbury*, 1981], as well as the heat flow data described above do not support a metapelite-dominated layer in the deep crust (e.g., KSZ, Ivrea). Alternatively, these layers could be composed of mixed mafic and felsic rocks in the amphibolite or granulite facies. In terms of chemical composition, it makes little difference whether these layers are modeled as intermediate or equal mixtures of mafic and felsic rocks (Figure 10). We therefore modeled these layers as 45% intermediate amphibolite facies gneisses, 45% mixed amphibolite and felsic amphibolite facies gneisses, and 10% metapelite.

6.3.3. Low V_p layers (6.2–6.5 km s^{-1}). Low-velocity layers typically occur at mid-crustal levels in Paleozoic and more recent fold belts and rifted margins. They also constitute the uppermost crust in shields and platforms (Fig. 2). Such layers are likely to be composed of felsic rocks in the granulite and amphibolite facies (Fig. 7), and we have modeled them as such. Several of these low velocity layers have average V_p of 6.5 km/sec, near the boundary between felsic and intermediate granulites. These layers are interpreted as equal mixtures of felsic and intermediate granulites.

6.4. Chemical Compositions of Granulites

The next step in our calculation is to assign a chemical composition to the mafic, intermediate, felsic, and pelitic granulites and amphibolite facies rocks. To do this, we used the data base of *Rudnick and Presper*

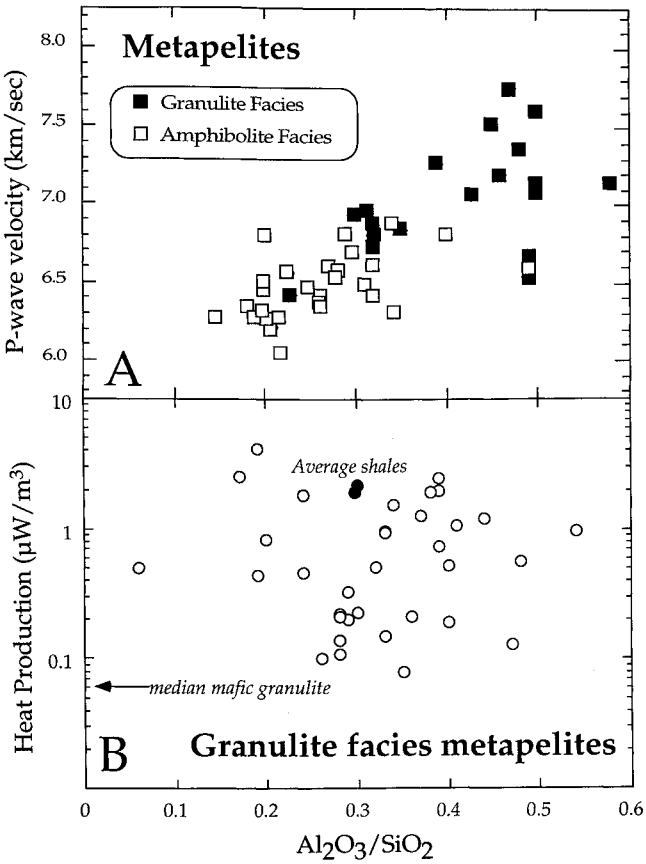

Figure 9. (a) Al_2O_3/SiO_2 versus P wave velocity for metapelites. See Table 4 for data sources. (b) Heat production versus Al_2O_3/SiO_2 for metapelitic xenoliths (data from *Rudnick and Presper* [1990]). Solid symbols represent average post-Archean shale compositions [*Krauskopf*, 1967; *Taylor and McLennan*, 1985]. Arrow marks the average heat production for mafic granulite xenoliths.

[1990], supplementing the granulite xenolith data with more recent data from the literature [*Halliday et al.*, 1993; *Hanchar et al.*, 1994; *McGuire and Stern*, 1993; *Mengel*, 1990; *Wendlandt et al.*, 1993]. We subdivided the database into averages of mafic granulites, intermediate granulites, felsic granulites, and metapelites, each of which is in turn subdivided into those occurring as xenoliths, post-Archean terrains, and Archean terrains (Table 6).

In general, the averages for major elements and the trace elements that are compatible or moderately incompatible agree well with the medians, indicating that the populations follow a normal distribution. For the highly incompatible trace elements, however, the medians can be significantly lower than the average (Table 6). We have chosen to use medians in our calculations rather than averages in order to minimize the effects of outliers for small sample populations [e.g., *Rock*, 1988].

Although the middle crust may be composed of rocks in the granulite facies in some regions, it is likely that amphibolite facies rocks make up a significant portion of the middle crust [e.g., *Stosch et al.*, 1992]. The use of granulites to model the middle crust will have little effect on the major element composition because amphibolite and granulite facies rocks of similar bulk compositions generally have similar *P* wave velocities (Figure 7). It will have an effect, however, on elements that are depleted by granulite facies metamorphism. Most specifically, we expect U, Cs, and possibly Rb, Th, K, and Pb to be lower in granulites than in their amphibolitic counterparts [*Rudnick et al.*, 1985; *Rudnick and Presper*, 1990].

If we assume that rocks in the middle crust are in the amphibolite facies and that these rocks (1) are not depleted in K, Rb, Cs, Th, and U and (2) have Th/U, K/U, K/Rb, and Rb/Cs ratios equal to those of the upper crust, we can use the Pb abundances of the granulites (assuming that Pb is not depleted by granulite facies metamorphism) and the Pb isotopic composition of the crust to calculate the abundances of U in amphibolite facies gneisses. The Pb isotope composition of the continental crust (i.e., $^{206}Pb/^{204}Pb = 18.2$, $^{207}Pb/^{204}Pb = 15.5$, and $^{208}Pb/^{204}Pb = 38$ [*Rudnick and Goldstein*, 1990]) suggests that the crust evolved with a time-integrated μ ($^{238}U/^{204}Pb$) of ~8, which corresponds to a U/Pb ratio of 0.13. Using this ratio and the Pb abundances for the different types of felsic and intermediate granulites, we calculated the U content of their amphibolite facies counterparts. Once U abundance is established, the Th abundance can be derived from Th/U = 3.8, the K abundance from K/U = 10,000, the Rb abundance from K/Rb = 260 and the Cs abundance from Rb/Cs = 25 [*McDonough et al.*, 1992; *Taylor and McLennan*, 1985]. For felsic granulites (both Archean and post-Archean), the calculations given above result in values for some mobile elements being higher in the granulites than in the amphibolite facies gneisses. This suggests that Pb may have been depleted by granulite facies metamorphism in these rocks. In these cases we increased Pb content in the amphibolite facies rocks until all of the mobile element abundances in the amphibolites are consistently higher than those of the granulites. The resulting compositions of amphibolite facies gneisses (Table 6) were used to model midcrustal layers.

6.5. Areal Extent of Crustal Type Sections

There are two schools of thought regarding the areal extent of different crustal provinces (i.e., Precambrian shields, Paleozoic orogenic belts, and Cenozoic-Mesozoic regions (Table 7)). One school [*Condie*, 1989; *Hurley and Rand*, 1969; *Sclater et al.*, 1980] argues that 60–70% of the crust is Precambrian in age. This estimate is based on the areal extent of inferred Precambrian crust (i.e., all crust of inferred Precambrian age that is exposed or covered by shallow sedimentary deposits on the continents). The second school [*Goodwin*, 1991; *Sprague and Pollack*, 1980] contends that only 50% of the continental crust is Precambrian.

TABLE 6. Average and Median Values for Different Types of Granulite (and Amphibolite) Facies Rocks

	Mafic											
	Archean Terrains			*Post-Archean Terrains*			*Xenoliths*[a]			*Archean Terrains*		
	Ave	*Med*	*N*	*Ave*	*Med*	*N*	*Ave*	*Med*	*N*	*Ave*	*Med*	*N*
SiO_2, wt. %	49.7	49.8	101	49.2	49.3	96	49.1	49.5	270	58.3	58.4	106
TiO_2, wt. %	0.95	0.96	101	1.32	1.25	95	1.00	0.84	266	0.83	0.78	106
Al_2O_3, wt. %	14.5	14.8	100	15.8	15.9	95	16.5	16.7	269	16.3	16.3	106
FeO_T, wt. %	11.3	11.1	101	9.2	9.4	65	9.02	8.91	269	7.3	7.2	106
MnO, wt. %	0.19	0.20	96	0.19	0.18	95	0.15	0.15	255	0.11	0.10	102
MgO, wt. %	8.53	7.25	100	8.14	7.3	95	8.56	8.24	269	3.6	3.3	106
CaO, wt. %	9.72	9.99	101	9.31	9.7	95	10.89	10.9	269	6.2	6.1	106
Na_2O, wt. %	2.56	2.59	100	2.39	2.51	94	2.45	2.51	269	4	4.1	106
K_2O, wt. %	0.70	0.58	100	0.85	0.62	94	0.38	0.28	236	1.55	1.1 (1.3)	106
P_2O_5, wt. %	0.19	0.12	98	0.3	0.22	87	0.20	0.12	258	0.27	0.23	105
Mg #, mol	57.4	53.8		56.2	53.6		62.8	62.2		46.8	45	
Li, ppm	15	13	7				6	6	14	11	9	9
Sc, ppm	39	41	23	45	43	33	35	34	92	17	17	15
V, ppm	216	195	67	261	257	55	216	219	173	128	121	81
Cr, ppm	464	229	92	345	153	74	353	252	192	155	103	90
Co, ppm	48	47	34	52	50	39	53	42	105	26	22	45
Ni, ppm	227	112	84	126	80	61	150	105	175	71	46	88
Cu, ppm	44	38	49	56	48	21	49	28	152	27	22	43
Zn, ppm	99	93	64	152	110	42	90	78	132	73	76	49
Ga, ppm	18	17	53	21	19	23	15	14	21	19	18	38
Rb, ppm	12	5	84	22	14	68	7	3	197	30	19 (41)	96
Sr, ppm	227	156	89	378	232	80	421	365	207	519	454	100
Y, ppm	25	22	73	39	31	47	16	13	151	22	20	85
Zr, ppm	94	64	86	196	106	78	76	40	181	163	130	96
Nb, ppm	6	5	71	9	6	33	9	4	102	7.5	7	76
Cs, ppm							1	0.11	32	0.9	0.2 (0.9)	5
Ba, ppm	294	137	75	332	184	66	275	175	179	691	512	97
La, ppm	31	8.5	70	25	14	43	8	5	121	38	30	68
Ce, ppm	37	20	72	48	24	41	19	12	122	74	58	67
Pr, ppm	5.5[b]	2.9[b]	2	6.7[b]	3.2[b]		2.5[b]	1.6[b]	37	8.7[b]	6.4[b]	4
Nd, ppm	27	14	25	31	14	26	11	8	15	31	20	32
Sm, ppm	5.4	3.1	37	9.0	5.8	28	2.81	2.3	135	5.7	4.1	36
Eu, ppm	1.0	0.9	37	2.3	1.5	35	1.07	0.96	123	1.5	1.2	37
Gd, ppm	5.5	3.9	16	6.9	4.7	21	3.06	2.71	63	4.4	3.5	24
Tb, ppm	1.0	0.6	27	1	0.8	27	0.47	0.41	87	0.66	0.5	19
Dy, ppm	7.8	4	13	4.2	3.6	7	2.99	2.67	40	4.3	2.9[b]	23
Ho, ppm	1.6[b]	0.8[b]	4	0.9[b]	0.8[b]		0.63	0.59[b]	54	0.81	0.60[b]	6
Er, ppm	4.3	2.2	13	2.5	2.5	6	1.84	1.68	41	2.1	1.6[b]	24
Yb, ppm	3.1	2.2	37	3.4	2.7	34	1.53	1.17	120	1.7	1.4	36
Lu, ppm	0.5	0.2	12	0.6	0.5	26	0.24	0.19	71	0.29	0.25	23
Hf, ppm	1.8	2	21	5.2	2.5	26	1.87	1.01	75	3.8	3.4	10
Ta, ppm	0.3	0.2	8	0.6	0.2	12	0.55	0.5	18	0.62	0.63	5
Pb, ppm	6	5	59	8.5	6	27	2.58	1.8	47	14	10	51
Th, ppm	1.8	1	39	6.4	1	23	0.6	0.3	55	2.3	1.0 (4.0)	37
U, ppm	0.7	0.5	24	2	0.55	13	0.21	0.08	36	0.54	0.4 (1.6)	24
H,[d] $\mu W\ m^{-3}$	0.37	0.25		1.06	0.27		0.13	0.06		0.43	0.27 (0.80)	

Numbers in parentheses represent estimated values for amphibolite facies rocks (see text for method of calculation).
[a]K, Sr and Ba values for kimberlite-hosted xenoliths were omitted owing to alteration effects.

These estimates assume that the 30% of submerged continental crust [*Cogley*, 1984] is younger. We therefore constructed two models using different crustal age distributions (Table 7). It is important to stress that the ages we are discussing are the observed crystallization ages of the crust, not growth ages (arguments of continental freeboard require that a large proportion (at least ~70%) of the crust was in place by the end of the Archean [*Armstrong*, 1991; *Taylor and McLennan*, 1995]; yet the amount of extant Archean crust is much lower than this).

The areal extent of shields and platforms is taken as the amount of Precambrian crust. In both models this constitutes the largest single portion of crust. The proportions of Archean to Proterozoic crust (14:86) are taken from Goodwin. The Phanerozoic crust in both models is divided as follows: 46% Paleozoic crust and 54% Cenozoic-Mesozoic crust (following subdivisions of Condie and Sprague and Pollack). In model 1, 30% of the crust is assigned to rifted margins, whereas in model 2, rifted margins constitute only 10% of the crust. In both models rifted margins are assumed to be

Intermediate						*Felsic*						*Metapelite*		
Post-Archean Terrains			*Xenoliths*			*Archean Terrains*			*Post-Archean Terrains*			*Xenoliths*		
Ave	*Med*	*N*	*Ave*	*Med*	*N*	*Ave*	*Med*	*N*	*Ave*	*Med*	*N*	*Ave*	*Med*	*N*
58.3	58.3	138	54.1	53.2	48	70.5	70.7	379	70.2	70.2	246	60.5	60.3	78
0.97	0.95	132	0.81	0.79	48	0.40	0.36	379	0.48	0.43	222	1.00	1.02	78
16.8	16.6	132	17.5	17.8	48	14.4	14.4	379	14.0	14.2	224	17.6	17.6	78
8.1	8	132	7.2	7.1	48	3.1	2.9	379	4	3.9	224	7.84	7.51	78
0.14	0.13	132	0.13	0.13	47	0.05	0.04	348	0.07	0.05	220	0.13	0.11	77
3.8	3.6	132	5.5	5.3	48	1.1	0.88	378	1.3	1.2	223	3.12	3.03	78
5.7	5.9	132	9.2	8.8	48	2.8	2.7	379	2.8	2.5	224	2.97	2.4	78
3.4	3.4	132	3.6	3.8	48	3.8	3.8	379	3.4	3.5	224	2.4	2.49	78
1.55	0.96 (1.7)	138	0.78	0.65	48	2.8	2.6 (3.2)	379	2.52	1.9 (2.5)	246	1.99	1.90	78
0.26	0.24	120	0.19	0.16	46	0.11	0.09	358	0.11	0.09	186	0.12	0.09	78
45.4	44.5		57.7	57.1		38.7	35.1		36.7	35.4		41.5	41.8	
9	10	5	10	10	2	15	15	10	7.4	7	21			
27	27	41	22	19	19	6	5	91	13	13	59	23	19	32
157	160	77	155	154	29	38	29	244	50	40	138	129	129	50
80	56	79	122	95	30	47	16	249	41	22	134	135	117	56
35	30	65	33	29	17	12	10	76	22	15	52	26	21	43
35	24	69	76	52	30	20	15	263	16	8	128	52	33	52
50	25	43	42	22	24	15	8	196	22	13	116	26	16	48
110	90	64	72	72	18	38	34	243	54	48	130	96	90	47
22	22	44	17	17	2	17	16	183	19	18	133			
42	22 (54)	111	12	5	33	71	57 (103)	366	78	58 (80)	204	51	42	72
408	346	126	549	435	41	285	257	353	222	185	215	331	284	69
30	24	86	23	17	25	24	11	286	35	22	151	44	33	35
188	120	112	127	54	38	229	184	332	254	156	163	248	210	48
11	8	37	10	7	15	8	5	232	13	8	78	21	14	29
3.2	2 (1.1)	5	0.07	0.04	3	0.62	0.5 (5.1)	42	1.7	1 (4.0)	18	0.73	0.9	23
470	400	105	498	380	33	823	693	361	568	453	170	730	700	53
23	18	71	14	10	29	44	34	276	31	19	127	36	24	43
56	50	65	32	22	29	71	54	274	82	56	143	71	50	44
7.4[b]	6.4[b]	4	3.7[b]	2.9[b]	8	9.7[b]	5.1[b]	15	10[b]	7.4[b]		8.4[b]	6.1[b]	3
31	26	31	13	12	23	43	18	74	39	32	45	32	23	47
6.4	5.5	35	3.7	2.8	30	5.7	2.9	110	4.2	4.6	13	5.9	5	50
2.2	1.6	33	1.4	1.2	29	1.4	1.3	110	2.3	1.9	13	1.48	1.4	44
4.9	4.1	20	3.1	2.8	18	4.0[b]	2.7[b]	32	7.7	4.4[b]	7	6.88	7.2	15
0.8	0.60[b]	22	0.58	0.48	17	0.56	0.32	91	0.84	0.6	11	1.05	0.90	40
4.5[b]	3.8[b]	13	2.8	2.8	8	3.5[b]	1.84[b]	52	5.1[b]	4.19[b]		7.75	6.8	22
0.82	0.75[b]	7	0.64	0.54	13	0.75[b]	0.36[b]	32	1.0[b]	0.93[b]	4	1.60[b]	1.08	11
2.2	1.95[b]	10	1.8	1.5	10	2.0[b]	0.84[b]	55	2.9	2.8[b]	6	4.5[b]	2.9	12
2.3	2.2	32	1.5	1.5	28	1.6	0.6	111	3.1	2.9	12	4.43	3.6	37
0.53	0.5	19	0.22	0.19	21	0.26	0.13	69	0.47	0.44	12	0.67	0.60	33
4.8	2.9	22	3.8	1.6	16	4.5	3.9	61	8.3	6.2	10	6.88	6	42
1.4	1.4	4	0.6[c]		1	0.58	0.35	34	0.8[c]	0.5[c]	1	1.3	1	15
15	13	55	2.9	2.9	11	17	14 (25)	226	22.5	16 (20)	129	12.3	12	28
9.6	2.2 (5.3)	27	1.4	0.25	14	12	5.5 (10)	217	12	7.7 (8.0)	53	7.53	4	41
0.95	0.8 (1.4)	21	0.15	0.08	10	1.44	1 (2.7)	121	0.81	0.7 (2.1)	48	0.58	0.5	35
1.06	0.45 (0.89)		0.20	0.09		1.50	0.87 (1.7)		1.27	0.89 (1.33)		0.85	0.57	

[b]Interpolated from the rare earth element (REE) pattern where the number of observations is low relative to that of an adjacent REE.
[c]Calculated assuming Nb/Ta = 16.
[d]Heat production.

Phanerozoic in age and are divided equally between Paleozoic and Cenozoic-Mesozoic crust. The remaining Paleozoic crust is assigned to Paleozoic orogenic belts, and the remaining Cenozoic-Mesozoic crust is further subdivided between extensional areas (3–3.5% of the total crust), contractional areas (2–2.5%), active rifts (1%), and arcs (6–7%). The latter assignments are somewhat arbitrary but based mainly on Condie's subdivisions. The small areal extent of these regions make them of less significance when the entire crust is considered, so errors in their area should not propagate into large errors when considering the whole crust.

6.6. A New Estimate of Crust Composition

Using the type sections, areas, lithological assignments to *P* wave velocities and chemical compositions given above, we estimated the composition of the lower, middle, and bulk continental crust. Table 8 gives the lower and total crust composition for the various type sections, whereas Table 9 gives the bulk lower, middle, and total crust compositions. Table 10 presents some relevant trace element ratios.

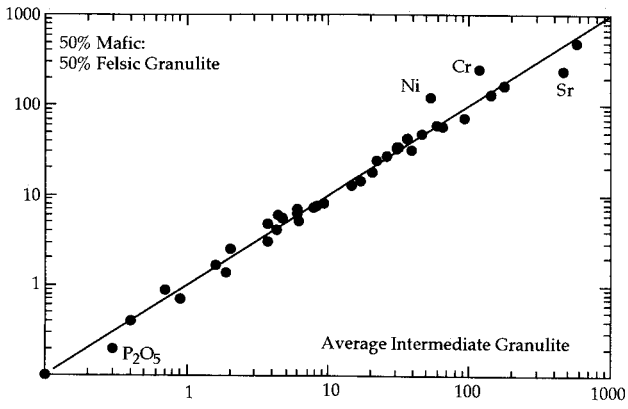

Figure 10. Comparison of major and trace element compositions between average intermediate (x axis) and mixed felsic-mafic (y axis) granulites. Each data point represents an individual element; points that deviate significantly from the 1:1 line are labeled.

We combined lower crustal rock types in the proportions dictated by the crustal type sections in Figure 2 and as discussed above. We used the average composition of mafic granulite xenoliths to model mafic granulites for two reasons: (1) we believe that xenoliths best represent lowermost crust and (2) compared with terrains, the majority of xenolith analyses were performed relatively recently, using analytical techniques that have better detection limits and higher precision than older techniques, especially at the lower concentrations that are typical of these rocks. For the upper crust we used *Taylor and McLennan*'s [1985] value for post-Archean regions and their average Archean upper crust for the Archean regions. Both models of areal distribution gave similar results for the lower and whole crusts, so only one value is presented in Table 8.

In our model the bulk lower crust is mafic and similar to previous estimates by *Poldervaart* [1955], *Pakiser and Robinson* [1966] and *Rudnick and Taylor* [1987] but significantly less evolved than the estimates of others (see review by *Fountain and Christensen* [1989]). (The lower crustal estimate of Taylor and McLennan includes that portion of crust below the upper crust (~upper third of the crust in their model) and above the Moho. Thus their "lower crust" corresponds to our combined middle and lower crusts, so the apparently large differences in composition are not as great as they seem.) The lower crust approaches the composition of a primitive basalt, having a high Mg # (100Mg/(Mg + ΣFe)), high Ni and Cr contents, and low abundances of heat-producing elements (HPE) (Table 9). The lower crust is light rare earth element

TABLE 7. Areal Percent of Different Age Continental Crust

	Hurley and Rand [1969]	*Condie [1989]*	*Goodwin [1991]*	*Sclater et al. [1980]*	*Sprague and Pollack [1980]*[a]	*Model 1*[b]	*Model 2*
Archean	5.6		7.0	20.0	5.2	7.0	9.0
Proterozoic	65.0		43.0	48.0	43.7	43.0	56.0
Paleozoic		19.0		8.0	24.0	23.0	16.0
Cenozoic-Mesozoic		23.0		24.0	27.1	27.0	19.0
Total	70.6	42.0	50.0	100.0	100.0	100.0	100.0
Total Precambrian	70.6	57.0	50.0	68.0	48.9	50.0	65.0
Total Phanerozoic	30.0	42.0		32.0	51.1	50.0	35.0

Breakdown of Cenozoic-Mesozoic Crust (27% and 19% of Total Crust)

	Model 1[c]	*Model 2*
Extensional areas	3.0	3.5
Contractional orogens	2.0	2.5
Active rifts	1.0	1.0
Rifted margins	15.0	5.0
Arcs	6.0	7.0
Total	27.0	19.0

Breakdown of Paleozoic Crust (23% and 16% of Total Crust)

	Model 1[c]	*Model 2*
Paleozoic orogens	8.0	11.0
Rifted margins	15.0	5.0
Total	23.0	16.0

[a] Continental shelves are included as Paleozoic crust.
[b] Precambrian crustal estimates from Goodwin; proportions of Paleozoic and Cenozoic-Mesozoic crusts from Sprague and Pollack.
[c] Rifted margins assumed to represent 30% of crust by area [*Cogley*, 1984] and are shared between Paleozoic and Cenozoic-Mesozoic ages.

TABLE 8. Major and Trace Element Concentrations of Lower and Total Crust for Different Type Sections

	Platform/ Shield		*(Archean)*	*Paleozoic Orogen*		*Mesozoic-Cenozoic Contractions*		*Continental Arcs*		*Rifted Margins*		*Active Rifts*		*Mesozoic-Cenozoic Extensions*	
	Lower	*Total*	*Total*	*Lower*	*Total*	*Lower*	*Total*	*Lower*	*Total*	*Lower*	*Total*	*Lower*	*Total*	*Lower*	*Total*
							Major Elements								
SiO_2, wt. %	52.4	57.8	55.2	55.0	61.0	58.0	62.5	50.6	57.3	50.6	60.2	55.0	60.5	58.0	64.8
TiO_2, wt. %	0.8	0.7	0.7	0.8	0.7	0.8	0.7	0.9	0.8	0.9	0.7	0.8	0.7	0.8	0.6
Al_2O_3, wt. %	16.5	15.8	15.4	16.4	15.7	16.1	15.6	16.8	16.2	16.8	15.8	16.4	15.9	16.1	15.2
FeO_T, wt. %	8.2	6.9	7.3	7.9	6.3	7.3	6.0	8.8	7.2	8.8	6.3	7.9	6.3	7.3	5.2
MnO, wt%	0.1	0.1	0.1	0.1	0.1	0.1	0.1	0.1	0.1	0.1	0.1	0.1	0.1	0.1	0.1
MgO, wt. %	7.1	4.7	4.9	6.0	3.9	4.8	3.3	7.7	5.1	7.7	4.3	6.0	4.0	4.8	2.6
CaO, wt. %	9.5	6.7	6.9	8.0	5.8	6.7	5.1	10.1	7.2	10.1	6.3	8.0	6.0	6.7	4.4
Na_2O, wt. %	2.7	3.1	3.1	2.8	3.2	3.0	3.4	2.5	3.1	2.5	3.2	2.8	3.3	3.0	3.5
K_2O, wt. %	0.6	1.7	1.2	0.8	1.9	1.0	2.3	0.4	1.6	0.4	2.1	0.8	2.1	1.0	2.7
P_2O_5, wt. %	0.1	0.2	0.2	0.1	0.2	0.1	0.2	0.1	0.2	0.1	0.2	0.1	0.3	0.1	0.2
Mg #, mol	61	55	54	57	53	54	49	61	56	61	55	57	53	54	47
							Trace Elements								
Li, ppm	6	11	11	6	10	7	11	5	10	5	11	6	12	7	12
Sc, ppm	30	22	20	28	21	26	19	33	24	33	21	28	20	26	16
V, ppm	194	141	162	174	118	151	105	210	150	210	122	174	120	151	82
Cr, ppm	213	128	162	175	101	132	76	239	141	239	114	175	100	132	57
Co, ppm	37	26	27	34	24	30	21	40	28	40	24	34	23	30	18
Ni, ppm	88	55	77	71	42	53	32	98	59	98	49	71	43	53	25
Cu, ppm	26	24	22	24	22	22	22	27	25	27	23	24	24	22	21
Zn, ppm	77	75	69	77	70	75	71	79	77	79	71	77	75	75	66
Ga, ppm	13	15	15	14	16	16	17	13	15	13	16	14	16	16	17
Rb, ppm	12	52	29	18	59	26	72	7	49	7	65	18	65	26	85
Sr, ppm	349	331	317	327	304	307	307	357	340	357	320	327	332	307	291
Y, ppm	16	19	16	18	20	20	22	15	19	15	20	18	21	20	22
Zr, ppm	69	119	105	86	129	106	144	57	111	57	127	86	136	106	156
Nb, ppm	5	11	7	6	11	7	13	5	11	5	13	6	14	7	15
Cs, ppm	0.3	2.2	0.7	0.6	3.5	0.9	3.2	0.2	2.1	0.2	3.0	0.6	2.9	0.9	4.2
Ba, ppm	263	379	339	303	403	353	443	228	364	228	397	303	425	353	467
La, ppm	9	17	18	11	18	14	20	7	16	7	18	11	20	14	22
Ce, ppm	21	40	36	28	44	36	50	16	37	16	43	28	46	36	54
Pr, ppm	2.6	4.8	4.1	3.6	5.4	4.7	6.1	2.1	4.5	2.1	5.1	3.6	5.5	4.7	6.5
Nd, ppm	11.4	19.0	15.4	15.6	22.2	19.9	24.3	9.2	17.9	9.2	20.5	15.6	21.5	19.9	26.2
Sm, ppm	2.8	3.8	3.3	3.4	4.1	3.9	4.4	2.6	3.7	2.6	3.8	3.4	4.1	3.9	4.4
Eu, ppm	1.1	1.1	1.1	1.2	1.3	1.4	1.3	1.0	1.1	1.0	1.2	1.2	1.1	1.4	1.3
Gd, ppm	3.1	3.5	3.1	3.4	3.8	3.7	3.9	3.0	3.5	3.0	3.6	3.4	3.7	3.7	4.0
Tb, ppm	0.5	0.6	0.5	0.5	0.6	0.6	0.6	0.5	0.5	0.5	0.6	0.5	0.6	0.6	0.6
Dy, ppm	3.1	3.4	2.9	3.4	3.6	3.6	3.7	3.0	3.4	3.0	3.5	3.4	3.5	3.6	3.8
Ho, ppm	0.7	0.7	0.6	0.7	0.8	0.8	0.8	0.7	0.7	0.7	0.8	0.7	0.8	0.8	0.8
Er, ppm	1.9	2.1	1.8	2.1	2.3	2.2	2.3	1.9	2.1	1.9	2.2	2.1	2.2	2.2	2.4
Yb, ppm	1.5	1.9	1.5	1.8	2.2	2.1	2.3	1.4	1.9	1.4	2.0	1.8	2.1	2.1	2.4
Lu, ppm	0.2	0.3	0.2	0.3	0.4	0.4	0.4	0.2	0.3	0.2	0.3	0.3	0.3	0.4	0.4
Hf, ppm	1.9	3.5	2.6	2.6	4.1	3.3	4.5	1.5	3.3	1.5	4.0	2.6	4.1	3.3	5.1
Ta, ppm	0.6	1.1	0.6	0.7	0.9	0.8	1.2	0.6	1.1	0.6	1.1	0.7	1.3	0.8	1.2
Pb, ppm	4.3	11.4	8.5	6.6	14.2	9.2	15.9	2.8	10.6	2.8	13.7	6.6	13.6	9.2	18.5
Th, ppm	1.2	5.1	3.0	2.1	5.8	3.0	7.1	0.7	4.7	0.7	6.3	2.1	6.3	3.0	8.3
U, ppm	0.2	1.3	0.7	0.3	1.4	0.5	1.8	0.1	1.2	0.1	1.6	0.3	1.6	0.5	2.1
							Heat								
Production, $\mu W\ m^{-3}$	0.18	0.84	0.51	0.30	0.96	0.42	1.17	0.12	0.79	0.12	1.05	0.30	1.04	0.42	1.38
Flow,[a] $mW\ m^{-2}$		36	22		36		61		32		27		29		43

[a]Crustal contribution to heat flow calculated with average crustal thicknesses given in Table 2.

TABLE 9. Major and Trace Element Composition of the Continental Crust

	Lower	*Middle*	*Upper*[a]	*Total*
	Major Elements			
SiO_2, wt. %	52.3	60.6	66.0	59.1
TiO_2, wt. %	0.8	0.7	0.5	0.7
Al_2O_3, wt. %	16.6	15.5	15.2	15.8
FeO_T, wt. %	8.4	6.4	4.5	6.6
MnO, wt. %	0.1	0.10	0.08	0.11
MgO, wt. %	7.1	3.4	2.2	4.4
CaO, wt. %	9.4	5.1	4.2	6.4
Na_2O, wt. %	2.6	3.2	3.9	3.2
K_2O, wt. %	0.6	2.01	3.40	1.88
P_2O_5, wt. %	0.1	0.1	0.4	0.2
Mg #, mol	60	48	47	54
	Trace Elements			
Li, ppm	6	7	20	11
Sc, ppm	31	22	11	22
V, ppm	196	118	60	131
Cr, ppm	215	83	35	119
Co, ppm	38	25	10	25
Ni, ppm	88	33	20	51
Cu, ppm	26	20	25	24
Zn, ppm	78	70	71	73
Ga, ppm	13	17	17	16
Rb, ppm	11	62	112	58
Sr, ppm	348	281	350	325
Y, ppm	16	22	22	20
Zr, ppm	68	125	190	123
Nb, ppm	5	8	25	12
Cs, ppm	0.3	2.4	5.6	2.6
Ba, ppm	259	402	550	390
La, ppm	8	17	30	18
Ce, ppm	20	45	64	42
Pr, ppm	2.6	5.8	7.1	5.0
Nd, ppm	11	24	26	20
Sm, ppm	2.8	4.4	4.5	3.9
Eu, ppm	1.1	1.5	0.9	1.2
Gd, ppm	3.1	4.0	3.8	3.6
Tb, ppm	0.48	0.58	0.64	0.56
Dy, ppm	3.1	3.8	3.5	3.5
Ho, ppm	0.68	0.82	0.80	0.76
Er, ppm	1.9	2.3	2.3	2.2
Yb, ppm	1.5	2.3	2.2	2.0
Lu, ppm	0.25	0.41	0.32	0.33
Hf, ppm	1.9	4.0	5.8	3.7
Ta, ppm	0.6	0.6	2.2	1.1
Pb, ppm	4.2	15.3	20	12.6
Th, ppm	1.2	6.1	10.7	5.6
U, ppm	0.2	1.6	2.8	1.42

[a]From *Taylor and McLennan* [1985], phosphorus data estimated, cesium from *McDonough et al.* [1992].

(LREE) enriched with a small (~14%) positive Eu anomaly ($Eu/Eu^* = 2Eu_n/(Sm_nGd_n)^{0.5}$), where the subscripted n indicates the values are normalized to chondritic meteorites) and contains higher concentrations of the compatible trace elements than the middle and upper crust (Tables 10 and 11; Figure 11).

The middle crust is intermediate in composition. It contains high concentrations of REE and a small positive Eu anomaly and is LREE-enriched (Figure 11). The HPE content of the middle crust is high but lower than that of the upper crust.

All existing models indicate that average continental crust is intermediate in composition, and our result is no exception (Table 11). This result is due more to mixing of mafic (lower crust) and felsic (upper crust) lithologies rather than a predominance of intermediate rocks in the crust. In detail, our crustal model is less evolved than most other estimates but is more evolved than *Taylor and McLennan*'s [1985] average crust. In addition, our estimate is considerably lower in FeO than that of Taylor and McLennan. It is significant that the Mg # of our model is the highest of any estimate, reflecting the generally high Mg # of mafic lower crustal xenoliths (Table 6).

Trace element compositions of the different crustal models are plotted in Figure 12. In contrast to the major elements, our average crustal model bears closest similarity to the estimates of *Weaver and Tarney* [1984] and *Wedepohl* [1994] and has markedly higher incompatible trace element contents than the average crust deduced by Taylor and McLennan. Using our continental crust composition and the composition of the primitive mantle from *McDonough and Sun* [1995], we calculate the proportion of incompatible trace elements that are contained within the continental crust (Figure 13). It is apparent from this figure that the largest differences between estimates are for the alkali elements, Ba, Pb, Th, and U. Our estimate places 35–55% of the silicate Earth's budget for these elements within the continental crust.

We now return to the question of heat production in

TABLE 10. Selected Trace Element Ratios and Heat Production in Continental Crust

	Lower	*Middle*	*Upper*[a]	*Total*
Zr / Hf	36	31	33	33
Th / U	5.9	3.9	3.8	3.9
K / U (10^3)	23.8	10.7	10.0	10.1
K / Rb	413	270	250	252
Rb / Cs	35	25	20	22
Rb / Sr	0.033	0.22	0.32	0.18
Sr / Nd	30	12	13	16
La / Nb	1.6	2.2	1.2	1.5
Sm / Nd	0.25	0.18	0.17	0.19
Eu / Eu*	1.14	1.09	0.66	0.96
U / Pb	0.047	0.103	0.140	0.113
μ[b]	2.9	6.4	9	7.1
Heat production, $\mu W\ m^{-3}$	0.18	1.02	1.8	0.93
Heat flow,[c] $mW\ m^{-2}$				37

[a]From *Taylor and McLennan* [1985], except for Cs value from *McDonough et al.* [1992].

[b]Calculated assuming bulk crust $^{207}Pb/^{204}Pb = 15.5$, $^{206}Pb/^{204}Pb = 18.2$ and $^{208}Pb/^{204}Pb = 38$ [*Rudnick and Goldstein*, 1990] and upper crust $^{207}Pb/^{204}Pb = 19.3$, $^{206}Pb/^{204}Pb = 15.7$ and $^{208}Pb/^{204}Pb = 39.1$ [*Zartman and Doe*, 1981].

[c]Crustal contribution to heat flow, assuming 40-km-thick crust with average density of 2.8 g cm^{-3}.

the continental crust. Whereas our estimate of shield-platform crustal composition has a rather high heat production of 0.92 $\mu W\ m^{-3}$ (which corresponds to a heat flow of 40 $mW\ m^{-2}$ for a 43-km-thick crust (Table 8)), the Archean component of this crust has a heat production of only 0.66 $\mu W\ m^{-3}$. This corresponds to a crustal heat flow component of 28 $mW\ m^{-2}$, a value consistent with the heat flow studies of Archean regions reviewed above. This suggests that the low and uniform heat flow observed in Archean shields is due to the combined effects of low mantle heat flow (due to the insulating effects of a thick lithospheric mantle?) and low crustal heat production.

TABLE 11. Compositional Estimates of the Continental Crust

	Shaw et al. [1986]	*Wedepohl [1994]*	*Weaver and Tarney [1984]*	*Taylor and McLennan [1985]*	*This Study*
SiO_2, wt. %	63.2	61.5	63.2	57.3	59.1
TiO_2, wt. %	0.7	0.68	0.6	0.9	0.7
Al_2O_3, wt. %	14.8	15.1	16.1	15.9	15.8
FeO_T, wt. %	5.60	5.67	4.90	9.10	6.6
MnO, wt. %	0.09	0.10	0.08	0.18	0.11
MgO, wt. %	3.15	3.7	2.8	5.3	4.4
CaO, wt. %	4.66	5.5	4.7	7.4	6.4
Na_2O, wt. %	3.29	3.2	4.2	3.1	3.2
K_2O, wt. %	2.34	2.4	2.1	1.1	1.9
P_2O_5, wt. %	0.14	0.18	0.19		0.2
Mg #, mol	50.1	53.4	50.5	50.9	54.4
Li, ppm		17		13	11
Sc, ppm	13	16		30	22
V, ppm	96	101		230	131
Cr, ppm	90	132	56	185	119
Co, ppm	26	26		29	25
Ni, ppm	54	66	35	105	51
Cu, ppm	26	26		75	24
Zn, ppm	71	66		80	73
Ga, ppm		15		18	16
Rb, ppm	76	76	61	32	58
Sr, ppm	317	334	503	260	325
Y, ppm	26	24	14	20	20
Zr, ppm	203	201	210	100	123
Nb, ppm	20	18	13	11	12
Cs, ppm				1	2.6
Ba, ppm	764	576	707	250	390
La, ppm		25	28	16	18
Ce, ppm		60	57	33	42
Pr, ppm				3.9	5.0
Nd, ppm		27	23	16	20
Sm, ppm		5.3	4.1	3.5	3.9
Eu, ppm		1.3	1.09	1.1	1.2
Gd, ppm		4.1		3.3	3.6
Tb, ppm		0.65	0.53	0.6	0.56
Dy, ppm				3.7	3.5
Ho, ppm		0.78		0.78	0.76
Er, ppm				2.2	2.2
Yb, ppm		2.0	1.5	2.2	2.0
Lu, ppm		0.36	0.23	0.3	0.33
Hf, ppm	5	4.9	4.7	3	3.7
Ta, ppm	4	1.1		1	1.1
Pb, ppm	20	14.8	15	8	12.6
Th, ppm	9	8.5	5.7	3.5	5.6
U, ppm	1.8	1.7	1.3	0.91	1.42
Heat production[a], $\mu W\ m^{-3}$	1.31	1.25	0.92	0.58	0.93
Heat flow,[b] $mW\ m^{-2}$	52	50	37	23	37

[a]Assumes an average density of 2.8 $g\ cm^{-3}$.
[b]Assumes a 40-km-thick crust.

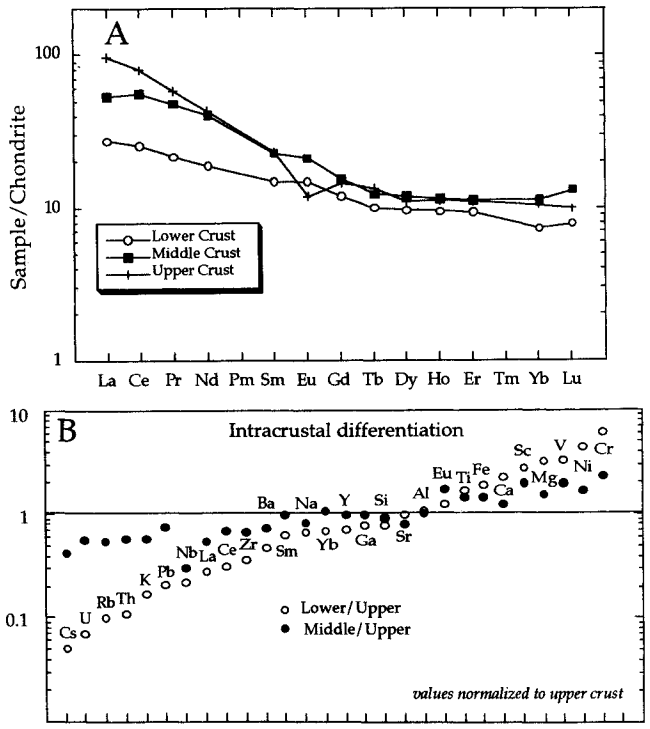

Figure 11. (a) Rare earth element patterns of upper [*Taylor and McLennan*, 1985], middle, and lower continental crust. (b) Relative enrichment/depletion of middle and lower crusts compared with upper crust.

Figure 14 presents a hypothetical continental cross section derived from the seismic data reviewed here. The crust is divided vertically into three layers on the basis of average seismic velocities determined for each type section. The use of a smooth pattern to illustrate the crustal layers is not meant to indicate lithological homogeneity (it is clear from a number of studies that the deep crust is lithologically diverse); the shading only indicates the average velocity of each layer (see Figure 2).

The diversity in average velocity, hence lithology, for the lower crust is reflected by the change in average SiO_2 and K_2O contents. These elements were chosen to illustrate chemical diversity because they are concentrated by igneous differentiation and therefore are sensitive indicators of the proportions of mafic to evolved rock types in the lower crust. Potassium contents of the lower crust vary by a factor of 3, with the highest values present in the lower crusts of extensional and contractional tectonic settings and the lowest values present in arcs and rifted margins, where

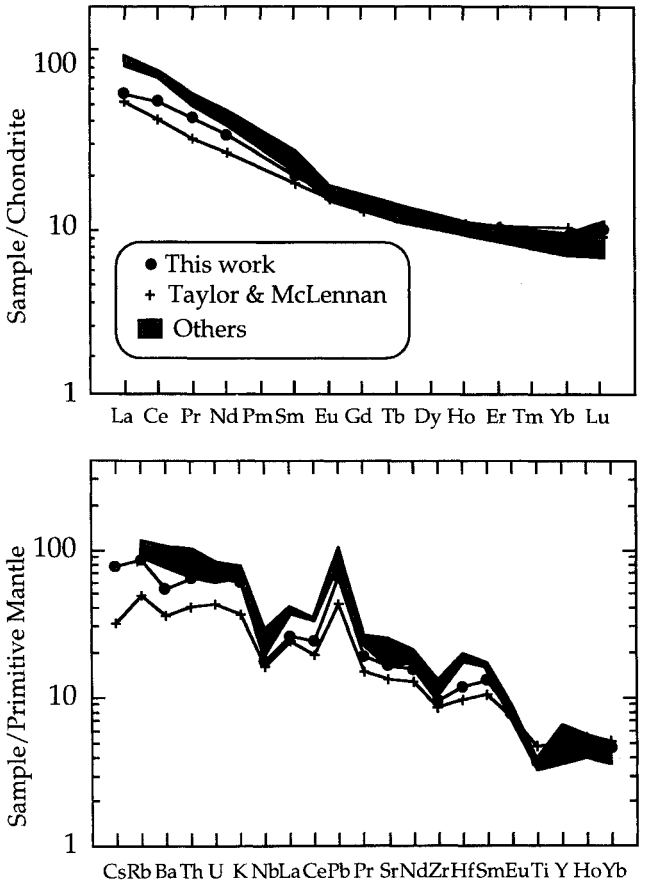

Figure 12. Comparisons of trace element content of continental crust determined from our model (solid circles) versus that of *Taylor and McLennan* [1985] (pluses) and others (*Weaver and Tarney* [1984], *Wedepohl* [1994], and *Shaw et al.* [1986]; shaded).

the lower crust appears to be dominated by mafic rock types. Shields and platforms, which constitute the largest volumetric proportion of the entire continental lower crust, also have relatively low K contents. Nevertheless, in comparison with oceanic crust (as sampled by mid-ocean ridge basalts), the mafic lower continental crust has ~10 to 30 times more K. SiO_2 varies sympathetically with K, but the overall variation is less (a factor of 1.1).

Delamination of the lower continental crust has been suggested to be an important process by which continental material is recycled into the convecting mantle [*Arndt and Goldstein*, 1989; *Kay and Kay*, 1991]. For this to be true, however, the lower crust must have an overall mafic composition so that it can transform to eclogite with a density exceeding that of the underlying mantle. If this process is shown to be geologically important, then our data suggest that significant quantities of incompatible trace elements may be lost from the continents in this manner owing to the presence of interlayered evolved rock types within a predominantly mafic lower crust.

7. CONCLUSIONS

The seismic, petrologic, and geochemical data reviewed here were used to develop a picture of the deep continental crust. Increasing average seismic velocities with depth indicate increasing proportions of mafic lithologies and increasing metamorphic grade. The lower crust consists of rocks in the granulite facies and has an average composition that varies between different tectonic provinces. The bulk lower crust has a mafic composition, approaching that of a primitive basalt. Felsic and intermediate lithologies are locally important in the lower crust and may give rise to seismic reflections that are observed in the lower crust of some regions. High-grade metamorphosed shales are also present in the lower crust, but their high heat production, coupled with their generally limited occurrence in lower crustal xenolith suites, suggests they are of minor volumetric significance in many areas. The highest-grade metapelites, which have lost a granitic melt fraction, have high seismic velocities and are seismically indistinguishable from mafic granulites. Such rocks are unlikely to be the cause of seismic reflections in the lower crust.

We have modeled the middle crust as consisting of rocks in the amphibolite facies, although granulites may also be present. Average middle crust *P* wave velocities are too low to be explained by dominantly mafic lithologies; thus the middle crust is modeled as a mixture of mafic, intermediate, and felsic amphibolite facies gneisses. This crustal layer has a significant amount of incompatible trace elements, including the heat-producing elements.

The bulk continental crust, modeled from the data presented here and using the upper crustal estimates of *Taylor and McLennan* [1985], has an intermediate composition and contains a significant proportion of the bulk Earth's highly incompatible trace element

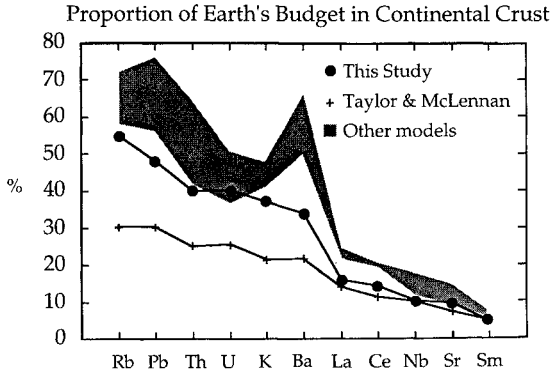

Figure 13. Proportion of elemental budget of bulk silicate Earth that is contained within the continental crust. The shaded region is range of model compositions listed in Table 11, circles are values from this study, and crosses are values from *Taylor and McLennan* [1985].

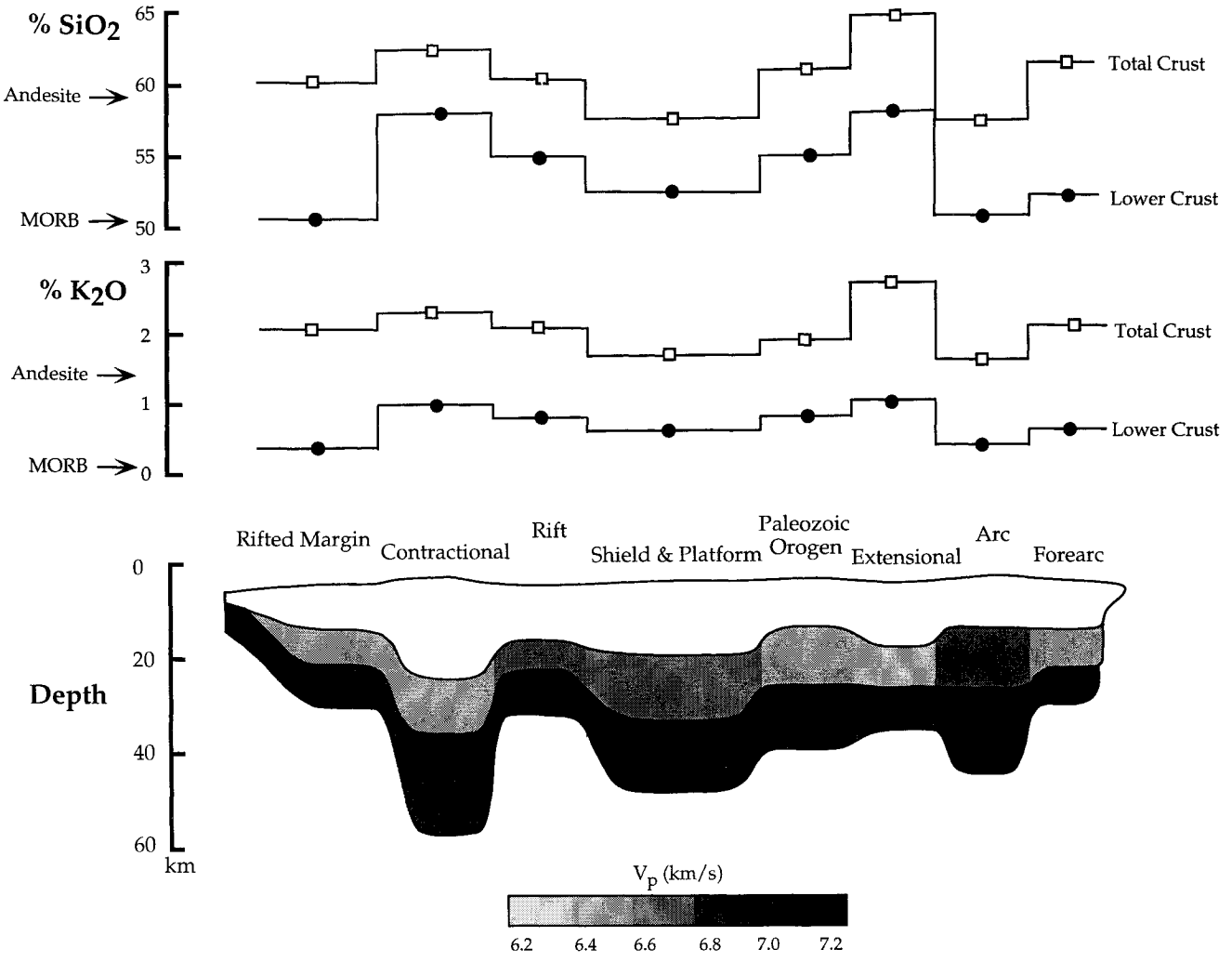

Figure 14. Hypothetical cross section of continental crust depicting average *P* wave velocities with depth for different type sections (scale given at bottom). Vertical exaggeration is approximately 17 times. An attempt was made to show the relative areal proportions of the different type sections, but to do this in absolute terms was not feasible owing to the very small areal extent of some type sections (e.g., active rifts constitute only 1% of total crustal area; see Table 7). Diversity in lithological assemblages of lower crust is reflected in the average K_2O and SiO_2 contents, shown above. Average normal mid-ocean ridge basalt (MORB) composition taken from *Hofmann* [1988]; average andesite composition taken from *Taylor and McLennan* [1985].

budget (35–55%). The basaltic lower continental crust has significantly greater incompatible trace element content compared with oceanic crust. If lower crustal delamination proves an important continental recycling process, then our data predict that significant amounts of incompatible trace elements may be returned to the mantle in this fashion.

ACKNOWLEDGMENTS. We thank Paul Troiano and Karen McIntosh for computing assistance. D.M.F.'s contribution was supported by NSF grants ISP-8011449, EAR-8300659, EAR-8410350, EAR-8720798, EAR-9003956, and EAR-9118318. Marilyn Holloway expertly assisted with preparation of tables. This work has benefited greatly from discussions with Paul Morgan, Walter Mooney, Scott Smithson, Al Levander, Bill McDonough, Ginny Sisson, and Anton Hales and reviews by Paul Morgan, Walter Mooney, Steve Bohlen, Scott McLennan, and Ian Jackson.

Thomas Torgersen was the editor responsible for this paper. He thanks Steve Bohlen and an anonymous referee for their technical reviews. He also thanks one anonymous cross-disciplinary reviewer.

REFERENCES

Aichroth, B., C. Prodehl, and H. Thybo, Crustal structure along the Central segment of the EGT from seismic-refraction studies, *Tectonophysics*, *207*, 43–64, 1992.

Armstrong, R. L., The persistent myth of crustal growth, *Aust. J. Earth Sci.*, *38*, 613–630, 1991.

Arndt, N. T., and S. L. Goldstein, An open boundary between lower continental crust and mantle: Its role in crust formation and crustal recycling, *Tectonophysics*, *161*, 201–212, 1989.

Asano, S., et al., Crustal structure in the northern part of the Philippine Sea plate as derived from seismic observations of Hatoyama off Izu Peninsula explosions, *J. Phys. Earth*, *33*, 173–189, 1985.

Ashwal, L. D., *Anorthosites*, 422 pp., Springer-Verlag, New York, 1993.

Ashwal, L. D., P. Morgan, S. A. Kelley, and J. A. Percival, Heat production in an Archean crustal profile and implications for heat flow and mobilization of heat-producing elements, *Earth Planet. Sci. Lett.*, *85*, 439–450, 1987.

Azbel, I. Y., A. F. Buyanov, V. T. Ionkis, N. V. Sharov, and V. P. Sharova, Crustal structure of the Kola Peninsula from inversion of deep seismic sounding data, *Tectonophysics*, *162*, 87–99, 1989.

BABEL Working Group, Integrated seismic studies of the Baltic shield using data in the Gulf of Bothnia region, *Geophys. J. Int.*, *112*, 305–324, 1993.

Babuška, V., Elasticity and anisotropy of dunite and bronzitite, *J. Geophys. Res.*, *77*, 6955–6965, 1972.

Baier, B., H. Berckhemer, D. Gajewski, R. W. Green, C. Grimsel, C. Prodehl, and R. Vees, Deep seismic sounding in the area of the Damara orogen, Namibia, South West Africa, in *Intracontinental Fold Belts*, edited by H. Martin, and F. W. Eder, pp. 885–900, Springer-Verlag, New York, 1983.

Bamford, D., K. Nunn, C. Prodehl, and B. Jacob, LISPB, IV, Crustal structure of northern Britain, *Geophys. J. R. Astron. Soc.*, *54*, 43–60, 1978.

Banda, E., E. Suriñach, A. Aparicio, J. Sierra, and E. Ruiz de la Parte, Crust and upper mantle structure of the central Iberian Meseta (Spain), *Geophys. J. R. Astron. Soc.*, *67*, 779–789, 1981.

Barnes, A. E., Moho reflectivity and seismic signal penetration, *Tectonophysics*, *232*, 299–307, 1994.

Barruol, G., D. Mainprice, H. Kern, M. de Saint Blanquat, and P. P. Compte, 3D seismic study of a ductile shear zone from laboratory and petrofabric data (Saint Barthélémy Massif, northern Pyrénées, France), *Terra Nova*, *4*, 63–67, 1992.

Bates, R. L., and J. A. Jackson (Eds) *Glossary of Geology*, 2nd ed., 749 pp., Am. Geol. Inst., Alexandria, Va., 1980.

Beaudoin, B. C., G. S. Fuis, W. J. Lutter, W. D. Mooney, and T. E. Moore, Crustal velocity structure of the northern Yukon-Tanana upland, central Alaska: Results from TACT refraction/wide-angle reflection data, *Geol. Soc. Am. Bull.*, *106*, 981–1001, 1994.

Birch, F., The velocity of compressional waves in rocks to 10 kbar, 1, *J. Geophys. Res.*, *65*, 1083–1102, 1960.

Birch, F., The velocity of compressional waves in rocks to 10 kbar, 2, *J. Geophys. Res.*, *66*, 2199–2224, 1961.

Blackwell, D. D., and J. L. Steele, Geothermal map of North America, *Geol. Soc. of Am.*, Boulder, Colo., 1991.

Bohlen, S. R., On the formation of granulites, *J. Metamorph. Geol.*, *9*, 223–229, 1991.

Bohlen, S. R., and K. Mezger, Origin of granulite terranes and the formation of the lowermost continental crust, *Science*, *244*, 326–329, 1989.

Boland, A. V., and R. M. Ellis, Velocity structure of the Kapuskasing uplift, northern Ontario, from seismic refraction studies, *J. Geophys. Res.*, *94*, 7189–7204, 1989.

Boland, A. V., and R. M. Ellis, A geophysical model for the Kapuskasing uplift from seismic and gravity studies, *Can. J. Earth Sci.*, *28*, 342–354, 1991.

Bott, M. H. P., *The Interior of the Earth: Its Structure, Constitution and Evolution*, 403 pp., Elsevier Sci., New York, 1982.

Bott, M. H. P., R. E. Long, A. S. P. Green, A. H. J. Lewis, M. C. Sinha, and D. L. Stevenson, Crustal structure south of the Iapetus suture beneath northern England, *Nature*, *314*, 724–727, 1985.

Brock, A., Heat flow measurements in Ireland, *Tectonophysics*, *164*, 231–236, 1989.

Boyd, F. R., Siberian geotherm based on lherzolite xenoliths from the Udachnaya kimberlite, U.S.S.R., *Geology*, *12*, 528–530, 1984.

Braile, L. W., et al., The Yellowstone–Snake River Plain seismic profiling experiment: Crustal structure of the eastern Snake River Plain, *J. Geophys. Res.*, *87*, 2597–2609, 1982.

Burke, M. M., and D. M. Fountain, Seismic properties of rocks from an exposure of extended continental crust—New laboratory measurements from the Ivrea zone, *Tectonophysics*, *182*, 119–146, 1990.

Burlini, L., and D. M. Fountain, Seismic anisotropy of metapelites from the Ivrea-Verbano zone and Serie dei Laghi (northern Italy), *Phys. Earth Planet. Inter.*, *78*, 301–317, 1993.

Cameron, K. L., J. V. Robinson, S. Niemeyer, G. J. Nimz, D. C. Kuentz, R. S. Harmon, S. R. Bohlen, and K. D. Collerson, Contrasting styles of pre-Cenozoic and mid-Tertiary crustal evolution in northern Mexico: Evidence from deep crustal xenoliths from La Olivina, *J. Geophys. Res.*, *97*, 17,353–17,376, 1992.

Campbell, I. H., and S. R. Taylor, No water, no granites—No oceans, no continents, *Geophys. Res. Lett.*, *10*, 1061–1064, 1985.

Cermák, V., Heat flow map of Europe, in *Terrestrial Heat Flow in Europe*, edited by V. Cermák and L. Rybach, pp. 3–40, Springer-Verlag, New York, 1979.

Cermák, V., Lithospheric thermal regimes in Europe, *Phys. Earth Planet. Inter.*, *79*, 179–193, 1993.

Chapman, D., and K. Furlong, Thermal state of the continental crust, in *Continental Lower Crust*, edited by D. M. Fountain, R. Arculus, and R. W. Kay, pp. 179–200, Elsevier Sci., New York, 1992.

Chapman, D. S., H. N. Pollack, and V. Cermák, Global heat flow with special reference to the region of Europe, in *Terrestrial Heat Flow in Europe*, edited by V. Cermák and L. Rybach, pp. 41–48, Springer-Verlag, New York, 1979.

Chen, Y. D., S. Y. O'Reilly, P. D. Kinny, and W. L. Griffin, Dating lower crust and upper mantle events: An ion microprobe study of xenoliths from kimberlitic pipes, South Australia, *Lithos*, *32*, 74–94, 1994.

Chian, D., and K. Louden, The structure of Archean-Ketilidean crust along the continental shelf of southwestern Greenland from a seismic refraction profile, *Can. J. Earth Sci.*, *29*, 301–313, 1992.

Christensen, N. I., Compressional wave velocities in metamorphic rocks at pressures to 10 kbar, *J. Geophys. Res.*, *70*, 6147–6164, 1965.

Christensen, N. I., Elasticity of ultrabasic rocks, *J. Geophys. Res.*, *71*, 5921–5931, 1966a.

Christensen, N. I., Shear-wave velocities in metamorphic rocks at pressures to 10 kbar, *J. Geophys. Res.*, *71*, 3549–3556, 1966b.

Christensen, N. I., Fabric anisotropy, and tectonic history of Twin Sisters Dunite, Washington, *Geol. Soc. Am. Bull.*, *82*, 1681–1694, 1971.

Christensen, N. I., Compressional wave velocities in possible mantle rocks to pressures of 30 kbar, *J. Geophys. Res.*, *79*, 407–412, 1974.

Christensen, N. I., and D. M. Fountain, Constitution of the lower continental crust based on experimental studies of seismic velocities in granulite, *Geol. Soc. Am. Bull.*, *86*, 227–236, 1975.

Christensen, N. I., and W. D. Mooney, Seismic velocity structure and composition of the continental crust: A global view, *J. Geophys. Res.*, *100*, 9761–9788, 1995.

Christensen, N. I., and R. Ramananantoandro, Elastic moduli and anisotropy of dunite to 10 kbar, *J. Geophys. Res.*, *76*, 4003–4010, 1971.

Christensen, N. I., and D. L. Szymanski, Origin of reflections from the Brevard fault zone, *J. Geophys. Res.*, *93*, 1087–1102, 1988.

Christensen, N. I., and W. W. Wepfer, Laboratory techniques for determining seismic velocities and attenuations, with applications to the continental lithosphere, in *Geophysical Framework of the Continental United States*, edited by L. C. Pakiser and W. D. Mooney, pp. 91–102, Geol. Soc. Am., Boulder, Colo., 1989.

Clowes, R. M., E. Gens-Lenartowicz, M. Demartin, and S. Saxov, Lithospheric structure in southern Sweden—Results from FENNOLORA, *Tectonophysics*, *142*, 1–14, 1987.

Cogley, J. G., Continental margins and the extent and number of the continents, *Rev. Geophys.*, *22*, 101–122, 1984.

Colburn, R. H., and W. D. Mooney, Two-dimensional velocity structure along the synclinal axis of the Great Valley, California, *Bull. Seismol. Soc. Am.*, *76*, 1305–1322, 1986.

Condie, K. C., *Plate Tectonics and Crustal Evolution*, 476 pp., Pergamon, New York, 1989.

Coolen, J. J. M. M. M., *Chemical Petrology of the Furua Granulite Complex, Southern Tanzania, GUA Pap. Geol.*, 13-1980, 258 pp., 1980.

Cull, J. P., Heat flow and regional geophysics in Australia, in *Terrestrial Heat Flow and the Lithosphere Structure*, edited by V. Cermák and L. Rybach, pp. 486–500, Springer-Verlag, New York, 1991.

Deichmann, N., J. Ansorge, and S. Mueller, Crustal structure of the southern Alps beneath the intersection with the European geotraverse, *Tectonophysics*, *126*, 57–83, 1986.

Dhaliwal, H., and E. K. Graham, A comparison of theoretical rock models with laboratory data, *Tectonophysics*, *188*, 373–383, 1991.

Duncan, R. A., and I. McDougall, Volcanic time-space relationships, in *Intraplate Volcanism in Eastern Australia and New Zealand*, edited by R. W. Johnson, pp. 43–54, Cambridge Univ. Press, New York, 1989.

Durrheim, R. J., and R. W. E. Green, A seismic refraction investigation of the Archaean Kaapvaal Craton, South Africa, using mine tremors as the energy source, *Geophys. J. Int.*, *108*, 812–832, 1992.

Durrheim, R. J., and W. D. Mooney, The evolution of the Precambrian lithosphere: Seismological and geochemical constraints, *J. Geophys. Res.*, *99*, 15,359–15,374, 1994.

Egloff, F., R. Rihm, J. Makris, Y. A. Izzeldin, M. Bobsein, K. Meier, P. Junge, T. Noman, and W. Warsi, Contrasting structural styles of the eastern and western margins of the southern Red Sea: The 1988 SONNE experiment, *Tectonophysics*, *198*, 329–353, 1991.

El-Isa, Z., J. Mechie, and C. Prodehl, Shear velocity structure of Jordan from explosion seismic data, *Geophys. J. R. Astron. Soc.*, *90*, 265–281, 1987a.

El-Isa, Z., J. Mechie, C. Prodehl, J. Makris, and R. Rihm, A crustal structure of Jordan derived from seismic refraction data, *Tectonophysics*, *138*, 235–253, 1987b.

Epili, D., and R. F. Mereu, The Grenville Front Tectonic Zone: Results from the 1986 Great Lakes onshore seismic wide-angle reflection and refraction experiment, *J. Geophys. Res.*, *96*, 16,335–16,348, 1991.

EUGENO-S Working Group, Crustal structure and tectonic evolution of the transition between the Baltic shield and the North German Caledonides (the EUGENO-S Project), *Tectonophysics*, *150*, 253–348, 1988.

Finlayson, D. M., Geophysical differences in the lithosphere between Phanerozoic and Precambrian Australia, *Tectonophysics*, *84*, 287–312, 1982.

Finlayson, D. M., C. D. N. Collins, and D. Denham, Crustal structure under the Lachlan fold belt, southeastern Australia, *Phys. Earth Planet. Inter.*, *21*, 321–342, 1980.

Finnerty, A. A., and F. R. Boyd, Thermobarometry for garnet peridotites: Basis for the determination of thermal and compositional structure of the upper mantle, in *Mantle Xenoliths*, edited by P. H. Nixon, pp. 381–402, John Wiley, New York, 1987.

Forsyth, D. A., M. Argyle, A. Okulitch, and H. P. Trettin, New seismic, magnetic, and gravity constraints on the crustal structure of the Lincoln Sea continent-ocean transition, *Can. J. Earth Sci.*, *31*, 905–918, 1994.

Fountain, D. M., Seismic velocities in granulite facies rocks and rocks from the Ivrea-Verbano and Strona-Ceneri zones: A study of continental crustal composition, Ph.D. dissertation, Univ. of Wash., Seattle, 1974.

Fountain, D. M., The Ivrea-Verbano and Strona-Ceneri zones, northern Italy: A cross-section of the continental crust—New evidence from seismic velocities of rock samples, *Tectonophysics*, *33*, 145–165, 1976.

Fountain, D. M., Is there a relationship between seismic velocity and heat production for crustal rocks?, *Earth Planet. Sci. Lett.*, *79*, 145–150, 1986.

Fountain, D. M., and N. I. Christensen, Composition of the continental crust and upper mantle; A review, *Mem. Geol. Soc. Am.*, *172*, 711–742, 1989.

Fountain, D. M., and M. H. Salisbury, Exposed cross-sections through the continental crust: Implications for crustal structure, petrology, and evolution, *Earth Planet. Sci. Lett.*, *56*, 263–277, 1981.

Fountain, D. M., and M. H. Salisbury, Seismic properties of the Superior Province crust based on seismic velocity measurements on rocks from the Michipicoten-Wawa-Kapuskasing terranes, Ontario (abstract), *Geol. Assoc. Can. Abstr. Program*, *11*, 69, 1986.

Fountain, D. M., M. H. Salisbury, and K. P. Furlong, Heat production and thermal conductivity of rocks from the Pikwitonei-Sachigo continental cross section, central Manitoba: Implications for the thermal structure of Archean crust, *Can. J. Earth Sci.*, *24*, 1583–1594, 1987.

Fountain, D. M., M. H. Salisbury, and J. Percival, Seismic structure of the continental crust based on rock velocity measurements from the Kapuskasing uplift, *J. Geophys. Res.*, *95*, 1167–1186, 1990.

Fountain, D. M., T. M. Boundy, H. Austrheim, and P. Rey, Eclogite-facies shear zones—Deep crustal reflectors?, *Tectonophysics*, *232*, 411–424, 1994a.

Fountain, D. M., P. Rey, and H. Austrheim, Seismic velocities across the garnet granulite-eclogite facies transition (abstract), *Eos Trans. AGU*, *75*(44), Fall Meet. suppl., 676, 1994b.

Fowler, C. M. R., *The Solid Earth*, 472 pp., Cambridge Univ. Press, New York, 1990.

Fowler, S. R., R. S. White, G. D. Spence, and G. K. Westbrook, The Hatton Bank continental margin, II, Deep structure from two-ship expanding spread seismic profiles, *Geophys. J.*, *96*, 295–309, 1989.

Frost, B. R., and K. Bucher, Is water responsible for geophysical anomalies in the deep continental crust?, A petrological perspective, *Tectonophysics*, *231*, 293–309, 1994.

Fuis, G. S., W. D. Mooney, J. H. Healy, G. A. McMechan, and W. J. Lutter, A seismic refraction survey of the Imperial Valley region, California, *J. Geophys. Res.*, *89*, 1165–1189, 1984.

Furlong, K. P., and D. S. Chapman, Crustal heterogeneities and the thermal structure of the continental crust, *Geophys. Res. Lett.*, *14*, 314–317, 1987.

Gajewski, D., and C. Prodehl, Seismic refraction investiga-

tion of the Black Forest, *Tectonophysics*, *142*, 27–48, 1987.

Gajewski, D., W. S. Holbrook, and C. Prodehl, A three-dimensional crustal model of southwest Germany derived from seismic refraction data, *Tectonophysics*, *142*, 49–70, 1987.

Gaulier, J. M., X. Le Pichon, N. Lyberis, F. Avedik, L. Geli, I. Moretti, A. Deschamps, and S. Hafez, Seismic study of the crust of the northern Red Sea and Gulf of Suez, *Tectonophysics*, *153*, 55–88, 1988.

Gettings, M. E., H. R. J. Blank, W. D. Mooney, and J. H. Healey, Crustal structure of southwestern Saudi Arabia, *J. Geophys. Res.*, *91*, 6491–6512, 1986.

Ginzburg, A., J. Makris, K. Fuchs, and C. Prodehl, The structure of the crust and upper mantle in the Dead Sea rift, *Tectonophysics*, *80*, 109–119, 1981.

Ginzburg, A., R. B. Whitmarsh, D. G. Roberts, L. Montadert, A. Camus, and F. Avedik, The deep seismic structure of the northern continental margin of the Bay of Biscay, *Ann. Geophys.*, *3*, 499–510, 1985.

Goff, J. A., K. Holliger, and A. Levander, Modal fields: A new method for characterization of random velocity heterogeneity, *Geophys. Res. Lett.*, *21*, 493–496, 1994.

Gohl, K., and S. B. Smithson, Structure of Archean crust and passive margin of southwest Greenland from seismic wide-angle data, *J. Geophys. Res.*, *98*, 6623–6638, 1993.

Goodwin, A. M., *Precambrian Geology*, 666 pp., Academic, San Diego, Calif., 1991.

Goodwin, E. B., and J. McCarthy, Composition of the lower crust in west central Arizona from three-component seismic data, *J. Geophys. Res.*, *95*, 20,097–20,109, 1991.

Grad, M., and U. Luosto, Seismic models of the crust of the Baltic shield along the SVEKA profile in Finland, *Ann. Geophys.*, *5*, 639–650, 1987.

Gupta, M. L., S. R. Sharma, and A. Sundar, Heat flow pattern and lithospheric thickness of peninsular India, in *Terrestrial Heat Flow and the Lithosphere Structure*, edited by V. Cermák and L. Rybach, pp. 283–307, Springer-Verlag, New York, 1991.

Guterch, A., M. Grad, and R. Materzok, Structure of the Earth's crust of the Permian basin in Poland, *Acta Geophys. Pol.*, *31*, 121–138, 1983.

Halchuk, S. C., and R. F. Mereu, A seismic investigation of the crust and Moho underlying the Peace River Arch, *Tectonophysics*, *185*, 1–9, 1990.

Hale, L. D., and G. A. Thompson, The seismic reflection character of the continental Mohorovičić discontinuity, *J. Geophys. Res.*, *87*, 4625–4635, 1982.

Halliday, A. N., A. P. Dickin, R. N. Hunter, G. R. Davies, T. J. Dempster, P. J. Hamilton, and B. G. Upton, Formation and composition of lower continental crust: Evidence from Scottish xenolith suites, *J. Geophys. Res.*, *98*, 581–608, 1993.

Hanchar, J. M., and R. L. Rudnick, Revealing hidden structures: The application of cathodoluminescence and back scattered electron imaging to dating zircons from lower crustal xenoliths, *Lithos*, in press, 1995.

Hanchar, J. M., C. F. Miller, J. L. Wooden, V. C. Bennett, and J.-M. G. Staude, Evidence from xenoliths for a dynamic lower crust, eastern Mojave desert, California, *J. Petrol.*, *35*, 1377–1415, 1994.

Harley, S. L., The origin of granulites: A metamorphic perspective, *Geol. Mag.*, *126*, 215–247, 1989.

Harley, S. L., Proterozoic granulite terranes, in *Proterozoic Crustal Evolution*, edited by K. C. Condie, pp. 301–359, Elsevier, New York, 1992.

Hart, R. J., L. O. Nicolaysen, and N. H. Gale, Radioelement concentrations in the deep profile through Precambrian basement of the Vredefort structure, *J. Geophys. Res.*, *86*, 10,639–10,652, 1981.

Hennet, C. G., J. H. Luetgert, and R. A. Phinney, The crustal structure in central Maine from coherency processed refraction data, *J. Geophys. Res.*, *96*, 12,023–12,037, 1991.

Hofmann, A. W., Chemical differentiation of the Earth: The relationship between mantle, continental crust, and oceanic crust, *Earth Planet. Sci. Lett.*, *90*, 297–314, 1988.

Holbrook, W. S., The crustal structure of the northwestern Basin and Range province, Nevada, from wide-angle seismic data, *J. Geophys. Res.*, *95*, 21,843–21,869, 1990.

Holbrook, W. S., and W. D. Mooney, The crustal structure of the axis of the Great Valley, California, from seismic refraction measurements, *Tectonophysics*, *140*, 49–63, 1987.

Holbrook, W. S., D. Gajewski, A. Krammer, and C. Prodehl, An interpretation of wide-angle compressional and shear wave data in southwest Germany: Poisson's ratio and petrological implications, *J. Geophys. Res.*, *93*, 12,081–12,106, 1988.

Holbrook, W. S., W. D. Mooney, and N. I. Christensen, The seismic velocity structure of the deep continental crust, in *Continental Lower Crust*, edited by D. M. Fountain, R. Arculus, and R. W. Kay, pp. 1–44, Elsevier Sci., New York, 1992.

Holbrook, W. S., G. M. Purdy, R. E. Sheridan, L. Glover III, M. Talwani, J. Ewing, and D. Hutchinson, Seismic structure of the U.S. Mid-Atlantic continental margin, *J. Geophys. Res.*, *99*, 17,871–17,891, 1994a.

Holbrook, W. S., E. C. Reiter, G. M. Purdy, D. Sawyer, P. L. Stoffa, J. A. Austin Jr., J. Oh, and J. Makris, Deep structure of the U.S. Atlantic continental margin, offshore South Carolina, from coincident ocean bottom and multichannel seismic data, *J. Geophys. Res.*, *99*, 9155–9178, 1994b.

Hole, J. A., R. M. Clowes, and R. M. Ellis, Interpretation of three-dimensional seismic refraction data from western Hecate Strait, British Columbia: Structure of the crust, *Can. J. Earth Sci.*, *30*, 1440–1452, 1993.

Holliger, K., and A. R. Levander, A stochastic view of lower crustal fabric based on evidence from the Ivrea zone, *Geophys. Res. Lett.*, *19*, 1153–1156, 1992.

Holliger, K., A. R. Levander, and J. A. Goff, Stochastic modeling of the reflective lower crust: Petrophysical and geological evidence from the Ivrea zone (northern Italy), *J. Geophys. Res.*, *98*, 11,967–11,980, 1993.

Horsefield, S. J., R. B. Whitmarsh, R. S. White, and J.-C. Sibuet, Crustal structure of the Goban Spur rifted continental margin, NE Atlantic, *Geophys. J. Int.*, *119*, 1–19, 1993.

Howie, J. M., K. C. Miller, and W. U. Savage, Integrated crustal structure across the south central California margin: Santa Lucia escarpment to the San Andreas fault, *J. Geophys. Res.*, *98*, 8173–8196, 1993.

Huang, S., and J. Wang, On variations of heat flow and *Pn* velocity–A case study from the continental area of China, *J. Geodyn.*, *13*, 13–28, 1991.

Hughes, S., and J. H. Luetgert, Crustal structure of the western New England Appalachians and the Adirondack Mountains, *J. Geophys. Res.*, *96*, 13,471–16,494, 1991.

Hughes, S., and J. H. Luetgert, Crustal structure of the southeastern Grenville province, northern New York State and eastern Ontario, *J. Geophys. Res.*, *97*, 17,455–17,479, 1992.

Hughes, S., J. H. Luetgert, and N. I. Christensen, Reconciling deep seismic refraction and reflection data from the Grenvillian-Appalachian boundary in western New England, *Tectonophysics*, *225*, 255–269, 1993.

Hurich, C. A., and S. B. Smithson, Compositional variation and the origin of deep crustal reflections, *Earth Planet. Sci. Lett.*, *85*, 416–426, 1987.

Hurley, P. M., and J. R. Rand, Pre-drift continental nuclei, *Science*, *164*, 1229–1242, 1969.

Iwasaki, T., M. A. Sellevoll, T. Kanazawa, T. Veggeland, and H. Shimamura, Seismic refraction crustal study along the Sognefjord, south-west Norway, employing ocean bottom seismometers, *Geophys. J. Int.*, *119*, 791–808, 1994a.

Iwasaki, T., T. Yoshii, T. Moriya, A. Kobayashi, M. Nishiwaki, T. Tsutsui, T. Iidaka, A. Ikami, and T. Masuda, Precise *P* and *S* wave velocity structures in the Kitakami massif, northern Honshu, Japan, from a seismic refraction experiment, *J. Geophys. Res.*, *99*, 22,187–22,204, 1994b.

Jackson, I., The petrophysical basis for the interpretation of seismological models of the continental lithosphere, *Spec. Publ. Geol. Soc. Aust.*, *17*, 81–114, 1991.

Jackson, I., R. L. Rudnick, S. Y. O'Reilly, and C. Bezant, Measured and calculated elastic wave velocities for xenoliths from the lower crust and upper mantle, *Tectonophysics*, *173*, 207–210, 1990.

Jacob, A. W. B., W. Kaminski, T. Murphy, W. E. A. Phillips, and C. Prodehl, A crustal model for a northeast-southwest profile through Ireland, *Tectonophysics*, *113*, 75–103, 1985.

Jaupart, C., Horizontal heat transfer due to radioactivity contrasts: Causes and consequences of the linear heat flow relation, *Geophys. J. R. Astron. Soc.*, *75*, 411–435, 1983.

Jessop, A. M., Terrestrial heat flow in Canada, in *Neotectonics of North America*, edited by D. B. Slemmons, E. R. Engdahl, M. D. Zoback, and D. D. Blackwell, pp. 437–444, Geol. Soc. of Am., Boulder, Colo., 1991.

Jones, A. G., Electrical properties of the lower continental crust, in *Continental Lower Crust*, edited by D. M. Fountain, R. Arculus, and R. W. Kay, pp. 81–144, Elsevier, New York, 1992.

Jones, M. Q. W., Heat flow in the Witwatersrand basin and environs and its significance for the South African shield geotherm and lithosphere thickness, *J. Geophys. Res.*, *93*, 3243–3260, 1988.

Jones, T., and A. Nur, The nature of seismic reflections from deep crustal fault zones, *J. Geophys. Res.*, *89*, 3153–3171, 1984.

Kaila, K. L., I. B. P. Rao, P. K. Rao, N. M. Rao, V. G. Krishna, and A. R. Sridhar, DSS studies over Deccan Traps along the Thuadara-Sendhwa-Sindad profile, across Narmada-Son lineament, India, in *Properties and Processes of Earth's Lower Crust*, *Geophys. Monogr. Ser.*, vol. 51, edited by R. F. Mereu, S. Müller, and D. M. Fountain, pp. 121–125, AGU, Washington, D. C., 1989.

Kan, R.-J., H.-X. Hu, R.-S. Zeng, W. D. Mooney, and T. V. McEvilly, Crustal structure of Yunnan province, People's Republic of China, from seismic refraction profiles, *Science*, *234*, 433–437, 1986.

Kanasewich, E. R., et al., Seismic studies of the crust under the Williston Basin, *Can. J. Earth Sci.*, *24*, 2160–2171, 1987.

Kanasewich, E. R., M. J. A. Burianyk, R. M. Ellis, R. M. Clowes, D. M. White, T. Côté, D. A. Forsyth, J. H. Luetgert, and G. D. Spence, Crustal velocity structure of the Omineca belt, southeastern Canadian Cordillera, *J. Geophys. Res.*, *99*, 2653–2670, 1994.

Kay, R. W., and S. M. Kay, Creation and destruction of lower continental crust, *Geol. Rundsch.*, *80*, 259–278, 1991.

Keller, G. R., R. B. Smith, and L. W. Braile, Crustal structure along the Great Basin–Colorado plateau transition from seismic refraction studies, *J. Geophys. Res.*, *80*, 1093–1098, 1975.

Kern, H., *P*- and *S*-wave velocities in crustal and mantle rocks under the simultaneous action of high confining pressure and high temperature and the effect of rock microstructure, in *High-Pressure Researches in Geoscience*, edited by W. Schreyer, pp. 15–45, E. Schweizerbart'sche, Stuttgart, Germany, 1982.

Kern, H., and A. Richter, Temperature derivatives of compressional and shear wave velocities in crustal and mantle rocks at 6 kbar confining pressure, *J. Geophys.*, *49*, 47–56, 1981.

Kern, H., and V. Schenk, Elastic wave velocities in rocks from a lower crustal section in southern Calabria (Italy), *Phys. Earth Planet. Inter.*, *40*, 147–160, 1985.

Kern, H., and V. Schenk, A model of velocity structure beneath Calabria, southern Italy, based on laboratory data, *Earth Planet. Sci. Lett.*, *87*, 325–337, 1988.

Kern, H., and J. M. Tubia, Pressure and temperature dependence of *P*- and *S*-wave velocities, seismic anisotropy and density of sheared rocks from the Sierra Alpujata (Ronda peridotites, southern Spain), *Earth Planet. Sci. Lett.*, *119*, 191–205, 1993.

Kern, H., and H.-R. Wenk, Fabric-related velocity anisotropy and shear wave splitting in rocks from the Santa Rosa mylonite zone, California, *J. Geophys. Res.*, *95*, 11,213–11,223, 1990.

Kern, H., C. Walther, E. R. Flüh, and M. Marker, Seismic properties of rocks exposed in the POLAR profile region—Constraints on the interpretation of refraction data, *Precambrian Res.*, *64*, 169–187, 1993.

Kerr, R. C., Convective crystal dissolution, *Contrib. Mineral. Petrol.*, in press, 1995.

Krauskopf, K. B., *Introduction to Geochemistry*, 721 pp., McGraw-Hill, New York, 1967.

Kremenetsky, A. A., and L. N. Ovchinnikov, The Precambrian continental crust: Its structure, composition and evolution as revealed by deep drilling in the U.S.S.R., *Precambrian Res.*, *33*, 11–43, 1986.

Kumazawa, M., H. Helmstaedt, and K. Masaki, Elastic properties of eclogite xenoliths from diatremes of the east Colorado plateau and their implication to the upper mantle structure, *J. Geophys. Res.*, *76*, 1231–1247, 1971.

Kushiro, I., Partial melting of mantle wedge and evolution of island arc crust, *J. Geophys. Res.*, *95*, 15,929–15,939, 1990.

Lambert, I. B., Investigations of high grade regional metamorphic and associated rocks, Ph.D. thesis, Aust. Natl. Univ., Canberra, 1967.

LASE Study Group, Deep structure of the U.S. East Coast passive margin from large aperture seismic experiments (LASE), *Mar. Pet. Geol.*, *3*, 234–242, 1986.

Leaver, D. S., W. D. Mooney, and W. M. Kohler, A seismic refraction study of the Oregon Cascades, *J. Geophys. Res.*, *89*, 3121–3134, 1984.

Le Bas, M. J., and A. L. Streckeisen, The IUGS systematics of igneous rocks, *J. Geol. Soc. London*, *148*, 825–833, 1991.

Levander, A. R., and K. Holliger, Small-scale heterogeneity and large-scale velocity structure of the continental crust, *J. Geophys. Res.*, *97*, 8797–8804, 1992.

Levander, A., R. W. Hobbs, S. K. Smith, R. W. England, D. B. Snyder, and K. Holliger, The crust as a heterogeneous "optical" medium, of "crocodiles in the mist," *Tectonophysics*, *232*, 281–297, 1994.

Lewis, T., Heat flux in the Canadian Cordillera, in *Neotectonics of North America*, edited by D. B. Slemmons,

E. R. Engdahl, M. D. Zoback, and D. D. Blackwell, pp. 445–456, Geol. Soc. of Am., Boulder, Colo., 1991.

Lister, J. R., and R. C. Kerr, Fluid-mechanical models of crack propagation and their application to magma transport in dykes, *J. Geophys. Res.*, *96*, 10,049–10,077, 1991.

Lizarralde, D., W. S. Holbrook, and J. Oh, Crustal structure across the Brunswick magnetic anomaly, offshore Georgia, from coincident ocean bottom and multichannel seismic data, *J. Geophys. Res.*, *99*, 21,741–21,757, 1994.

Long, R. E., P. A. Matthews, and D. P. Graham, The nature of crustal boundaries: Combined interpretation of wide-angle and normal incidence seismic data, *Tectonophysics*, *232*, 309–318, 1994.

Luetgert, J. H., and C. E. Mann, Avalon terrane in eastern coastal Maine: Seismic refraction-wide-angle reflection data, *Geology*, *18*, 878–881, 1990.

Luetgert, J. H., H. M. Benz, and S. Madabhushi, Crustal structure beneath the Atlantic coastal plain of South Carolina, *Seismol. Res. Lett.*, *65*, 180–191, 1994.

Luetgert, J. H., C. E. Mann, and S. L. Klemperer, Wide-angle deep crustal reflections in the northern Appalachians, *Geophys. J. R. Astron. Soc.*, *89*, 183–188, 1987.

Luosto, U., and H. Korhonen, Crustal structure of the Baltic shield based on off-Fennolora refraction data, *Tectonophysics*, *128*, 183–208, 1986.

Luosto, U., E. R. Flüh, C.-E. Lund, and W. Group, The crustal structure along the POLAR profile from seismic refraction investigations, *Tectonophysics*, *162*, 51–85, 1989.

Luosto, U., T. Tiira, H. Korhonen, I. Azbel, V. Burmin, A. Buyanov, I. Kosminskaya, V. Ionkis, and N. Sharov, Crust and upper mantle structure along the DSS Baltic profile in SE Finland, *Geophys. J. Int.*, *101*, 89–110, 1990.

Lutter, W. J., and R. L. Nowack, Inversion for crustal structure using reflections from the PASSCAL Ouachita experiment, *J. Geophys. Res.*, *95*, 4633–4646, 1990.

MacGregor-Scott, N., and A. Walter, Crustal velocities near Coalinga, California, modeled from a combined earthquake/explosion refraction profile, *Bull. Seismol. Soc. Am.*, *78*, 1475–1490, 1988.

Mackie, D. J., R. M. Clowes, S. A. Dehler, R. M. Ellis, and P. Morel-à-l'Huissier, The Queen Charlotte Islands refraction project, II, Structural model for transition from Pacific plate to North American plate, *Can. J. Earth Sci.*, *26*, 1713–1725, 1989.

Manghnani, M. H., R. Ramananantoandro, and S. P. Clark Jr., Compressional and shear wave velocities in granulite facies rocks and eclogites to 10 kbar, *J. Geophys. Res.*, *79*, 5427–5446, 1974.

Marillier, F., M. Dentith, K. Michel, I. Reid, B. Roberts, J. Hall, J. Wright, K. Louden, P. Morel-à-l'Huissier, and C. Spencer, Coincident seismic-wave velocity and reflectivity properties of the lower crust beneath the Appalachian front, west of Newfoundland, *Can. J. Earth Sci.*, *28*, 94–101, 1991.

Marillier, F., et al., Lithoprobe East onshore-offshore seismic refraction survey—Constraints on interpretation of reflection data in the Newfoundland Appalachians, *Tectonophysics*, *232*, 43–58, 1994.

McCarthy, J., S. P. Larkin, G. S. Fuis, R. W. Simpson, and K. A. Howard, Anatomy of a metamorphic core complex: Seismic refraction/wide-angle reflection profiling in southeastern California and western Arizona, *J. Geophys. Res.*, *96*, 12,259–12,291, 1991.

McDonough, D. T., and D. M. Fountain, Reflection characteristics of a mylonite zone based on compressional wave velocities of rock samples, *Geophys. J. R. Astron. Soc.*, *93 & P 547–558*, 1988.

McDonough, D. T., and D. M. Fountain, *P*-wave anisotropy of mylonitic and infrastructural rocks from a Cordilleran metamorphic core complex: The Ruby-East Humboldt Range, Nevada, *Phys. Earth Planet. Inter.*, *78*, 319–336, 1993.

McDonough, W. F., and S.-S. Sun, Composition of the Earth, *Chem. Geol.*, *120*, 223–253, 1995.

McDonough, W. F., S.-S. Sun, A. E. Ringwood, E. Jagoutz, and A. W. Hofmann, Potassium, rubidium, and cesium in the Earth and Moon and the evolution of the mantle of the Earth, *Geochim. Cosmochim. Acta*, *56*, 1001–1012, 1992.

McGuire, A. V., and R. J. Stern, Granulite xenoliths from western Saudi Arabia: The lower crust of the late Precambrian Arabian-Nubian shield, *Contrib. Mineral. Petrol.*, *114*, 395–408, 1993.

Mechie, J., C. Prodehl, and G. Koptschalitsch, Ray path interpretation of the crustal structure beneath Saudi Arabia, *Tectonophysics*, *131*, 333–352, 1986.

Mechie, J., G. R. Keller, C. Prodehl, S. Caciri, L. W. Braile, W. D. Mooney, D. Gajewski, and K.-J. Sandmeier, Crustal structure beneath the Kenya rift from axial profile data, *Tectonophysics*, *236*, 179–200, 1994.

Mehnert, K. R., The Ivrea zone, A model of the deep crust, *News Jahrb. Mineral. Abh.*, *125*, 156–199, 1975.

Ménard, G., and P. Molnar, Collapse of a Hercynian Tibetan plateau into a late Paleozoic European basin and range, *Nature*, *334*, 235–237, 1988.

Mengel, K., Crustal xenoliths from Tertiary volcanics of the northern Hessian depression, Petrological and chemical evolution, *Contrib. Mineral. Petrol.*, *104*, 8–26, 1990.

Mereu, R. F., et al., The 1982 COCRUST experiment across the Ottawa-Bonnechere graben and Grenville Front in Ontario and Quebec, *Geophys. J. R. Astron. Soc.*, *84*, 491–514, 1986.

Mezger, K., Temporal evolution of regional granulite terranes: Implications for the formation of lowermost continental crust, in *Continental Lower Crust*, edited by D. M. Fountain, R. Arculus, and R. W. Kay, pp. 447–478, Elsevier Sci., New York, 1992.

Miller, J. D., and N. I. Christensen, Seismic signature and geochemistry of an island arc: A multidisciplinary study of the Kohistan accreted terrane, northern Pakistan, *J. Geophys. Res.*, *99*, 11,623–11,642, 1994.

Mjelde, R., Shear waves from three-component ocean bottom seismographs off Lofoten, Norway, indicative of anisotropy in the lower crust, *Geophys. J. Int.*, *110*, 283–296, 1992.

Mooney, W. D., and T. M. Brocher, Coincident seismic reflection/refraction studies of the continental lithosphere: A global review, *Rev. Geophys.*, *25*, 723–742, 1987.

Mooney, W. D., and N. I. Christensen, Composition of the crust beneath the Kenya rift, *Tectonophysics*, *236*, 391–408, 1994.

Mooney, W. D., and R. Meissner, Continental crustal evolution observations, *Eos Trans. AGU*, *72*, 537–541, 1991.

Mooney, W. D., and R. Meissner, Multi-genetic origin of crustal reflectivity: A review of seismic reflection profiling of the continental lower crust and Moho, in *Continental Lower Crust*, edited by D. M. Fountain, R. Arculus, and R. W. Kay, pp. 45–80, Elsevier Sci., New York, 1992.

Mooney, W. D., M. E. Gettings, H. R. Blank, and J. H. Healy, Saudi Arabian seismic refraction profile: A traveltime interpretation of crustal and upper mantle structure, *Tectonophysics*, *111*, 173–246, 1985.

Morel-à-l'Huissier, P., A. G. Green, and C. J. Pike, Crustal refraction surveys across the Trans-Hudson orogen/Williston basin of south central Canada, *J. Geophys. Res.*, *92*, 6403–6420, 1987.

Morgan, J. V., P. J. Barton, and R. S. White, The Hatton Bank continental margin, III, Structure from wide-angle OBS and multichannel seismic refraction profiles, *Geophys. J. Int.*, *98*, 367–384, 1989.

Morgan, P., The thermal structure and thermal evolution of the continental lithosphere, in *Structure and Evolution of the Continental Lithosphere*, *Phys. Chem. Earth*, vol. 15, edited by H. N. Pollack and V. R. Murthy, pp. 107–193, Pergamon, New York, 1984.

Morgan, P., and W. D. Gosnold, Heat flow and thermal regimes in the continental United States, in *Geophysical Framework of the Continental United States*, edited by L. C. Pakiser and W. D. Mooney, pp. 493–522, Geol. Soc. of Am., Boulder, Colo., 1989.

Mutter, J. C., and C. M. Zehnder, Deep crustal structure and magmatic processes: The inception of seafloor spreading in the Norwegian-Greenland Sea, in *Early Tertiary Volcanism and the Opening of the NE Atlantic*, edited by A. C. Morton and L. M. Parson, pp. 35–48, Geol. Soc., London, 1988.

Nagao, T., and S. Uyeda, Heat flow measurements in the northern part of Honshu, northeast Japan, using shallow holes, *Tectonophysics*, *164*, 301–314, 1989.

Newton, R. C., and D. Perkins III, Thermodynamic calibration of geobarometers based on the assemblages garnet-plagioclase-orthopyroxene (clinopyroxene)-quartz, *Am. Mineral.*, *67*, 203–222, 1982.

Nicolayson, L. O., R. J. Hart, and N. H. Gale, The Vredefort radioelement profile extended to supracrustal strata at Carletonville, with implications for continental heat flow, *J. Geophys. Res.*, *86*, 10,653–10,661, 1981.

Nyblade, A. A., and H. N. Pollack, A global analysis of heat flow from Precambrian terrains: Implications for the thermal structure of Archean and Proterozoic lithosphere, *J. Geophys. Res.*, *98*, 12,207–12,218, 1993.

Nyblade, A. A., H. N. Pollack, D. L. Jones, F. Podmore, and M. Mushayandebvu, Terrestrial heat flow in east and southern Africa, *J. Geophys. Res.*, *95*, 17,371–17,384, 1990.

Okubo, Y., and T. Matsunaga, Curie point depth in northeast Japan and its correlation with regional thermal structure and seismiscity, *J. Geophys. Res.*, *99*, 22,363–22,371, 1994.

O'Reilly, S. Y., I. Jackson, and C. Bezant, Equilibration temperatures and elastic wave velocities for upper mantle rocks from eastern Australia: Implications for the interpretation of seismological models, *Tectonophysics*, *185*, 67–82, 1990.

Padovani, E. R., J. Hall, and G. Simmons, Constraints on crustal hydration below the Colorado plateau from V_p measurements on crustal xenoliths, *Tectonophysics*, *84*, 313–328, 1982.

Pakiser, L. C., and R. Robinson, Composition and evolution of the continental crust as suggested by seismic observations, *Tectonophysics*, *3*, 547–557, 1966.

Parsons, T., N. I. Christensen, and H. G. Wilshire, Velocities of southern Basin and Range xenoliths: Insights on the nature of lower-crustal reflectivity and composition, *Geology*, *23*, 129–132, 1995.

Paterson, M. S., *Experimental Rock Deformation: The Brittle Field*, 254 pp., Springer-Verlag, New York, 1978.

Peselnick, L., and A. Nicolas, Seismic anisotropy in an ophiolite peridotite: Application to oceanic upper mantle, *J. Geophys. Res.*, *83*, 1227–1235, 1978.

Pinet, C., and C. Jaupart, The vertical distribution of radiogenic heat production in the Precambrian crust of Norway and Sweden: Geothermal implications, *Geophys. Res. Lett.*, *14*, 260–263, 1987.

Pinet, C., C. Jaupart, J.-C. Mareschal, C. Gariepy, G. Bienfait, and R. Lapointe, Heat flow and structure of the lithosphere in the eastern Canadian shield, *J. Geophys. Res.*, *96*, 19,941–19,963, 1991.

Poldervaart, A., The chemistry of the Earth's crust, *Spec. Pap. Geol. Soc. Am.*, *62*, 119–144, 1955.

Prodehl, C., J. Schlittenhardt, and S. W. Stewart, Crustal structure of the Appalachian highlands in Tennessee, *Tectonophysics*, *109*, 61–76, 1984.

Reid, I., Velocity structure of reflective lower crust beneath the Grand Banks of Newfoundland, *J. Geophys. Res.*, *98*, 9845–9859, 1993.

Reid, I. D., Crustal structure of a nonvolcanic rifted margin east of Newfoundland, *J. Geophys. Res.*, *99*, 15,161–15,180, 1994.

Reid, I., and C. E. Keen, Deep structure beneath a rifted basin: Results from seismic refraction measurements across the Jeanne d'Arc basin, offshore eastern Canada, *Can. J. Earth Sci.*, *27*, 1462–1471, 1990.

Reid, M. R., S. R. Hart, E. R. Padovani, and G. A. Wandless, Contribution of metapelitic sediments to the composition, heat production, and seismic velocity of the lower crust of southern New Mexico, *Earth Planet. Sci. Lett.*, *95*, 367–381, 1989.

Reston, T. J., The structure of the crust and uppermost mantle offshore Britain: Deep seismic reflection profiling and crustal cross-sections, in *Exposed Cross-Sections of the Continental Crust*, edited by M. H. Salisbury and D. M. Fountain, pp. 603–621, Kluwer Acad., Norwell, Mass., 1990.

Rey, P., D. M. Fountain, and W. P. Clement, *P*-wave velocity across a ductile shear zone and its associated strain gradient: Consequences for crustal reflectivity, *J. Geophys. Res.*, *99*, 4533–4548, 1994.

Rock, N. M. S., Summary statistics in geochemistry: A study of the performance of robust estimates, *Math. Geol.*, *20*(3), 243–275, 1988.

Roy, R. F., D. D. Blackwell, and F. Birch, Heat generation of plutonic rocks and continental heat flow provinces, *Earth Planet. Sci. Lett.*, *5*, 1–12, 1968.

Rudnick, R. L., Xenoliths—Samples of the lower continental crust, in *Continental Lower Crust*, edited by D. M. Fountain, R. Arculus, and R. W. Kay, pp. 269–316, Elsevier Sci., New York, 1992.

Rudnick, R. L., and S. L. Goldstein, The Pb isotopic compositions of lower crustal xenoliths and the evolution of lower crustal Pb, *Earth Planet. Sci. Lett.*, *98*, 192–207, 1990.

Rudnick, R. L., and I. N. S. Jackson, Measured and calculated elastic wave speeds in partially equilibrated mafic granulite xenoliths: Implications for the properties of an underplated lower continental crust, *J. Geophys. Res.*, *100*, 10,211–10,218, 1995.

Rudnick, R. L., and T. Presper, Geochemistry of intermediate- to high-pressure granulites, in *Granulites and Crustal Evolution*, edited by D. Vielzeuf and P. Vidal, pp. 523–550, Kluwer Acad., Norwell, Mass., 1990.

Rudnick, R. L., and S. R. Taylor, The composition and petrogenesis of the lower crust: A xenolith study, *J. Geophys. Res.*, *92*, 13,981–14,005, 1987.

Rudnick, R. L., and I. S. Williams, Dating the lower crust by ion microprobe, *Earth Planet. Sci. Lett.*, *85*, 145–161, 1987.

Rudnick, R. L., S. M. McLennan, and S. R. Taylor, Large ion lithophile elements in rocks from high-pressure granulite facies terrains, *Geochim. Cosmochim. Acta*, *49*, 1645–1655, 1985.

Rudnick, R. L., W. F. McDonough, M. T. McCulloch, and S. R. Taylor, Lower crustal xenoliths from Queensland, Australia: Evidence for deep crustal assimilation and

fractionation of continental basalts, *Geochim. Cosmochim. Acta*, *50*, 1099–1115, 1986.

Salisbury, M. H., and D. M. Fountain, The seismic velocity and Poisson's ratio structure of the Kapuskasing uplift from laboratory measurements, *Can. J. Earth Sci.*, *31*, 1052–1063, 1994.

Sapin, M., X.-J. Wang, A. Hirn, and Z. X. Xu, A seismic sounding in the crust of the Lhasa block, Tibet, *Ann. Geophys.*, *3*, 637–646, 1985.

Sawka, W. N., and B. W. Chappell, The distribution of radioactive heat production in I- and S-type granites and residual source regions: Implications to high heat flow areas in the Lachlan fold belt, Australia, *Aust. J. Earth Sci.*, *33*, 107–118, 1986.

Sclater, J. G., C. J. Jaupart, and D. Galson, The heat flow through oceanic and continental crust and the heat loss of the Earth, *Rev. Geophys.*, *18*, 269–311, 1980.

Shalev, E., J. Park, and A. Lerner-Lam, Crustal velocity and Moho topography in central New Hampshire, *J. Geophys. Res.*, *96*, 16,415–16,427, 1991.

Shaw, D. M., J. J. Cramer, M. D. Higgins, and M. G. Truscott, Composition of the Canadian Precambrian shield and the continental crust of the Earth, in *The Nature of the Lower Continental Crust*, edited by J. B. Dawson, et al., pp. 257–282, Geol. Soc., London, 1986.

Shen, X., Crust and upper mantle thermal structure of Xizang (Tibet) inferred from the mechanism of high heat flow observed in south Tibet, in *Terrestrial Heat Flow and the Lithosphere Structure*, edited by V. Cermák and L. Rybach, pp. 293–307, Springer-Verlag, New York, 1991.

Sheraton, J. W., A. C. Skinner, and J. Tarney, The geochemistry of the Scourian gneisses of the Assynt district, in *The Early Precambrian of Scotland and Related Rocks of Greenland*, edited by R. G. Park and J. Tarney, pp. 13–30, Univ. of Keele, Keele, England, 1973.

Sheriff, R. E., *Encyclopedic Dictionary of Exploration Geophysics*, 376 pp., Soc. of Explor. Geophys., Tulsa, Okla., 1991.

Shive, P. N., R. J. Blakely, B. R. Frost, and D. M. Fountain, Magnetic properties of the lower continental crust, in *Continental Lower Crust*, edited by D. M. Fountain, R. Arculus, and R. W. Kay, pp. 145–177, Elsevier Sci., New York, 1992.

Siegesmund, S., T. Takeshita, and H. Kern, Anisotropy of V_p and V_s in an amphibolite of the deeper crust and its relationship to the mineralogical, microstructural and textural characteristics of the rock, *Tectonophysics*, *157*, 25–38, 1989.

Simmons, G., Velocity of shear waves in rocks to 10 kbar, 1, *J. Geophys. Res.*, *69*, 1123–1130, 1964.

Sinno, Y. A., P. H. Daggett, G. R. Keller, P. Morgan, and S. H. Harder, Crustal structure of the southern Rio Grande rift determined from seismic refraction profiling, *J. Geophys. Res.*, *91*, 6143–6156, 1986.

Spence, G. D., and I. Asudeh, Seismic velocity structure of the Queen Charlotte basin beneath Hecate Strait, *Can. J. Earth Sci.*, *30*, 787–805, 1993.

Spera, F. J., Aspects of magma transport, in *Physics of Magmatic Processes*, edited by R. B. Hargraves, pp. 265–323, Princeton Univ. Press, Princeton, N. J., 1980.

Sprague, D., and H. N. Pollack, Heat flow in the Mesozoic and Cenozoic, *Nature*, *285*, 393–395, 1980.

Stauber, D. A., Crustal structure in northern Nevada from seismic refraction data, in *Geothermal Resources Council, Special Report*, pp. 319–332, Geotherm. Resour. Counc., Davis, Calif., 1983.

Stosch, H.-G., A. Schmucker, and C. Reys, The nature and geological history of the deep crust under the Eifel, Germany, *Terra Nova*, *4*, 53–62, 1992.

Suetnova, E., R. Carbnell, and S. Smithson, Magma in layering at the Moho of the Basin and Range of Nevada, *Geophys. Res. Lett.*, *20*, 2945–2948, 1993.

Suyehiro, K., and A. Nishizawa, Crustal structure and seismicity beneath the forearc off northeastern Japan, *J. Geophys. Res.*, *99*, 22,331–22,347, 1994.

Taylor, S. R., Growth of planetary crusts, *Tectonophysics*, *161*, 147–156, 1989.

Taylor, S. R., and S. M. McLennan, *The Continental Crust: Its Composition and Evolution*, 312 pp., Blackwell, Cambridge, Mass., 1985.

Taylor, S. R., and S. M. McLennan, The geochemical evolution of the continental crust, *Rev. Geophys.*, *33*, 241–265, 1995.

Tréhu, A. M., A. Ballard, L. M. Dorman, J. F. Gettrust, K. D. Klitgord, and A. Schreiner, Structure of the lower crust beneath the Carolina trough, U.S. Atlantic continental margin, *J. Geophys. Res.*, *94*, 10,585–10,600, 1989.

Tsuchiyama, A., Melting and dissolution kinetics: Application to partial melting and dissolution of xenoliths, *J. Geophys. Res.*, *91*, 9395–9406, 1986.

Valasek, P. A., R. B. Hawman, R. A. Johnson, and S. B. Smithson, Nature of the lower crust and Moho in eastern Nevada from "wide-angle" reflection measurements, *Geophys. Res. Lett.*, *14*, 1111–1114, 1987.

Valdes, C. M., W. D. Mooney, S. K. Singh, R. P. Meyer, C. Lomnitz, J. H. Luetgert, C. E. Helsley, B. T. R. Lewis, and M. Mena, Crustal structure of Oaxaca, Mexico, from seismic refraction measurements, *Bull. Seismol. Soc. Am.*, *76*, 547–563, 1986.

Vielzeuf, D., and J. R. Holloway, Experimental determination of the fluid-absent melting relations in the pelitic system: Consequences for crustal differentiation, *Contrib. Mineral. Petrol.*, *98*, 257–276, 1988.

Vitorello, I., and H. N. Pollack, On the variation of continental heat flow with age and the thermal evolution of the continents, *J. Geophys. Res.*, *85*, 983–995, 1980.

von Huene, R., and D. W. Scholl, Observations at convergent margins concerning sediment subduction, subduction erosion, and the growth of the continental crust, *Rev. Geophys.*, *29*, 279–316, 1991.

Weaver, B. L., and J. Tarney, Rare earth geochemistry of Lewisian granulite-facies gneisses, northwest Scotland: Implications for the petrogenesis of the Archaean lower continental crust, *Earth Planet. Sci. Lett.*, *51*, 279–296, 1980.

Weaver, B. L., and J. Tarney, Empirical approach to estimating the composition of the continental crust, *Nature*, *310*, 575–577, 1984.

Wedepohl, K. H., The composition of the continental crust (abstract), *Mineral. Mag. 58*, suppl., 959–960, 1994.

Wells, P. R. A., Thermal models for the magmatic accretion and subsequent metamorphism of continental crust, *Earth Planet. Sci. Lett.*, *46*, 253–265, 1980.

Wendlandt, E., D. J. DePaolo, and W. S. Baldridge, Nd and Sr isotope chronostratigraphy of Colorado plateau lithosphere: Implications for magmatic and tectonic underplating of the continental crust, *Earth Planet. Sci. Lett.*, *116*, 23–43, 1993.

Wolf, L. W., and J. J. Cipar, Through thick and thin: A new model for the Colorado Plateau from seismic refraction data from Pacific to Arizona Crustal Experiment, *J. Geophys. Res.*, *98*, 19,881–19,894, 1993.

Yan, Q. Z., and J. Mechie, A fine structural section through the crust and lower lithosphere along the axial region of the Alps, *Geophys. J.*, *98*, 465–488, 1989.

Yuan, T., G. D. Spence, and R. D. Hyndman, Structure

beneath Queen Charlotte Sound from seismic-refraction and gravity interpretation, *Can. J. Earth Sci.*, *29*, 1509–1529, 1992.

Zartman, R. E., and B. R. Doe, Plumbotectonics—The model, *Tectonophysics*, *75*, 135–162, 1981.

Zeis, S., D. Gajewski, and C. Prodehl, Crustal structure of southern Germany from seismic refraction data, *Tectonophysics*, *176*, 59–86, 1990.

Zelt, B. C., R. M. Ellis, and R. M. Clowes, Crustal velocity structure in the eastern Insular and southernmost Coast belts, Canadian Cordillera, *Canadian J. Earth Sci.*, *30*, 1014–1027, 1993.

Zelt, C. A., and R. M. Ellis, Seismic structure of the crust and upper mantle in the Peace River Arch region, Canada, *J. Geophys. Res.*, *94*, 5729–5744, 1989.

Zelt, C. A., and D. A. Forsyth, Modeling wide-angle seismic data for crustal structure: Southeastern Grenville province, *J. Geophys. Res.*, *99*, 11,687–11,704.

Zelt, C. A., and R. B. Smith, Seismic traveltime inversion for 2-D crustal velocity structure, *Geophys. J. Int.*, *108*, 16–34, 1992.

Zhu, H., and J. E. Ebel, Tomographic inversion for the seismic velocity structure beneath northern New England using seismic refraction data, *J. Geophys. Res.*, *99*, 15,331–15,357, 1994.

Zucca, J. J., The crustal structure of the southern Rhinegraben from re-interpretation of seismic refraction data, *J. Geophys.*, *55*, 13–22, 1984.

D. M. Fountain, Department of Geology and Geophysics, University of Wyoming, P. O. Box 3006, Laramie, WY 82071.

R. L. Rudnick, Department of Earth and Planetary Sciences, Harvard University, 20 Oxford Street, Cambridge, MA 02138. (e-mail: rudnick@eps.harvard.edu)